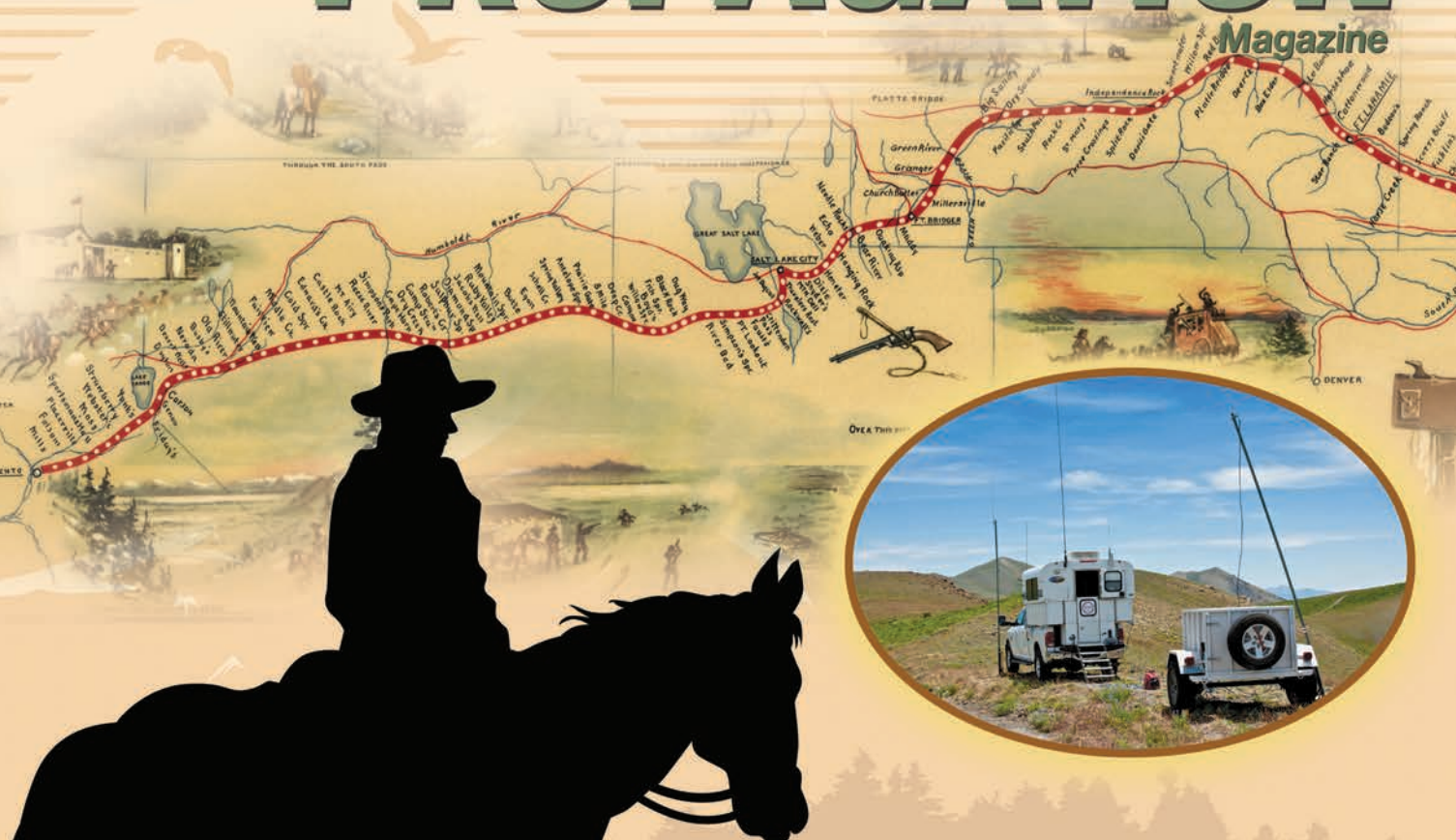CONSIDER PUBLISHING YOUR JOB OPENINGS AT NO COST

IEEE Antennas & PROPAGATION Magazine

COMMUNICATION CHALLENGES

Ham Radio and the Pony Express

◆IEEE

Making Waves in Texas

Call for Papers

The 2020 IEEE Texas Symposium on Wireless & Microwave Circuits & Systems

Baylor University, Waco, Texas   April 2–3, 2020

The Texas Symposium on Wireless and Microwave Circuits and Systems invites paper submissions for the 2020 conference, to be held at the Baylor Research and Innovation Collaborative (https://www.baylor.edu/bric/) in Waco, Texas, on April 2–3, 2020.

Authors from Texas and elsewhere are invited to submit papers based on their original and previously unpublished work in all areas listed below:

- RF and microwave circuits and systems
- 5G and millimeter-wave wireless technologies
- Wireless technologies for biomedical applications
- Computational Electromagnetics
- Antennas, propagation, and electromagnetics
- Spectrum management and coexistence
- Active and passive devices
- Microwave metrology

- Wireless power transfer
- Electromagnetic materials and modeling
- Wireless and optical communications
- Geophysical and subsurface modeling
- Photonics
- Radar and sensing
- Internet of Things
- Emerging wireless technologies

Papers accepted for publication and presented at the conference will be submitted to IEEE Xplore®.

Travel grants will be awarded to students of selected papers to offset registration and travel costs.

Paper Submission Timeline:

- Deadline for submission of full paper: **Feb. 3, 2020**
- Author notification: March 2, 2020 (earlier notification may be requested for foreign submissions)
- Deadline for submission of final paper and presentation: March 16, 2019

Conference website for more information and for submission of papers: www.TexasSymposium.org

Organizing Committee:

General Chairs
David R. Jackson, University of Houston
Shahrokh Saeedi, The University of Oklahoma

Technical Program Chair
Jennifer Kitchen, Arizona State University

Technical Program Co-Chairs
Wooyeol Choi, Oklahoma State University
Taiyun Chi, Rice University

Conference Advisor
Oren Eliezer, Apogee Semiconductor

Publicity Chairs
Rashaunda Henderson, University of Texas at Dallas
Pedro Rodriguez-Garcia, Baylor University

Publications Chair
Ifana Mahbub, University of North Texas

Local Arrangements Chairs
Charles Baylis, Baylor University
Yang Li, Baylor University

Webmaster
Tien Le, University of North Texas

Student Posters and Presentations Chair
Donald Lie, Texas Tech University

Sponsors and Exhibitors Chairs
Oren Eliezer, Apogee Semiconductor
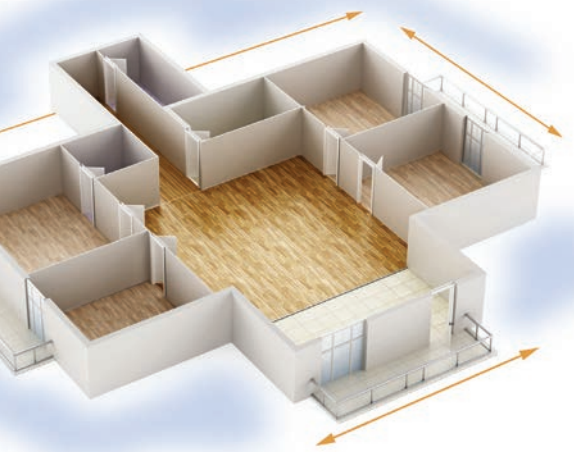Casey Latham, Keysight Technologies

Tutorials Chair
Jiefu Chen, University of Houston

Finance Chair
Brandon Herrera, Baylor University

Call for Sponsors/Exhibitors: Companies interested in sponsoring and/or exhibiting at the event – please contact Oren Eliezer (OrenE@ieee.org) or Casey Latham (CaseyLatham@ieee.org).
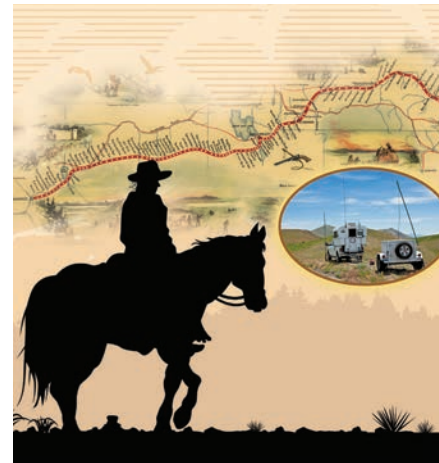
IEEE Antennas & PROPAGATION

Magazine

FEATURES

ON THE COVER

This issue's cover feature is all about ham radio and the Pony Express Re-Ride. Also in this issue is an overview of ray-based strategies for channel characterization and an article regarding a new propagation model based on Fresnel zones. Happy reading!

MISSION STATEMENT:

IEEE Antennas and Propagation Magazine publishes feature articles and columns that describe engineering activities within its scope, taking place in industry, government, and universities. All feature articles are subject to peer review. Emphasis is placed on providing the reader with a general understanding of either a particular subject or of the technical challenges being addressed by various organizations, as well as their capabilities to cope with these challenges. Review, tutorial, and historical articles are welcome.

DEPARTMENTS

Address editorial correspondence to the Editor-in-Chief Francesco P. Andriulli, Dept. Electronics and Telecommunications, Politecnico di Torino, Corso Duca degli Abruzzi 24 10129, Turin, Italy; email: apm-eic@ieee.org.

General information for contributors: Contributions to *IEEE Antennas and Propagation Magazine* are accepted through ScholarOne Manuscripts at https://mc.manuscriptcentral.com/apm-ieee. Contributors are encouraged to contact the magazine editor-in-chief before submitting their articles to inquire whether their prospective submission is within the scope of the magazine. Article formatting requirements vary based on the type of article. The authors are asked to consult http://ieeeauthorcenter.ieee.org/ and https://www.ieeeaps.org/publications/ieee-antennas-and-propagation-magazine for general instructions. Manuscripts should be in English. The editor-in-chief reserves the right to accept, reject, and/or edit any and all material submitted. Submission of material will be interpreted as assignment and release of copyright and any and all other rights as if the standard IEEE copyright and US Export Control Compliance Forms had been signed by the copyright owner. All material associated with contributions may be discarded after the issue containing the contribution goes to press, unless otherwise requested. The nominal deadline for material not requiring peer review or extensive editing is 120 days prior to the start of the month of publication. Contact the editor-in-chief if you have timely material that cannot make this deadline. All feature articles are subject to full peer review per IEEE policy. There is a limit of ten double-column printed pages for all articles. All contributions to

departments are reviewed by the associate editor(s) for that department, with additional peer review as deemed necessary by the associate editor. Conference reports should be no more than two pages and contain no more than five figures.

Digital Object Identifier 10.1109/MAP.2019.2943581

SUSTAINABLE FORESTRY INITIATIVE
Certified Chain of Custody
At Least 10% Certified Forest Content
www.sfiprogram.org
SFI-01681

How do you adapt the real world for electromagnetics simulations?
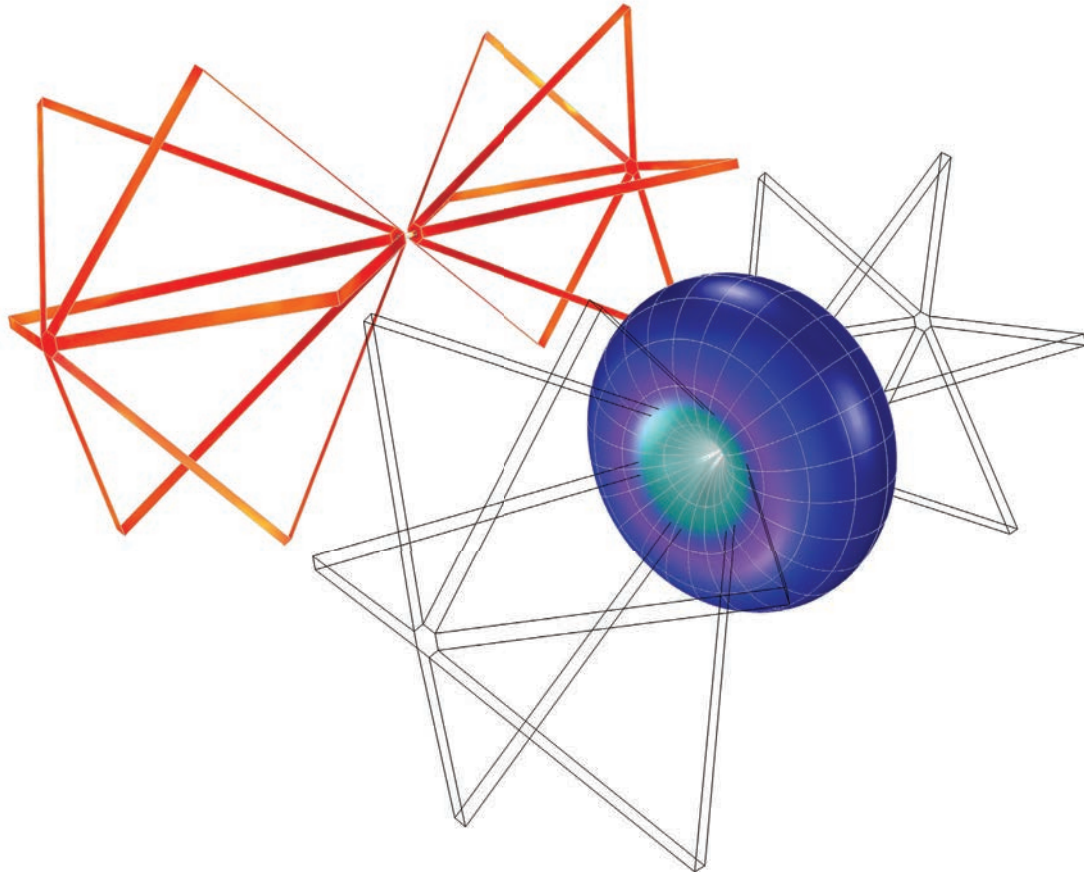
Visualization of the electric field norm and far-field radiation pattern of a biconical frame antenna.

When the ultimate goal is to design more efficient and productive electronic devices, design engineers need to run antenna measurements. If you know what attributes of the real world are important, you could instead test the designs with simulation.

The COMSOL Multiphysics® software is used for simulating designs, devices, and processes in all fields of engineering, manufacturing, and scientific research. See how you can apply it to electromagnetics simulation.

comsol.blog/EM-simulations

COMSOL

Francesco Andriulli

Communication: Then and Now

The quest for fast communication is not unique to modern times, as even when messages were transmittable only by snail mail, there was a strong demand for swift delivery. This demand, at a point in history right at the dawn of telegraph technology, was addressed by the Pony Express, a mail delivery service that used brave horse riders to connect St. Joseph, Missouri, to Sacramento, California. That era may seem like a lifetime ago when compared to today's technology, where electromagnetic waves have changed the way people communicate. This, however, is not always the case. In fact, once a year, the legend of the Pony Express is revived, with horse riders carrying mail across the country. Unlike previous times, however, today's brave riders are never really alone during their endeavors: a unit of ham radio operators provides riders with assistance and emergency communication with their radio coverage. I am sure that you will find the topic interesting, so please take a moment to read the article written by Furse et al. in this issue of *IEEE Antennas and Propagation Magazine* (*APM*). Their detailed account is amazing, and I am sure it will be inspiring for many ham radio operators (and friends) around the world.

This issue also features a contribution by Azpilicueta et al., which offers an overview of ray-based strategies for channel characterization and presents a new hybrid solution in this field. Readers will also enjoy the article penned by Osterman and Ritoša, where a new propagation model based on Fresnel zones is provided. Last but not least, be sure to check out our column contributions, which, in this issue, are particularly intriguing.

ONLINE MATERIAL

When preparing a manuscript for submission to *APM*, all prospective authors are encouraged to present a readable, broad-in-scope, results-focused main article, which is made available in print and online (IEEE *Xplore*). More technical and field-specific material pertaining to your article should be submitted as "supplemental material," which will be available in IEEE *Xplore* and linked to the main article via a QR code. Take advantage of this feature, as there is no page limit on the online material. To increase your chances of a successful submission to *APM*, please see these and other author guidelines in the updated document available at https://www.ieeeaps.org/publications/ieee-antennas-and-propagation-magazine.

PROPOSE A TOPIC FOR A FUTURE SPECIAL ISSUE

We are currently inviting proposals for *APM* special issues. We have already approved three special issues for 2020 and have the resources necessary to examine additional topics. The focus of special issues/sections could be on either established or emerging research topics relevant for the IEEE Antennas and Propagation Society. Cross-disciplinary topics are equally welcome. You can send your proposal to apm-eic@ieee.org with 1) a title and short abstract, 2) a list of prospective guest editors and their affiliations, and 3) a tentative list of potential contributors. We look forward to receiving your proposals!

HAPPY HOLIDAY SEASON!

As 2019 comes to a close, I would like to join the editorial board and the publishing team of *APM* in wishing you a joyful holiday season and a great 2020. May it be filled with exciting scientific and technological advances in our beautiful research field!
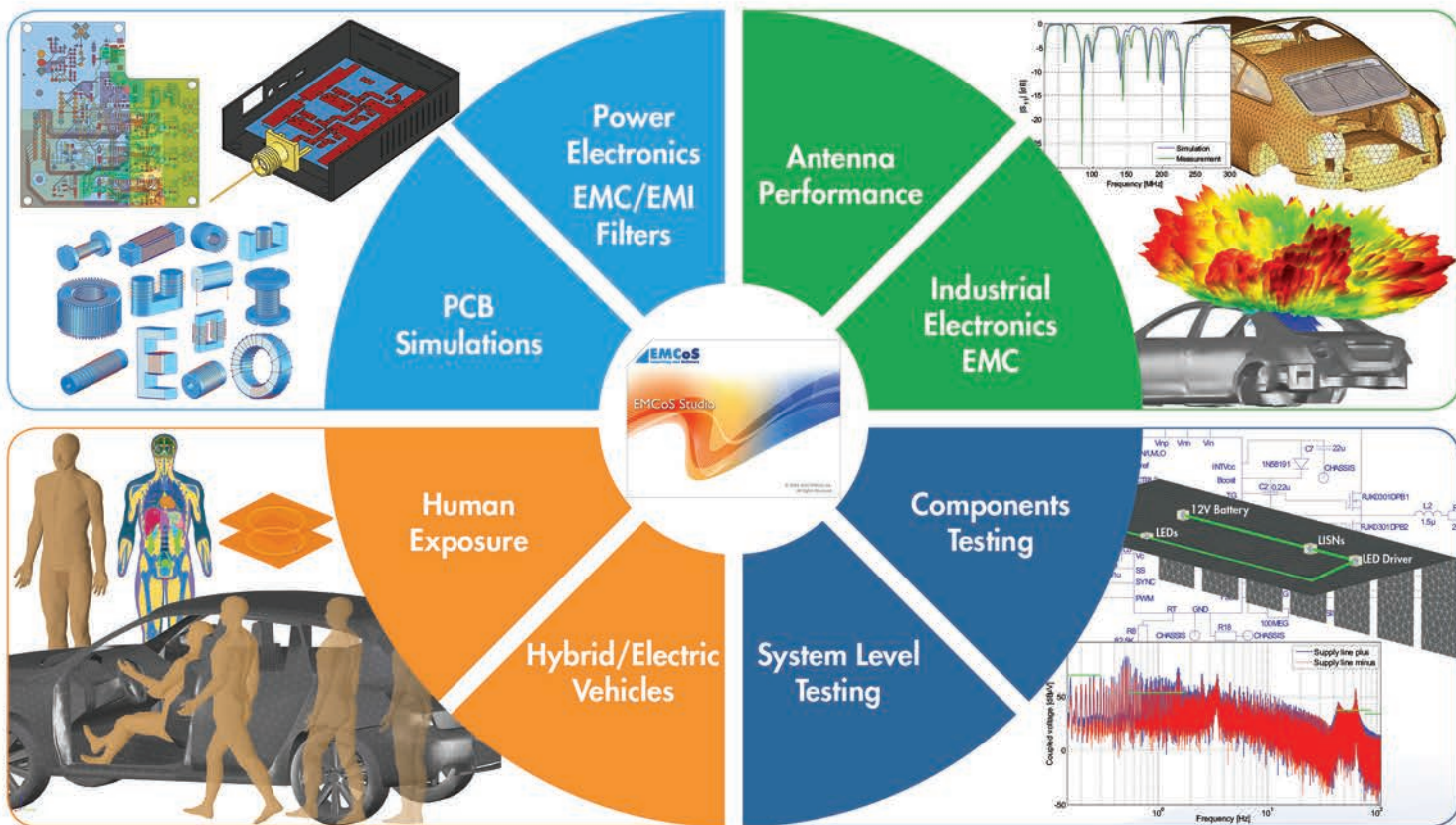
Koichi Ito

Looking Back and Looking Forward

How time flies! This is my last "President's Message" in *IEEE Antennas and Propagation Magazine*. It has been my great honor to serve the IEEE Antennas and Propagation Society (AP-S) as president. First, I would like to thank the AP-S officers, i.e., President-Elect Mahta Moghaddam, Secretary Felix Vega, and Treasurer Don McPherson; the four most-junior Past Presidents Weng Cho Chew, Ahmed Kishk, Mike Jensen, and Roberto Graglia; Honorary Life Member Ross Stone; and many other past presidents, all of whom have always offered assistance as well as helpful comments and suggestions. I would also like to thank the Administrative Committee (AdCom) members, the editors-in-chief of the Society's publications, all chairs of standing committees of the AdCom, AP-S representatives, and relevant IEEE staff for their efforts and hard work in their capacities. Furthermore, I would like to express my appreciation to AP-S volunteers and members for their participation in various AP-S activities.

IEEE OPEN JOURNAL OF ANTENNAS AND PROPAGATION

The Society's first fully open-access publication, *IEEE Open Journal of*

> I would like to express my appreciation to AP-S volunteers and members for their participation in various AP-S activities.

Antennas and Propagation, is currently accepting article submissions. It originally was planned to be published as *IEEE Journal of Special Topics in Antennas and Propagation*, but before its publication, AP-S requested that the IEEE change it into a gold open-access journal. Special thanks go to Prof. Konstantina Nikita, its editor-in-chief, as well as the AP-S Publications Committee for their all of their hard work, which helped produce this journal in such a short period. Please visit https://www.ieeeaps.org/ieee-ojap for more details. We warmly ask you and your group to submit papers to this new journal.

IEEE AP-S C.J. REDDY TRAVEL GRANT

The IEEE AP-S C.J. Reddy Travel Grant is a tremendously valuable gift to the Society, particularly to graduate students. Dr. C.J. Reddy has made a substantial donation to the IEEE

Foundation to establish the IEEE AP-S C.J. Reddy Travel Grant for Graduate Students. It will enable one or more graduate students to attend our annual flagship conference, the IEEE International Symposium on Antennas and Propagation and the U.S. National Committee for the International Union of Radio Science Meeting. Dr. Reddy's intention is that this endowment be used beginning in 2020 to provide long-term support. The AP-S Education Committee is handling this new program. On behalf of the AP-S, I would like to extend our sincere appreciation to Dr. Reddy, and I thank the Education Committee for handling the additional workload.

Prof. Mahta Moghaddam will take over as president of AP-S for 2020. I have no doubt that she will do an excellent job. I wish the best to her as well as the newly elected president-elect and AdCom members. I will continue to serve the Society as a past president and as a volunteer. Finally, I wish all of you a healthy, happy, and successful year in 2020.

Meisong Tong

Chapter Funding, Chapter Activity Committee, and Outstanding Chapter Awards

In this issue of *IEEE Antennas and Propagation Magazine*, I would like to welcome and express my gratitude to the many new Chapter officers who altruistically volunteer their time for our Society members. I would also like to remind our Chapter officers of the coming deadlines for submitting 2019 annual reports and for 2020 Chapter activity funding requests. The deadline for submitting 2019 annual reports is 1 March 2020. The report template and preparation guidelines can be found on the IEEE Antennas and Propagation Society (AP-S) Chapter webpage (http://www.ieeeaps.org/chapters.html). Annual support and special project funding requests should be sent before March 2020 to akpoddar@ieee.org. Chapter chairs should apply for the travel grant to attend the Chapter Chairs Meeting (CCM) at the 2020 IEEE International Symposium on Antennas and Propagation and the U.S. National Committee of the International Union of Radio Science Meeting, which will be held 4–11 July 2020 in Montréal, Canada.

I am pleased to report that, as of December 2019, we have received a record of 121 annual reports for Chapter activities. To continue providing services to our AP-S members and Chapters, the Chapter Activity Committee (CAC) chairs and members have been contacting our Chapter chairs throughout the year, supplying assistance and membership engagement networking. This has helped resolve issues with dormant Chapters, including the formation of new ones. Special thanks go to Dr. Poddar, CAC chair, for his leadership and dedicated service to our Chapters and members. His efforts have led to a rapid increase in the number of AP-S Chapters and a steady growth in membership, when other Societies have shown a decline in memberships. If any of our members are interested in establishing a new AP-S Chapter, please feel free to contact Dr. Poddar or me (mstong@tongji.edu.cn). We will guide you through the Chapter's petition process.

2019 CAC MEMBERS

In January 2019, the AP-S Administrative Committee approved the following membership of the CAC for serving members worldwide:

- Ajay K. Poddar (chair)
- Don McPherson (vice chair)
- Edip Niver (Regions 1–6)
- Anisha Apte (Regions 1–6)
- Charlotte Blair (Regions 1–6)
- Har Dayal (Regions 1–6)
- Vladimir Okhmatovski (Region 7)
- Zhizhang Chen (Region 7)
- Amir Boag (Region 8)
- Vikas Monebhurrun (Region 8)
- Felix Vega (Region 9)
- Meisong Tong (Region 10)

- Jawad Siddiqui (Region 10)

I encourage our members to serve the CAC. If you are interested, please send your nomination to the AP-S president for the consideration of serving the CAC in 2020.

2019 OUTSTANDING AP-S CHAPTER AWARD

Choosing the Outstanding Chapter Award winner is a rigorous process involving many factors (technical events, involvement with local IEEE volunteers, membership drive, mentoring new volunteers, and engagement). The members of the Chapter Award Committee include

- chair: Prof. Weng Cho Chew (2018 AP-S president)
- coordinator: Dr. Ajay K. Poddar (AP-S CAC chair)
- member 1: Prof. Mykhaylo Andriychuk (2017 Outstanding Chapter Award recipient, West Ukraine Chapter)
- member 2: Prof. Qun Wu (2017 Outstanding Chapter Award recipient, Harbin Chapter)
- member 3: Prof. Shun-Yun Lin (2015 Outstanding Chapter Award recipient, Tainan Chapter)
- member 4: Prof. Debatosh Guha (2014 Outstanding Chapter Award recipient, Kolkata Chapter).

I want to thank Prof. Weng Cho Chew and the Chapter Award Committee members for reviewing the nominations. This year, a total of 11 Chapter Award

FIGURE 1. (a) Prof. Yahia Antar (10th from the right) shown with the attendees and Chapter officers. (b) Prof. Alejandro Alvarez Melcon (fifth from the left) gathered with the attendees and Chapter officers.

nominations were sent to the CAC, of which three were selected as the award winners. The winners of first, second, and third place Outstanding Chapter Award are North Jersey, Poland, and Hong Kong Chapter, respectively.

The Outstanding Chapter Award consisted of US$1,000 and a plaque as a token of recognition of volunteerism and technical activities for the benefit of members and the growth of the AP-S. In addition, the officers of winning Chapters were able to use a US$1,950 travel grant to attend the Outstanding Chapter Award function and the Chapter Chairs Luncheon Meeting.

YOUNG PROFESSIONAL EVENTS

Last year, Young Professionals in Space 2018 took place at the Universidad Politécnica de Cataluña, Barcelona, Spain, from 17 to 21 July. The five-day event was packed with expert talks, lectures, workshops, and rocket launches! This event was cosponsored and supported by the AP-S CAC and several IEEE sister Societies including

- IEEE Geoscience and Remote Sensing Society
- IEEE Microwave Theory and Techniques (MTT) Society
- IEEE Aerospace and Electronic Systems Society
- IEEE Industrial Electronics Society

and Region 8's Young Professionals. This year, the AP-S CAC again cosponsored Young Professionals in Space, at

the Dubai World Center, United Arab Emirates, from 4 to 6 November 2019.

CHAPTERS' EVENTS
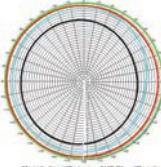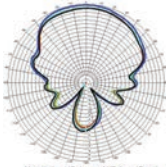
IEEE AP/MTT JOINT CHAPTER (MOROCCO SECTION)

The IEEE AP/MTT Joint Chapter (Morocco Section) organized a one-day visit for Prof. Yahia Antar from the Royal Military College of Canada on Tuesday, 30 April 2019, at the Faculty of Sciences, Tétouan. His visit was sponsored by the AP-S. The one-day public lecture, "Antennas for Wireless Communications and for Sensors: Some Recent Advances and Future Trends," addressed some current and new emerging directions of research in antenna systems. The event provided an opportunity for engineers, researchers, and students to discuss the recent trends in antennas, especially antennas for 5G communication. The speaker, attendees, and IEEE AP/MTT Joint Chapter (Morocco Section) officers are shown in Figure 1(a).

On 2 May 2019, the Chapter also arranged for a one-day visit from Prof. Alejandro Alvarez Melcon of the Universidad Politécnica de Cartagena, Spain, at the Faculty of Sciences, Tétouan. His visit was also sponsored by the AP-S. Prof. Melcon gave the public talk "Leaky Waves Antennas," which was a good opportunity for master's and Ph.D. students to see the latest

developments in this hot topic of great importance to the AP-S. More than 30 participants from various universities attended this event [as shown in Figure 1(b)].
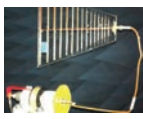
FIGURE 2. (a) Prof. Meisong Tong presents his Distinguished Lecture at the Xi'an Chapter in China. (b) Prof. Tong (bottom row, center) with the main faculty members and Chapter officers at The National Key Laboratory of Antennas and Microwave Technology, Xidian University, Xi'an, China.

IEEE AP/EMC/VT JOINT CHAPTER, NEW JERSEY COAST SECTION

Project Diana, the 1940s U.S. Armed Forces effort that used radar to bounce signals off the moon, was a post-World War II project that became a forerunner of satellite communication systems. The New Jersey Coast Section and AP/EMC/VT Joint Chapter decided to pursue obtaining historic IEEE Milestone status. The citation from the IEEE History Committee reads:

On 10 January 1946, a team of military and civilian personnel at Camp Evans, Fort Monmouth, New Jersey, USA, reflected the first radar signals off the moon using specially modified SCR-270/1 radar. The signals took 2.5 s to travel to the moon and back to the Earth. This achievement, Project Diana, marked the beginning of radar astronomy and space communications.

IEEE AP/MTT NORTH JERSEY JOINT CHAPTER

The North Jersey AP/MTT Joint Chapter hosted the 33rd Annual Symposium and Mini-Show on Thursday, 3 October 2019, at the Hanover Manor in East Hanover, New Jersey. The conference presented a series of 10 lectures that described the state of the art in drone technology; digital predistortion; 5G multiple-input, multiple-output; closed-loop circuits; antennas; directional filters; satellites; arrays; atomic clocks; and a special talk from the Women in Engineering Chapter. The speakers, all leaders in their respective fields, represented General Dynamics, AeroDefense, Nokia Bell Labs, Keysight Technologies, ET Industries, Futurewei, WTG CommAgility, Advancing the Wireless Revolution, and Microchip Technology. The Mini-Show presented a group of displays and demonstrations of state-of-the-art products from leading companies in the aforementioned technology categories. The exhibits included components, subsystems, test equipment, and CAD tools. Registration is online, there is no charge to attend, and IEEE membership is not required to attend the event. Additional information about the event can be found at http://sites.ieee.org/northjersey/.

IEEE AP/MTT XI'AN JOINT CHAPTER

On 13 May 2019, Prof. Meisong Tong visited Xidian University and gave a distinguished lecture at The National Key Laboratory of Antennas and Microwave Technology in Xi'an, China. Prof. Tong was warmly welcomed by Prof. Ying Liu, the director of the laboratory and Xi'an Chapter's chair.

During the morning session, Prof. Tong gave his distinguished lecture on the topic of nontraditional numerical methods for solving electromagnetic problems [Figure 2(a)]. Hundreds of faculty members, researchers, and students from Xidian University and the Chapter attended the seminar. Prof. Tong has done substantial research on integral

FIGURE 3. Prof. Meisong Tong (center) with the student volunteers who organized the conference.

equation methods in computational electromagnetics. He has made prominent contributions and achievements in developing nontraditional numerical methods, especially the Nyström and meshless methods. During the seminar, Prof. Tong introduced the background, principles, advantages, and typical applications of nontraditional numerical methods in detail. After the seminar, Prof. Tong interacted cordially with the attendees and was photographed together with the main faculty members and Chapter officers [Figure 2(b)]. The attendees expressed that they benefited a great deal from Prof. Tong's lecture and hoped to have more such lectures in the future (Figure 3).

IEEE AP-S STUDENT BRANCH CHAPTER OF TONGJI UNIVERSITY

The IEEE AP-S student members from the Student Branch Chapter (SBC) of Tongji University, Shanghai, China, enthusiastically served as volunteers for the 2019 IEEE International Conference on Computational Electro-

> More than 100 graduate students from several universities in Shanghai, including the prestigious Fudan University and Shanghai Jiao Tong University, attended the forum.

magnetics, which was hosted by Tongji University and held at Shanghai Majesty Plaza Hotel from 20 to 22 March 2019. The student members provided courteous and professional assistance during the organization of the well-known conference, including webpage design and maintenance, on-site registration, designing and disseminating publicity materials, reception and banquet preparation, guest pickup and drop off, and so on. Their thoughtful volunteerism was deeply appreciated by the attendees.

Following the conference, the SBC invited three renowned scholars, Prof. Tapan K. Sarkar, Prof. Roberto D. Graglia, and Dr. Vikass Monebhurrun (who all participated in the conference) (Figure 4), to visit Tongji University on 25 March 2019. There, Prof. Sarkar presented "The Physics, Mathematics, and Realization of Radio Wave Propagation in a Cellular Wireless Communication System," and Dr. Monebhurrun gave the talk "Numerical Calibration of Electric Field Probe for Specific Absorption Rate Measurement." Their stimulating talks were well received by attendees and evaluated highly. During the presentations, the students mingled with the speakers, proposing and discussing many problems and theories, especially on the subject of electromagnetic theory related to 5G communication. The scholars also shared their rich experience with the students on how to be a good researcher.

The SBC of Tongji University also cosponsored "The 11th Shanghai Graduate Academic Forum" with the SBC of East China Normal University, Shanghai, China, which was held at East China Normal University on 11 May 2019 (Figure 5). More than 100 graduate students from several universities in Shanghai, including the prestigious Fudan University and Shanghai Jiao Tong University, attended the forum. The graduate students talked with each other about how to track cutting-edge and frontier research topics, review literatures, interact with advisors, conduct high-quality research work, and so on. The forum received great support from the East China Normal University and has come to have a greater impact for Shanghai's graduate students.

FIGURE 4. The student members with (standing behind sign, from left to right) Dr. Vikass Monebhurrun, Prof. Tapan K. Sarkar, and Prof. Roberto D. Graglia.

FIGURE 5. The student representatives of branch Chapters at four universities in Shanghai, China.

Cynthia M. Furse, Charles Killian, Gerald Hasty, and Bob Nelson

Ham Radio and the Pony Express

Providing communication in remote areas.

The Pony Express provided mail service between Sacramento, California, and St. Joseph, Missouri, using relays of horse-mounted riders from 3 April 1860 to October 1861. The route, shown in Figure 1, was roughly 1,966 mi (3,164 km) long, through country inhabited mainly by Native Americans with a few scattered white settlements in the western United States. The Pony Express is reenacted annually, with riders galloping day and night to carry the mail across the country. Ham radio operators provide emergency communication for this event across the remotest sections of the route, using a variety of base and repeater stations,

handheld and vehicle-supported radios; ultrahigh frequency (UHF), very HF (VHF), and HF bands; and an array of deployed antennas, described in this article.

INTRODUCTION

The Pony Express crossed both the rugged Rocky Mountains and the Sierra Nevada range, through two states (Missouri and California) and six territories (Kansas, Nebraska, Colorado, Wyoming, Utah, and Nevada). Running day and night, in all weather, riders galloped from 5 to 20 mi (80 to 320 km), depending upon the terrain, between stations, swapped to a fresh horse in 2 min or less, and continued on to the next station, covering a total of 100 mi (1,600 km) before switching riders. All the same, this 10-day transcontinental

delivery time was a breakthrough in communication speed, cutting the time required for mail delivery by stagecoach (21 days) in half. This feat required 80 riders, more than 400 horses, 184 stations, and several hundred support personnel. In a whirlwind delivery, the Pony Express brought news of President Abraham Lincoln's election to the West Coast in a record-setting seven days and 17 h.

The riders were often teenage boys. A famous advertisement allegedly read, "Wanted: Young, skinny, wiry fellows not over eighteen. Must be expert riders, willing to risk death daily. Orphans preferred." However, the ad has never been found, and many historians question its veracity. "Buffalo" Bill Cody claimed to have been a Pony Express rider, and he later glamorized the Pony Express in his "Buffalo Bill's Wild West Show," capturing imaginations and turning its young riders into national heroes. The horses were outfitted with special lightweight saddles, and the mail was carried in a leather mail bag, called a *mochila*—four locked pouches, called *canteens*, attached to a leather saddle cover that fit over the saddle, held in place by the weight of the rider sitting on it. When the rider would pull up to a station, he would exchange the mochila from his tired horse to a fresh mount, swing up, and gallop off.

The Pony Express was never intended to be long term nor the only system of delivery. Mail was still carried overland in wagons and stagecoaches. Ponies carried only express mail, at US$5 a half ounce (14 g), the equivalent of more than US$140 today. The transcontinental telegraph, already well on its way to linking the frontier when the Pony Express began operating, merely sealed the doom of the operation, which was already collapsing due to conflicts with Native Americans, harsh winter conditions, and financial mismanagement. The riders of the Pony Express made a last gallop across the country in November 1861, soon to be replaced by the transcontinental telegraph, depicted in Figure 2.

But the romance of the Pony Express never really faded away. In 1923 a Re-Ride, from St. Joseph to Sacramento (not necessarily following the original Pony Express trail), was kicked off by a signal from President Calvin Coolidge. In 1935, 300 Boy Scouts carried the mail from west to east, following the original trail. In 1960, for the Pony Express Centennial, the mail was carried simultaneously both east and west. Following this ride, the National Pony Express Association (NPEA) was organized, and a Re-Ride of the famous journey between St. Joseph, Missouri, and Sacramento, California, has been an annual event since 1985. Each state organizes mounted relay teams, with rides between 2 and 10 mi (3.2 and 16 km) each, before passing off the mochila to the next rider. Riders are sworn in as temporary mail carriers taking the same oath as the original riders, and the 50-lb (23-kg) mochila contains actual U.S. mail [souvenir letters from the Pony Express, which cost US$5 (the same as in 1860) to send].

The Pony Express originally ran through a remote frontier, typically following stagecoach routes with vast empty expanses between small urban areas. Stage stations served as home bases where riders stopped, and smaller stations between them provided places just to exchange horses. Today, much of the trail remains remote and rugged with majestic mountains to scale, primitive roads to follow, long distances between water, and miles and miles of nothing but miles. Imagine galloping a strong horse under a full moon through a remote desert where it can be 40 mi (64 km) or more to a telephone, 125 mi (200 km) between gas stations, and the only traffic consists of wild mustangs, antelope, and coyote. Often, the only domestic thing that is seen is a range cow.

With no cell phone coverage and long distances without access to emergency care, amateur radio (ham) operators provide tactical and emergency communications for various events in these areas, such as races, bike events, and the Pony Express Re-Ride. In Utah and parts of California, they follow in a truck behind the riders, as seen in Figure 3. In Nevada and most of California, they are posted along the trail. Either way, they provide information on the location of the pony and rider and are there in case of an emergency. Figure 1 shows a map of the ham radio support (marked by blue dots) along the trail, as well as the locations of repeater stations, and so on used along the way.

Ham reports, plus a satellite tracker in the locked mail pouch, track the mochila as it traverses the country. The tracking is updated continuously on the NPEA website and is followed by people all over the world [1]. This helps riders to saddle up and be ready when the mail is coming, and reports the locations of rider exchanges for people who want to see and cheer on the riders as they come through. Their reports from the trail are uploaded to the NPEA website. But the most important communication the ham operators can provide is for emergency assistance—injuries, medical issues, runaway horses, flat tires and truck problems, lost riders, and so on.

This article is about the details of the ham radio support for the Pony Express Re-Ride and the challenges of providing communication for long distances in remote areas with rugged mountains and deserts, through quite literally rain, hail, sleet, snow, mud, and the dark of night. The trail and terrain through each state are a little different, requiring different ham radio support, as described next.

CALIFORNIA HAM SUPPORT

California hams cover the whole stretch of the Re-Ride from Old Sacramento, California, to the Nevada border or close to it. There are 43 exchanges (covering 143 mi in 23 h), 42 of which are accessible for ham coverage to report to net

control the rider in/out times. Ham support is particularly necessary in the High Sierra mountains, where cell phone coverage is spotty. There are two different trails used for the Re-Ride, depending on if the ride is from east-to-west (when the mochila and amateur reporting are handed off to Nevada Express and the Sierra Intermountain Emergency Radio Association (SIERA) hams at Woodfords, California) or west-to-east (when they pick up the mochila from Nevada at the border in South Lake Tahoe). The terrain varies from the high Sierras where the rider and the hams are far from the road to the great Sacramento Valley and Old Sacramento with traffic and potentially irritated motorists, annoyed for
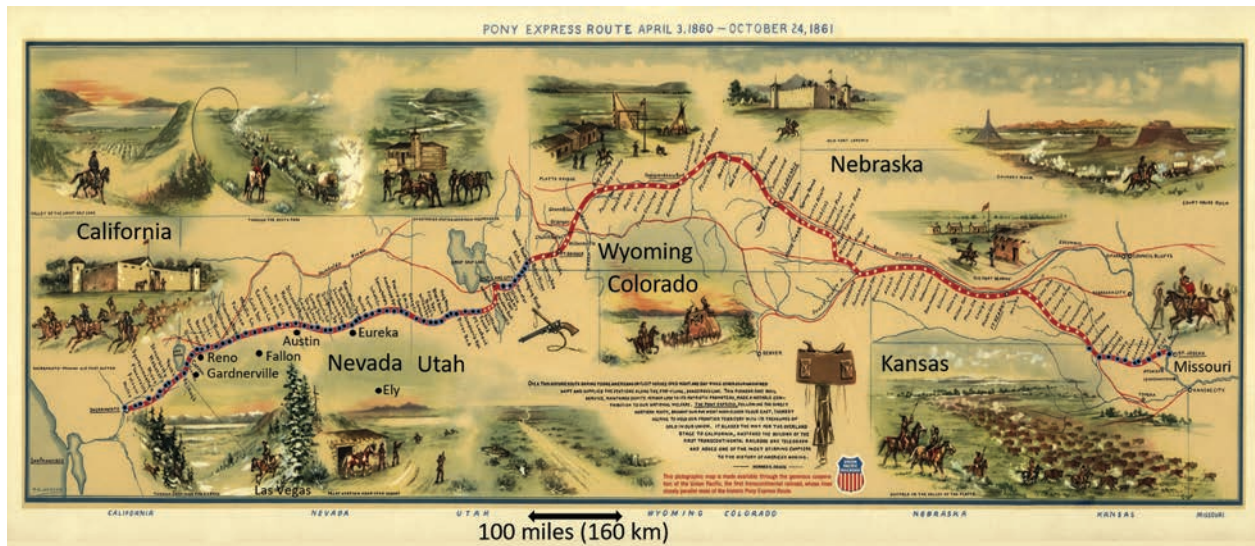
FIGURE 1. The Pony Express (1860–1861) carried the mail between St. Joseph, Missouri, and Sacramento, California, about 1,900 mi (3,100 km) in 10 days, running day and night in all weather. The annual Pony Express Re-Ride closely follows most of the original routes. Some areas are as remote as they were in the mid-19th century. Blue dots indicate portions of the Re-Ride through Utah and Nevada supported by ham operators. (Source: Wikipedia; courtesy of the Library of Congress.)

FIGURE 2. The romance of the Pony Express, of a young rider galloping headlong across the desert, continues to capture imaginations to this day. Wire-line communication—the telegraph—brought a quick end to the Pony Express. (Source: The Utah Historical Society; courtesy of the Library of Congress.)

any delay in their travel. In these urban areas, the ham pick-up truck travels close behind the horse and rider, protecting them from cars.

California has 23 h to get the mail through the state, with ham coverage all the way. Two net controllers split the shift, and an operation officer manages the whole route, with two ride captain ham shadows who stay with the captain and relay information that is pertinent to the smooth operation of the ride. There is also a shadow following the ride lieutenants. The exchanges are usually 5 mi (8 km) apart. Usually, there are 20 hams taking part in the Re-Ride, leapfrogging from one place to the other.

Repeater 146.805 in Pollock Pines, California, covers 95% of the trail. The other 5% is covered by linking into the SIERA's repeater in Minden, California. Although there are areas where cell phone communication is readily available, the repeater is used for the whole trip, so all the information goes through the net control and keeps the hams on the route in the link as to what is happening. Unlike their peers in other states, the hams do not follow the pony, especially in the Sierras, because a jeep cannot get through.

NEVADA HAM SUPPORT

Amateur radio is a hobby that encompasses many different interests. Some like contests, using low power, or building equipment. Others like serving their communities by providing public service communications support, and the Pony Express ham radio support is only one example of such an activity. The SIERA solicits volunteers to help with the NPEA Pony Express Re-Ride each year, and ham radio operators throughout the state of Nevada step up to provide communication support for this annual event.

In Nevada, ham support is provided for the entire Re-Ride from east to west. Throughout the route, cell phone coverage is sparse. Nevada is one of the longest remote stretches in the Pony Express Re-Ride. Ham operators provide communication support from repeaters on mountain summits to areas that are flat, harsh desert. Stations can be sweltering during the day and icy cold, and it can sometimes snow at night. Jeff (K7BCV) and Sue (KI7CTT) Cauhape spent the first 15 years on Overlook Pass West (see Figure 4), north of Eureka, Nevada, where they strung out an 80-m (covering 3.5–4 MHz, roughly 130 ft long) antenna up the hillside and also hoisted a mast for a 40-m (covering 7–7.3 MHz, about 65-ft-long) antenna. Huddling over VHF and HF radios powered by a deep-cycle battery in the back of a Jeep, they helped cover the state. Now, they use a mobile antenna system that was made by MFJ. It consists of two pairs of verticals that can be mounted on the back bumper of the Jeep on separate 12-ft (3.6-m) masts to form dipoles. In addition to providing communication support, they also shelter the riders as they wait, often hours, for the mail (Figure 5).

Austin, Nevada, is a very small community located near the center of the state on U.S. Route 50 close to the path that the original Pony Express riders used. The 2010 Census listed the population of Austin as 192. Nearby, the Austin Summit is about 8,500 ft (2,600 m) above sea level and has a view of a major part

FIGURE 3. Utah ham operators in the Rover follow rider Cindy Furse on her horse, Tesla, through Utah's West Desert. Note the leather mochila mail pouches (carrying a GPS transponder locked in with the mail) on either side of the horse and the antennas protruding from either side of the Rover. (Source: Jamie Marvadakis; used with permission.)

FIGURE 4. Ham radio support on Overlook Pass West includes dipole antennas, VHF and HF radio links, and shelter from the weather. (Source: Sue Cauhape; used with permission.)

FIGURE 5. In wet and soggy years, ham stations sometimes also provide shelter from the weather for both ham operators and Pony Express riders. The horse, Patriot Commander, is making it clear he'd like to come all of the way into the tiny tent. (Source: Sue Cauhape; used with permission.)

of the state. The dirt forest road from Route 50 to the summit is poorly maintained and difficult to climb. In 2018, Bob Nelson made it to the summit in a pickup truck pulling a small utility trailer (shown in Figure 6) and set up communications with the mobile operators who track the progress of the Pony Express riders both along the roads that are used and at checkpoints in areas where the riders are cross-country. As can be seen in Figure 6, he set up two tall poles with dual-band J-pole antennas, one set on the VHF simplex frequency (146.55 MHz) to communicate with the mobile and checkpoint operators and one set to communicate with the repeater (KC5ARS) near Fallon, Nevada (147.345 MHz) to reach the base stations, which were all in the Reno to Gardnerville, Nevada, area. That repeater was 117 mi (188 km) away, and the operators were somewhat surprised at how good the signal was in both directions throughout the two-and-a-half days of the Nevada Pony Express transit. Dipole antennas on two HF frequencies (3.965 and 7.230 MHz) were set up as a backup but were not used. The Pony Express runs 24/7, and the ham support does as well. Originally expecting to support only a 4-h shift near the Austin transit, the unexpectedly good coverage led Nelson to work a full 18 h without a break, as the Pony ran across the state.

Nelson's station is made up of equipment that is built into a camper shell on the back of a pickup truck (shown in Figure 6) and a linear amplifier that is stationed at his home. In the camper are 15 two-way radios, several modems, two laptop computers, and three 50-Ah, 12-V batteries. Everything in the truck runs on 12 V of dc, except the air conditioner. The utility trailer contains all the camping gear and two small Honda generators. The radios are mostly commercial Motorola radios and cover the 1.8–900-MHz radio bands. Nelson operates four HF radios with three of them in the truck and one in a very-low-noise area just at the north end of Las Vegas. He operates this from wherever he is using an Internet device to link the control head to the radio. The camper was custom built for Nelson by Alaskan Campers of Winlock, Washington. The top rises and lowers using a hydraulic system so that when up, as in the photos, it has a full 6-ft-tall

FIGURE 6. This photo shows the 2018 setup at the peak of the Austin Summit. There are two dipoles off to the right of the photo, and the 19-ft whip on the camper shell was used for various HFs through an autotuner.

interior, but when lowered, it is slightly above the pickup cab, which makes driving much easier.

After the communication success in 2018, Nelson and three other operators [Frank Kostelac (N7ZEV), Linda Kostelac (KC7IIT), and Keith Gordon (K7KSG)] planned to support communication from Austin Summit, sharing the workload in shifts over the two-and-a-half days that the Pony Express was crossing Nevada. About a week before the event, they were told that the road to the summit was so bad the maintenance crews for the microwave relay station on the summit were still using a tracked snowcat to get to the top. Kostelac came up with the idea of building a cross-band repeater that would operate on solar power with batteries for nighttime, and he proposed using his Jeep, outfitted for off-road work, with which he was sure he could reach the summit. The remaining equipment would be set up at the Austin Airport, which was line of sight to Austin Peak. Gordon, who is a corporate pilot, arranged access at the airport through the Austin Airport Authority, which was very supportive of the effort. The Austin Airport Authority not only provided use of the airport grounds but also gave the radio operators access to the lounge, bathroom, shower, and electric power. Kostelac and Gordon took the equipment up to the summit and set it up while Nelson set up the antennas and radio equipment at the airport. The cross-band repeater operated on the VHF frequency (146.55 MHz) to the mobiles and on the UHF frequency (446.025 MHz) to the airport. They were not able to reach the Fallon, Nevada, repeater from the airport, so they used the HF radios on 3.965 and 7.230 MHz with dipoles cut for those frequencies. These dipole antennas were set up using some surplus Collins Radio antennas, which have coils of wire and a simple mechanical computer that enable pulling out just the right amount of wire for the desired frequency. They also have a balun and work remarkably well. They also set up an 80-ft (24.4-m) wire about 10 ft (3 m) off the ground fed with an SGC autotuner. They used that radio for trying various frequencies and principally for Winlink transmission and reception as a backup to the HF voice communications. Nelson also used Winlink [2] (using the fast Pactor mode), which he has found to be a particularly effective tool in emergency and public service communications. Winlink gateways (from Nevada to Utah, California, Mexico, and sometimes Oregon) or a Winlink capable station can pass email or peer-to-peer traffic.

In all, four HF radios were used. One was connected to each of the dipole antennas, one was connected to the 80-ft wire, and the fourth was Nelson's remote radio in Las Vegas, Nevada, operated through the Internet using a Verizon hotspot for connection to long-term evolution (LTE). That radio is connected to a terminated folded dipole for HF, so it covers the HF spectrum. The base stations were about 150 mi (240 km) from the airport and about 350 mi (560 km) from the Las Vegas radio. The propagation conditions worked out that either the local radio at the airport or the Las Vegas radio was in solid contact with the base stations every time they needed to communicate. They also had one VHF radio in the truck at the airport on the simplex 146.55-MHz frequency and one UHF radio on the cross-band repeater UHF frequency (446.025 MHz), which could have been used if needed.

During the 2019 Pony Express Re-Ride, the team began communicating with the mobiles to the east of the airport, north of Ely, Nevada, and were able to communicate most of the way to Fallon, Nevada, covering about 200 mi (320 km) of the Re-Ride route. The airport was on the Re-Ride route, so the ham operators stationed at the airport saw the riders as they passed. Numerous mobile and checkpoint operators helped throughout the two-and-a-half day event. They used mobile and handheld VHF radios to contact the airport crew via the cross-band repeater. They also manned several base stations in the Reno, Nevada, to Gardnerville, Nevada, region, posting information day and night on the riders' progress.

Plans for the 2020 Pony Express Re-Ride include three cross-band repeaters. One will be set up as it was in 2019 to communicate with the mobiles and checkpoints along the route. The second will communicate with one of the repeaters near Fallon, Nevada, as in 2018, and a third will communicate with a repeater near Ely, Nevada, which should have coverage most of the way to the Utah border. The support team hopes to set up again at the Austin Airport.

The equipment inside the camper is shown in Figures 7 and 8. In Figure 7, the Pelican case on the left contains the control head and speaker for the remotely operated radio at the north end of Las Vegas. One of the laptop computers is to the right of that unit and is the main operating position. There are two 110-W Motorola MCS 2000 commercial VHF radios, one with a dual-control head so that it can be operated from the cab of the pickup. Below the VHF radio is a Motorola UHF digital mobile radio. There are two Motorola Micom HF radios to the right of the VHF radios. One is a Micom 2, and the other is a Micom 3. These are 125-W commercial HF radios. In the center is the controller for the three 100-W solar panels that run all the equipment within the camper. Below the tabletop are stored the two cross-band repeaters, one that operates VHF to HF connecting to the Micom radios and one that is VHF to UHF as well as some backup VHF and 900 MHz radios. The UHF radio covers both the amateur 70 cm band and the General Mobile Radio Service frequencies. To the right of those radios is the telephone patch equipment that provides two means of providing phone patch capabilities, a direct hard-wired line when at home and on the road either voice over IP or a standard analog phone using a Verizon LTE hotspot. This hotspot also enables control of the Las Vegas radio from the camper. In Figure 8, three of the modems are shown. These include the SCS Pactor 3/4 modem, the RapidM RM2 modem for the military M110A mode, and the Kantronics packet modem. There is also a modem for Winmor that is behind the computer. Antenna hardware (not shown) includes two dual-band J-pole antennas, a UHF beam, a 900-MHz collinear antenna, a dual-band log periodic antenna, and two Collins Radio adjustable dipole antennas. Many feet of coaxial cable, fiberglass poles, and nylon guy ropes are used to set up the antennas.

Ham radio support for an event as remote, long, and challenging as the Pony Express Re-Ride requires the skill and cooperation of a huge team of ham radio operators. Because of the late spring, the dirt roads were mostly impassable, so they used two jeeps to set up a cross-band radio on the summit instead of setting the relay station on the summit. (Figure 9).

FIGURE 8. Three of the modems are shown. These include the SCS Pactor 3/4 modem, the RapidM RM2 modem for the military M110A mode, and the Kantronics Packet Modem. A modem for Winmor is behind the computer.

FIGURE 7. Radios and control units inside the camper.

FIGURE 9. Operators who manned the Austin, Nevada, relay site shown are (from left): Robert Nelson (WA3PAD), Frank Kostelac (N7ZEV), Linda Kostelac (KC7IIT), and in the camper, Keith Gordon (K7KSG).

UTAH HAM SUPPORT

Ham operators provide support for the Utah segment of the Pony Express Re-Ride on both the east and west sides of the state where cell phone coverage is limited or nonexistent. The ride through the central part of the state goes through Salt Lake City and the surrounding urban areas, so ham coverage is not required there. The eastern ride from Barker Ranch on the Utah–Wyoming border to the This Is the Place Monument on the eastern side of Salt Lake City is a steep (paved) mountain road with deep canyons that sometimes limit even

FIGURE 10. Servers, VHF radios, and switches are rack-mounted behind the driver's seat. Operator stations are to the left, and the radios can be operated from the driver's seat as well.

FIGURE 11. The Rover carries VHF mobile communication equipment, six crossed-dipole antennas, and two operators. Here, it is almost ready to start the night ride support, following the pony across Utah's west desert.

ham coverage. West of Salt Lake City from Camp Floyd, Utah, to Ibapah on the Nevada border is a gravel road through desolate desert. Wild horses and coyote are often seen. The Re-Ride is generally scheduled on a weekend where a full moon lights the way through the desert at night.

The eastern part of the state is covered by two repeaters, K7HEN located on Lewis Peak and W7SP located on Farnsworth Peak. The route through Utah's western desert utilizes four linked repeaters provide by W7EO. The repeaters are located at Vernon, Wendover Peak, Black Mountain, and South Mountain in and around the Tooele, Utah, area. Typically, 15–20 amateur radio operators volunteer their time to provide communications along the roughly 36-h route. One or more vehicles equipped with amateur radio equipment (for example Figures 10 and 11) and operators accompany the horse and rider along each of the routes. A net control operator monitors the repeaters, relaying the position of the pony and being ready to handle emergency communications if required.

Mobile ham support is provided by the Rover (shown in Figures 3 and 11), a 1978 Dodge Kary van that had once been a crime scene investigation sheriff's vehicle, complete with running water and an on-board generator. Charles (Chuck) Killian (WB6YOK) and Gerald Hasty (AD7QF) gutted the vehicle, fitting it out with two operator positions (Figure 12). They installed a high-capacity battery stack, a rack with VHF radios (2 m, 144–148 MHz), Internet and keyboard video mouse switches, and seven Dell servers. Several crossed-dipole antennas on masts that can be raised when the vehicle is stopped, as well as several field-deployable antennas, are included. Today, they have a single vmWare host that supports several guests. They can access OpenStreetMap an Asterisk private-branch exchange, to enable phone connections, computer systems for the two operators, radio location equipment, and more. The Rover is an ongoing project, and they are currently adding equipment that supports an amateur radio emergency data network at the microwave frequencies of 2.4, 3, and 5 GHz to allow the remote sharing of the Rover capabilities with others in the line of sight.

FIGURE 12. Chuck Killian (right) and another ham operator, waiting for the rider to bring the mail. They will support the next team of riders running the mail across the desert overnight. Many ham operators, such as Killian (shown wearing the official Pony Express uniform), also join the NPEA.

The practical and logistical issues of providing continuous communication support day and night over long distances in challenging, remote locations stress the systems (mechanical, electrical, and human). A pickup truck and trailer (the Rover support vehicle) provide a second large generator and enough gas, food, and water for three days, as well as more complex antenna systems, as needed. Quick snack food and freeze-dried food with water heated on a propane stove are the norm. Cold water from the Rover's fridge is a luxury in the desert heat and dust.

WYOMING, NEBRASKA, COLORADO, KANSAS, AND MISSOURI

The route through Nebraska and Colorado mainly follows the Platte River Valley and Interstate 80, and cell phone coverage is generally available. Ham radio support has been provided some years but not others.

Through Kansas and Missouri, the route follows both well-established roads (where the ham support may include marking railroad crossings), as well as more primitive dirt roads, rarely graded. Mud and washed out bridges have required rerouting riders, and the ham operators have helped to communicate these changes, collaborating with the local sheriff offices to ensure the safety of the Re-Ride. Severe weather warnings (rain, hail, and even one tornado warning) have also been shared so that riders could take cover. Ham operators have also helped with a couple of emergencies including a wheel coming off a trailer (it was found about 3 mi back down the road) and the loss of a rider's pocket Bible (carried by the riders, as in the original Pony Express; this was also found back down the trail). The challenges of covering the ride (see Figure 13), which takes more than 30 h, requires the cooperation and collaboration of numerous dedicated volunteer ham operators plus local law enforcement, weather service, and the Pony Express captains who organize their teams of horses and riders. Each state-line crossing is cause for celebration, and bragging rights are won for the relays that keep the mail on time or make up time when it gets behind.

FIGURE 13. Kansas ham operators follow the rider in a mobile home, supporting the ride day and night. (Source: Dennis Mason; used with permission.)

CONCLUSIONS

The Pony Express, although short lived, remains a romantic icon of the Old West frontier. The 1,900-mi (3,100-km) mail run is rerun in 10 days each year (day and night, through all weather) by teams of dozens of horses and riders, carrying the mail between Sacramento, California, and St. Joseph, Missouri. Much of the Re-Ride closely follows the original trail, and much of this remains rugged and remote, even today, with little or no cell phone coverage. Volunteer ham radio operators provide communications support throughout these remote areas, helping organize the ride by sharing where the mail-carrying rider is and providing emergency communications as needed.

Perhaps it is poetic, in an engineering sort of way. The Pony Express was the high-speed communication link of its time. It was soon outpaced by the transcontinental telegraph, only to ride again a century and a half later, supported by ham radio. In the cheer of the riders—"Go! Pony!"

AUTHOR INFORMATION

Cynthia M. Furse (cfurse@ece.utah.edu) is a professor of electrical and computer engineering at the University of Utah and a Pony Express Re-Rider. She has applied her expertise in electromagnetics to sensing and communication in complex lossy scattering media such as the human body, geophysical prospecting, ionospheric plasma, and aircraft wiring networks. She is a Fellow of the IEEE.

Charles Killian (ckillian@xmission.com) works at Dell EMC as a configuration administrator for systems that support the supply chain for products produced by Dell EMC. His current focus is on emergency communications of all kinds, serving several agencies, and microwave digital communications utilizing mesh networks. He is a Member of the IEEE.

Gerald Hasty (xp@sumofiber.net) is currently retired. His research interests include working with radios in remote locations.

Bob Nelson (nelsonrk@ix.netcom.com) has organized and participated in many exercises and real-world events as a volunteer operator. He is an American Radio Relay League Official Emergency Station and an operator in the Amateur Radio Emergency Service.

REFERENCES

[1] National Pony Express Association, "Follow the Ride." Accessed on: Aug. 29, 2019. [Online]. Available: https://nationalponyexpress.org/annual-Re-Ride/follow-the-ride/
[2] Winlink Global Radio Email. Accessed on: Aug. 29, 2019. [Online]. Available: https://www.winlink.org/

Leyre Azpilicueta, Francisco Falcone, and Ramakrishna Janaswamy
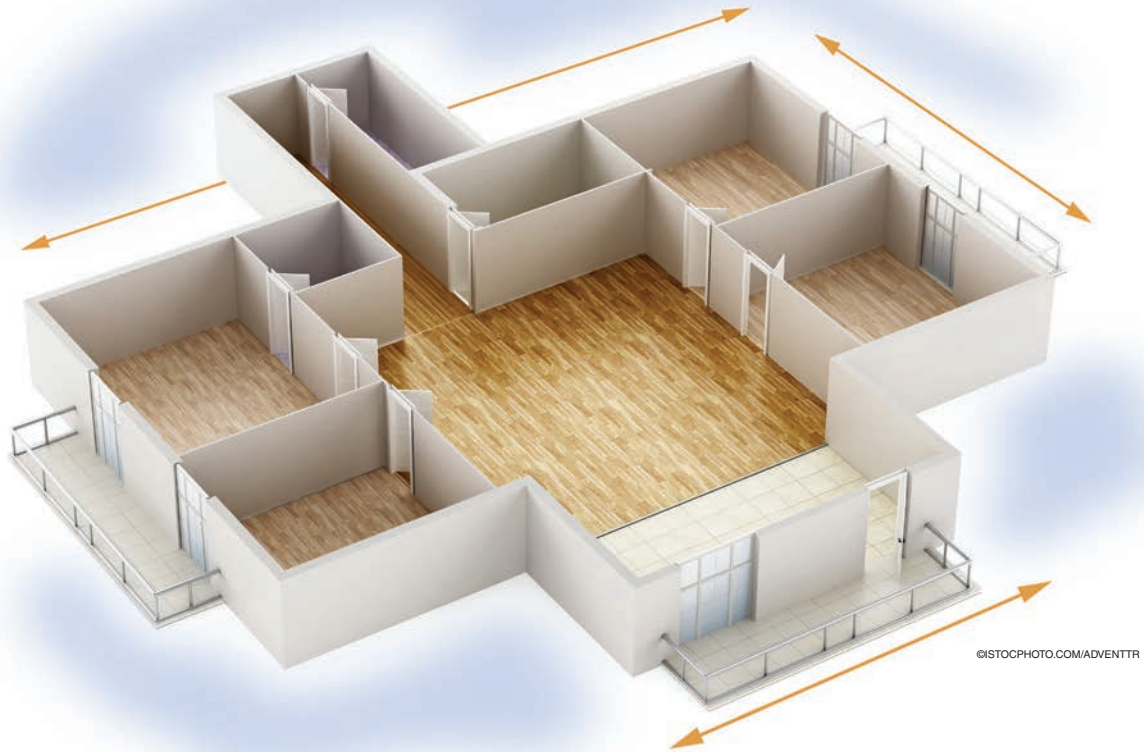
©ISTOCPHOTO.COM/ADVENTTR

Hybrid Computational Techniques

*Electromagnetic propagation analysis
in complex indoor environments.*

In this article, we compare deterministic methodologies for characterizing channel behavior in heterogeneous and composite scenarios. These techniques include one that combines a 3D ray launching (RL) approach based on geometrical optics (GO), a second based on GO and the uniform theory of diffraction (UTD), and another that includes a diffusion equation (DE) method based on the equation

of transfer. A new methodology based on the GO and DE is presented and shown to achieve accurate results when compared with real measurements. The proposed technique provides a computational time reduction of up to 90% compared to the conventional approach using GO with the UTD and DE.

LOCATING TRANCEIVERS

With the growth in demand for wireless communications systems in recent years, the need for efficient tools to characterize

electromagnetic propagation in different complex environments has increased significantly. Among the essential tools needed in one capable of determining the best locations for transceivers in a wireless communication system. This means the ability to estimate coverage/capacity relationships without having to take real measurements, which are costly and take up a lot of time. To devise tools with this estimating capability so important in designing wireless communication systems and networks, more efficient and accurate prediction propagation approaches must be developed. Such improved approaches will help in radio planning as well as in performing system-level design and optimization tasks, such as coverage/capacity analysis in heterogeneous network operation or energy efficiency analysis in wireless sensor networks [1].

Empirical methods, such as COST-231, Walfish-Bertoni, and Okumura Hata, were the first methods used to predict initial coverage [2], [3]. They are fast, in terms of computational time needed for simulation, but their results need to be calibrated based on real measurements with linear regression methods.

Meanwhile, deterministic methods [4], [5] can be divided in two groups. In the first group are methods based on full-wave simulation approaches, such as method of moment or finite difference time domain [6]. In the second group are those methods based on geometrical approximations, such as RL and ray tracing (RT) [7]. These methods deliver precise results, but the simulation computational time can be unaffordable if the analyzed scenario is complex and large. Such methods are usually used in combination with the UTD to predict radio coverage [8], [9]. It has been shown in the literature that RT and RL approaches provide a reasonable balance between accuracy and computational time, which is why they are the most used for multipath propagation prediction in urban and complex indoor environments.

Evidence in the literature demonstrates the dispersive behavior of electromagnetic waves in a discrete random medium with sufficient multiple scattering [10], [11]. Taking this into account, it is highly advantageous to consider diffuse scattering when assessing the performance of wireless electromagnetic channels.

Researchers have implemented this phenomenon in deterministic approaches. Reference [12] describes a diffuse scattering implementation in a 3D urban propagation environment. References [13] and [14], while showing the influence of diffuse scattering when analyzing narrowband and wideband characteristics, present a field prediction technique that considers reflection, diffraction, and diffuse scattering, demonstrating that diffuse scattering plays an important role in electromagnetic propagation. Reference [15] presents a novel and efficient hybrid model that is both 2D site-specific and statistical for modeling the presented mean addition of diffused scattering.

However, these approaches, depending on the precision required, may call for unreasonably costly computational complexity. Currently, researchers, taking up the challenge of reducing simulation computational time, are suggesting various speed-up approaches. Reference [16] presents a novel deterministic approach to modeling radio-wave propagation channels. With this approach, fewer transmitted rays are used in the simulation scenario, whereas intermediate points can be predicted using a neural network. In [17], several acceleration techniques to improve the storage of data and processing are shown. Some authors have worked on acceleration techniques by decomposing the 3D problem into two 2D subproblems [18], [19], whereas in [20] the methodology of splitting the 3D wave propagation into 2D planes is shown. In [21] and [22], the medium is tessellated using rectangular and triangular meshes, respectively. In [23], a database preprocessing and discretization of the environment is proposed. Finally, two methods presented in [24] aim to cut down the high number of rays and the huge input database handled by the algorithm.

In light of the earlier analysis of diverse propagation approaches, it is extremely important to consider deterministic models that convey precise results within a reasonable simulation computational time. Our analysis of different deterministic approaches leads to the conclusion that a novel and efficient hybrid GO/DE methodology to assess electromagnetic propagation in heterogeneous and composite indoor scenarios achieves the best results in terms of accuracy and simulation computational time. The proposed approach has been presented in [25]. It is an acceleration technique combining the full GO with the UTD and DE (GO/UTD/DE) approaches. This article presents different realistic scenarios in which the different approaches are applied. The novel technique delivers accurate results and is computationally more efficient when compared to the full GO/UTD/DE technique, with a rise in a mean error of 0.27 dB. Figure 1 describes the presented work, showing the advantages and disadvantages of each one of the cases analyzed.

RL APPROACH

To perform wireless channel analysis, a 3D RL algorithm has been developed in-house on GO and its extension, the UTD. The main principle of RL techniques is that, based on an addition of optic and electromagnetic theories, the radiated wave is approximated as a set of rays that propagate along the space.

Rays are launched as defined in the spherical coordinate system at an elevation angle θ and an azimuth angle ϕ. The parameters of the antenna as well as the radiation pattern are

> ### Currently, researchers, taking up the challenge of reducing simulation computational time, are suggesting various speed-up approaches.

considered. Parameters, such as frequency of operation, number of multipath reflections, angular resolution, and the dimension of cuboids, are introduced.

Each ray propagates in the space as a single optical wavefront. The electric field E created by an antenna with a radiated power P_{rad} with a directivity $D_t(\theta_t, \phi_t)$ and polarization ratio $(X^\perp, X^\|)$ at a distance r in the free space is calculated as follows by [26]:

$$E_i^\perp = \sqrt{\frac{P_{rad} D_t(\theta_t, \phi_t) \eta_0}{2\Pi}} \frac{e^{-j\beta_0 r}}{r} X^\perp L^\perp, \qquad (1)$$

$$E_i^\| = \sqrt{\frac{P_{rad} D_t(\theta_t, \phi_t) \eta_0}{2\Pi}} \frac{e^{-j\beta_0 r}}{r} X^\| L^\|, \qquad (2)$$

where $\beta_0 = 2\pi f_c \sqrt{\varepsilon_0 \mu_0}$, $\varepsilon_0 = 8.854 \times 10^{-12}$ F/m, $\mu_0 = 4\pi \times 10^{-7}$ H/m, and $\eta_0 = 120\pi$ Ω. f_c is the transmission frequency and $L^{\perp\|}$ is the path loss coefficients for each polarization. When this ray finds an object in its path, two new rays are created: a reflected ray and a transmitted ray. These rays have new angles provided by Snell's law [27].

A full 3D scenario is created before simulation in which objects, walls, transmitters (Tx), receivers (Rx), and the complete set of elements within the simulation environment are considered. A volumetric grid is implemented that stores the different parameters and characteristics of each ray propagating in the space. In consequence, the whole area is separated into several cuboids of fixed dimensions. When a ray enters a specific cuboid, its parameters are saved in a matrix. Dispersive material properties within the considered frequency range for all of the elements within the scenario are also taken into account.

RL MODELING WITH EDGE CONTRIBUTIONS

One of the main problems of the GO-only approach is that it cannot estimate correctly the received field in shadow areas originated by edges or discontinuities of the obstacles in the scenario (Figure 2). The reason this approach cannot estimate correctly in such cases is because the GO-only approach only accounts for the direct, reflected, and refracted rays heading to unexpected areas that correspond to the boundaries where these rays exist. To explain this diffraction phenomenon, Keller [28] stated that, when GO rays leave the edge of the obstacles, they are diffracted rays, and they follow the rules of the generalized Fermat's principle [29]. However, where the GO rays present discontinuities, this formulation had inaccuracies in shadow and reflection regions. To solve these problems, uniform solutions to the asymptotic expressions were used. The first one is the UTD developed by Kouyoumjian and Pathak [30] from the asymptotic expansion by Pauli Clemmow [31]. The second one is the uniform asymptotic solution (UAT) obtained by Lee and Deschamps [32]. The UAT obtains the fields by removing two terms with infinite
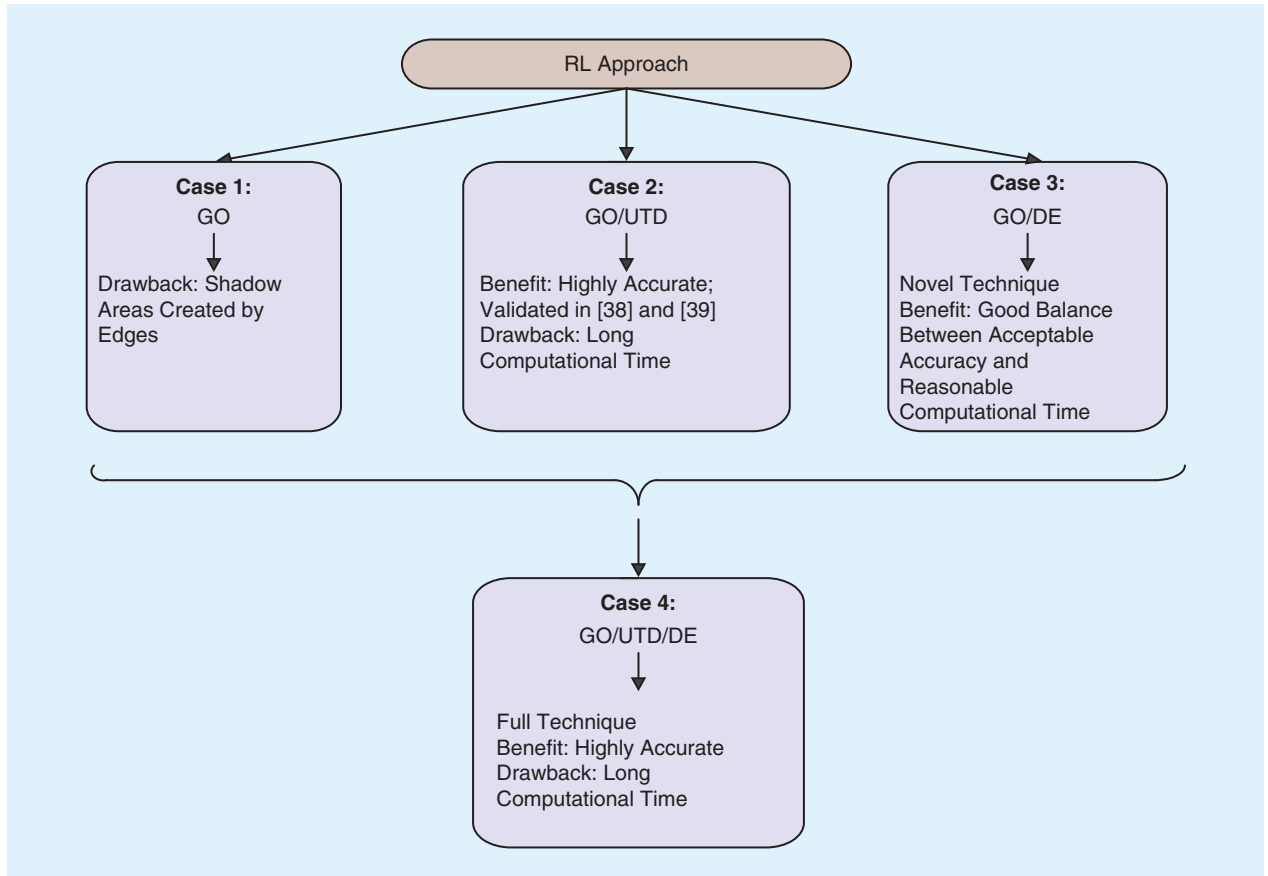
FIGURE 1. A diagram showing scheme with the different deterministic approaches under consideration and the benefits and drawbacks of each one.

values at the shadow borders, while the UTD is numerically easier to be implemented.

The GO/UTD approach has been widely used to predict mobile communication propagation for both urban [33], [34] and indoor [35], [36] environments. In the software developed in house, the UTD has been implemented by computing the diffraction coefficients on the edges of the diffractive elements with the finite conductivity 2D diffraction coefficients given by [37] as follows:

$$D^{\|\perp} = \frac{-e^{(-j\pi/4)}}{2n\sqrt{2\pi k}} \left\{ \begin{array}{l} \cot\left(\frac{\pi+(\Phi_2-\Phi_1)}{2n}\right)F(kLa^+(\Phi_2-\Phi_1)) \\ +\cot\left(\frac{\pi-(\Phi_2-\Phi_1)}{2n}\right)F(kLa^-(\Phi_2-\Phi_1)) \\ +R_0^{\|\perp}\cot\left(\frac{\pi-(\Phi_2+\Phi_1)}{2n}\right)F(kLa^-(\Phi_2+\Phi_1)) \\ +R_n^{\|\perp}\cot\left(\frac{\pi+(\Phi_2+\Phi_1)}{2n}\right)F(kLa^+(\Phi_2+\Phi_1)) \end{array} \right\}$$

(3)

where $n\pi$ is the wedge angle; F, L, and $a\pm$ are defined in [37]; and $R_{0,n}$ is the reflection coefficient for the respective polarization for the 0 face or n face. Figure 3 shows Φ_2 and Φ_1 angles in (3).

The diffracted field is calculated by (4) as follows:

$$E_{\text{UTD}} = e_0 \frac{e^{-jks_1}}{s_1} D^{\perp\|} \sqrt{\frac{s_1}{s_2(s_1+s_2)}} e^{-jks_2},$$

(4)

where $D^{\perp\|}$ is the diffraction coefficient in (3) and s_1, s_2 corresponds with the distances source-edge and edge-Rx point, respectively, as represented in Figure 3. The path loss propagation is considered at each spatial point of the 3D scenario, considering the losses of propagation due to different material properties, at different distances d, with an attenuation constant α(Np/m), and a phase constant β(rad/m). The total field is calculated considering all of the incident vectorial fields inside each cuboid of the defined spatial mesh. Thus, the main principle of the RL techniques is that, for a given carrier frequency, at a specific bandwidth, where the materials are assumed to be spatially homogeneous and temporally nondispersive in the band of interest, the impulse response of the channel can be determined. Consequently, considering this information, the entire characterization of a stationary channel can be done.

The proposed simulation code has been extensively tested as a valid methodology to characterize electromagnetic propagation in complex scenarios [38], [39], interference analysis [40], or electromagnetic dosimetry evaluation in wireless systems [41]. It has been demonstrated that the principle of GO/UTD gives precise radio-wave propagation results when a whole 3D environment is considered. Nevertheless, the significant disadvantage of the algorithm is the high and perhaps unaffordable computational simulation time needed for complex and large scenarios. To manage this issue and achieve precise results within an affordable computational simulation time, the GO/DE technique has been analyzed and compared for different realistic scenarios. The technique has achieved good results. The DE technique neglects the edge contributions and considers absorption and scattering electromagnetic phenomena caused by the obstacles. The main

purpose of this article is to validate the power prediction tool in different complex and large scenarios and to demonstrate that it achieves precise results within an affordable computational time. The following methodology compares the GO/DE method with the complete GO/UTD/DE technique (which considers all electromagnetic phenomena) in terms of accuracy and simulation time required. We show that the novel approach gives precise results while reducing simulation time.

DE APPROACH

RL MODELING WITH DE

Evidence in the literature shows that in discrete random media with enough multiple scattering, electromagnetic waves have a diffusive behavior. Under the assumption of uniform scattering, the DE simplifies the equation of transfer in the classical transport theory [42].

Following the approach described in [11], [25], and [43], a new module for implementation in the 3D RL tool has been developed. This new module is based on the DE and considers absorption and scattering losses caused by obstacles. It can be implemented in both the GO-only approach
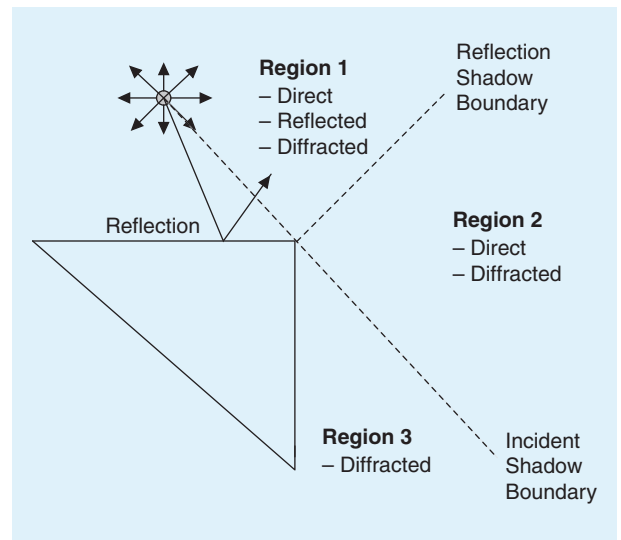
FIGURE 2. An illustration of the regions described by GO rays.
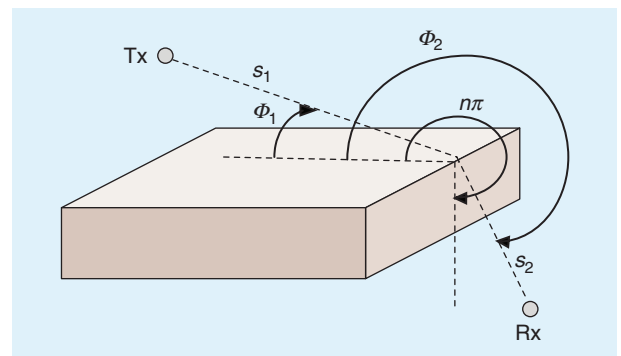
FIGURE 3. A diagram showing geometry for wedge diffraction coefficients.

and the GO/UTD technique. In this sense, the full GO/UTD/DE methodology is the most precise approach because it considers all of the electromagnetic phenomena encountered in a composite and heterogeneous scenario, i.e., reflection, refraction, diffraction, and diffuse scattering. Nevertheless, the computational simulation time of this full technique can be unaffordable for complex and large scenarios, as is demonstrated in the following sections. In this article, the comparison between different techniques for different scenarios is presented, showing that the GO/DE approach, which does not consider edge diffraction, achieves the best balance between computational time and accuracy. Although this technique does not consider edge diffraction, the following sections show that the impact of edge diffraction need not be considered if the field is averaged while considering all of the obstacles (with the respective locations and orientations) within the whole 3D environment. As a result, computational time is trimmed considerably.

The GO/DE approach has been presented in [25]. The new technique is based on the statement that if the obstacles' area

> **The DE technique neglects the edge contributions and considers absorption and scattering electromagnetic phenomena caused by the obstacles.**

density is more than 10%, then diffusion approaches can be applied to indoor scenarios [43]. The principle is that the whole 3D environment is divided in terms of horizontal and vertical 2D planes. Afterward, the 2D planes with diffusive behavior are treated with the DE methodology, considering scattering and absorption losses due to obstacles.

The statistical average of the Poynting vector magnitude at any spatial location of the 3D scenario is the notion of specific intensity, on which the DE approach is based. In 2D, the specific intensity can be described as a function of three input arguments: one angular coordinate ξ, providing the azimuthal direction of the average Poynting vector, and two spatial coordinates $\rho = (x, y) \equiv (r_a, \varphi)$, where r_a is the radial distance and φ is the azimuthal angle. The specific intensity, after normalization, is given by $I(\rho, \xi) = U_d(\rho) + \hat{s} \cdot \vec{F}(\rho)/\pi$, where U_d is the average intensity (in units of watts per meter), the flux density vector (in units of watts per meter) is $\vec{F}$ and $\hat{s} = \hat{x} \cos \xi + \hat{y} \sin \xi$. Their relationship is given by the following:

$$U_d(\rho) = \frac{1}{2\pi} \int_0^{2\pi} I(\rho, s) d\xi, \qquad (5)$$

$$\vec{F}(\rho) = \frac{1}{2\pi} \int_0^{2\pi} \hat{s} I(\rho, s) d\xi. \qquad (6)$$

Following the formulation stated in [11], which is based on transport theory, the excess loss on a decibel scale can be expressed as follows:

$$L_{\text{ex}}^T(r_a) \sim \frac{10\sqrt{2}\, \sigma_g p_0 \log e}{A_0} r_a - 5 \log \left(\frac{\pi p_0 \sigma_g r_a}{\sqrt{2}\, A_0} \right), \qquad (7)$$

where p_0 is the density of the obstacles in the space, A_0 is the average obstacle cross-sectional area, σ_g [m] is the geometrical cross section of the obstacles per unit length, and r_a is the radial distance between the Tx and the Rx.

For those horizontal or vertical planes that behave diffusively, the DE model has been applied (Figure 4). As stated in the section "RL Approach," the whole 3D scenario is divided into a grid, leading to a number of cuboids of fixed size. In the algorithm, we can define cuboid volume as input parameters. Depending of this cuboid's size, the vertical and horizontal 2D planes are created, which could be different depending on the layout of the entire scenario. The methodology has included calculations of the obstacle density for each 2D vertical and horizontal plane. The obstacle density is calculated by the area occupied by obstacles per total area of the region of interest. Afterward, the planes with an obstacle area density greater than 10% have been treated with DE.
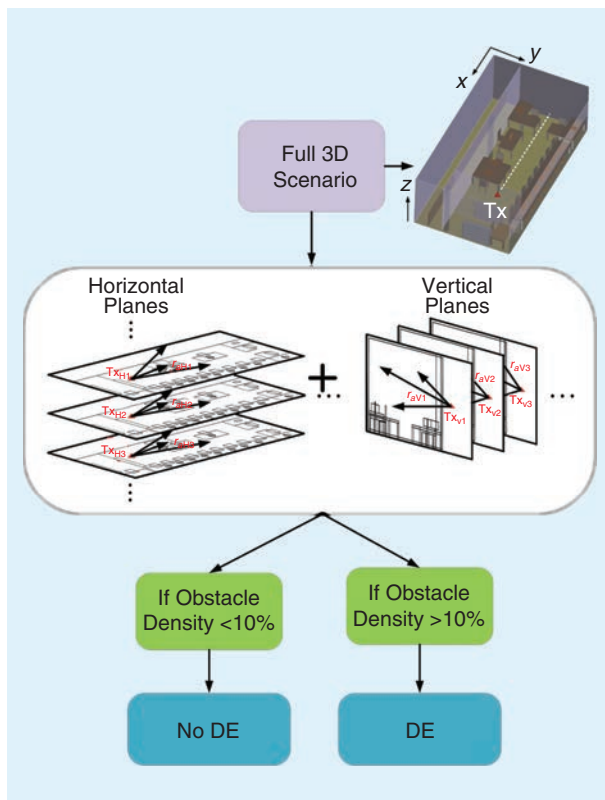
FIGURE 4. A diagram showing schematic view of the new approach.

Considering the large size of obstacles when compared to the investigated wavelength, it can be assumed that the transmission and absorption cross sections are approximately equal to the geometric cross section [42].

FIGURE 5. An aerial view of the scenarios under consideration: (a) typical office environment, (b) first floor of a house, and (c) floor with several meeting rooms and offices. To facilitate illustration, ceilings are not shown.

SIMULATION RESULTS AND VALIDATION OF THE ALGORITHM

First, different simulations of typical complex indoor environments were done with the different approaches. The scenarios we considered (Figure 5) were (a) an office environment, (b) eight rooms on the first floor of a house, and (c) a floor with several meeting rooms and offices. These three scenarios were chosen because they represent typical complex indoor environments. All scenarios have several obstacles, i.e., tables of different dimensions and shapes, chairs, furniture, computers, shelves, and so on. The dimensions of the scenarios are $13 \times 7 \times 4.2$ m for (a), $9 \times 7.25 \times 2.6$ m for (b), and $29.5 \times 20.45 \times 3.8$ m for (c). The simulations accounted for every obstacle within each scenario as well as the walls of different materials, with a wall thickness of 10 cm for the three cases, which are also shown in the schematic view of the scenarios. The major obstacles in the first scenario are the tables and chairs as well as the personal computers on the tables, while in the second scenario, more walls are considered because the space is divided into many rooms. Different types of furniture with different material properties are also considered. The third scenario, compared to the other two, has more walls and more metallic structures, such as the lift. Roughness of surfaces have not been considered. The values of permittivity and conductivity employed in the simulated scenarios are defined in Table 1 [45].

Table 2 presents the considered simulation input parameters for the GO/UTD/DE approach. A different resolution for the cuboids has been chosen according to a convergence analysis of cuboid size in comparison with the dimensions of the scenarios [45]. The cuboid mesh resolution of the different scenarios generates a different number of planes in the xy-, yz-, and xz-planes, which are presented in Table 3, along with the number of planes with an obstacle density larger than 10%. In the case of the first scenario (office environment), only the horizontal plane that considers tables and chairs exceeds the obstacle area density of 10%, with an obstacle density in this particular plane of 15.49%. For the house, several planes exceed the obstacle density of 10%. In these 2D horizontal and vertical planes, DEs have been applied to obtain precise results for those planes. The third scenario does not have any plane with an obstacle density greater than 10%. Because of that, it has been treated also with DEs to show that in this case the mean error is larger when the DE is applied to those

TABLE 1. RL MATERIAL PROPERTIES.		
Parameters	**Permittivity (ε_r)**	**Conductivity (σ) [S/m]**
Air	1	0
Plywood	2.88	0.21
Brick wall	4.11	0.0364
Glass	6.06	10^{-12}
Concrete	5.66	0.142
Metal	4.5	4×10^7
Polycarbonate	3	0.2

IEEE ANTENNAS & PROPAGATION MAGAZINE // DECEMBER 2019   **25**

planes with a density less than 10%. Thus, only those planes with an obstacle density larger than 10% must be treated with the DE approach [43].

The impact of furniture in the office environment was assessed. Furniture is a big factor in weakening the signal. Figures 6–8 show the xy-planes of received power for a height of 0.8 m. For these simulations, the full GO/UTD/DE approach was used. Results show how much furniture influences radio-wave propagation: more obstacles result in greater interference.

Figure 9 shows the received power distribution as a function of obstacle density variation along the x-axis at $y = 5.75$ m. As expected, higher fading losses are observed as the propagating paths encounter higher furniture density.

The objective is to assess the impact of the scattering in this complex indoor scenario. For that purpose, several simulations were developed with the implementation of DE modeling. Then, a comparison was been made between the GO-only approach, the GO approach with edge contributions, and the full GO/UTD/DE method. The comparison of received power for the different techniques along the x-axis for $y = 4.5$ m is shown in Figure 10, which presents the comparison between GO-only approach, the GO/UTD approach, the GO/DE approach, and the full GO/UTD/DE approach. It can be seen that the edge contributions of the GO/UTD and GO/UTD/DE techniques can enhance the channel performance in certain points as the received power is higher on the whole than with the GO/DE approach. However, the scattering and absorption due to obstacles, which is always present in practical situations, reduces the received power in almost every spatial point of the space. In light of this, we see the importance of accounting for the scattering phenomena to achieve precise results to characterize adequately the wireless channel.

TABLE 2. SIMULATION PARAMETERS IN THE RL SOFTWARE.

Frequency	2.4 GHz
Tx power	0 dBm
Antenna gain	5 dBi
Horizontal plane angle resolution ($\Delta\Phi$)	1°
Vertical plane angle resolution ($\Delta\theta$)	1°
Reflections	7
Cuboid resolution	5 cm / 30 cm / 1 m

dBm: decimal-milliwatts.

TABLE 3. THE NUMBER OF PLANES GENERATED BY THE CUBOID MESH RESOLUTION.

Scenario	Cuboid Mesh Resolution			Obstacle Density
	xy-Planes	yz-Planes	xz-Planes	
Office environment	84	260	140	>10% in one plane
One-story house	9	25	31	>10% in several planes
Floor with several rooms	4	21	30	<10% in all planes

FIGURE 7. An xy-plane of received power (dBm) for 0.8-m height considering only the tables in the office environment.

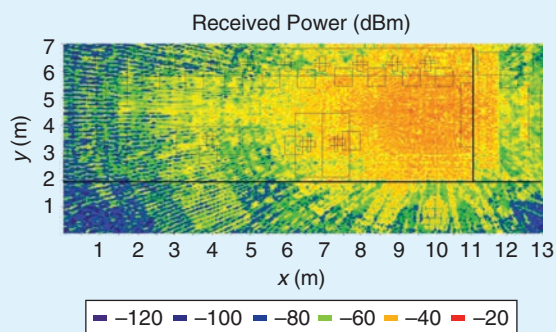**FIGURE 6.** An xy-plane of received power (dBm) for 0.8-m height accounting for all of the furniture in the office environment.
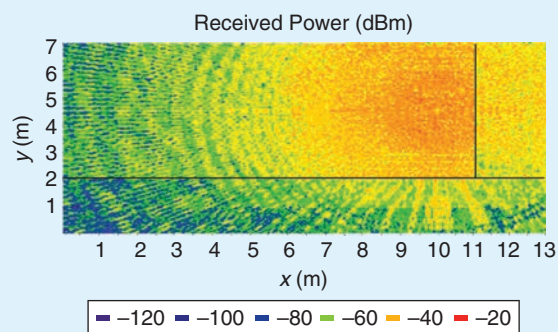
FIGURE 8. An xy-plane of received power (dBm) for 0.8-m height without obstacles in the office environment.

It can also be observed from Figure 10 that the GO-only approach predicts higher levels of received power along the entire radial. However, the full method, which accounts for all electromagnetic phenomena, predicts lower values and is more accurate because it considers more losses mainly due to scattering and diffraction. The figure also depicts the location of obstacles, given by the vertical dashed lines, in which larger variability in estimated losses can be observed.
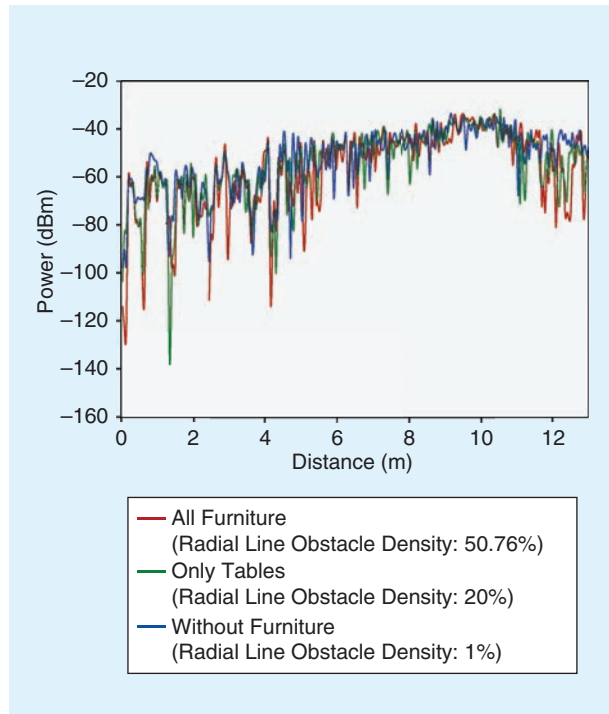
FIGURE 9. The distribution of received power for the three cases considered: all furniture (red), only tables (green), and without furniture (blue) in the office environment.
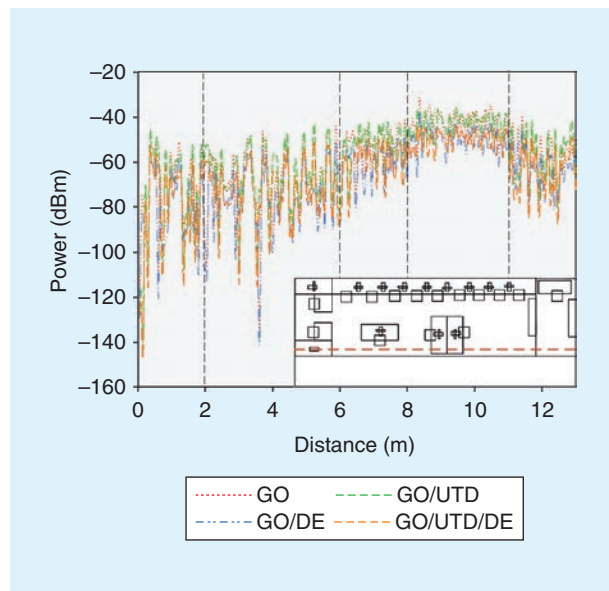
FIGURE 10. The comparison between received power lines in dBm for the GO-only approach, the GO/UTD approach, the GO/DE approach, and the full GO/UTD/DE approach in the office environment.
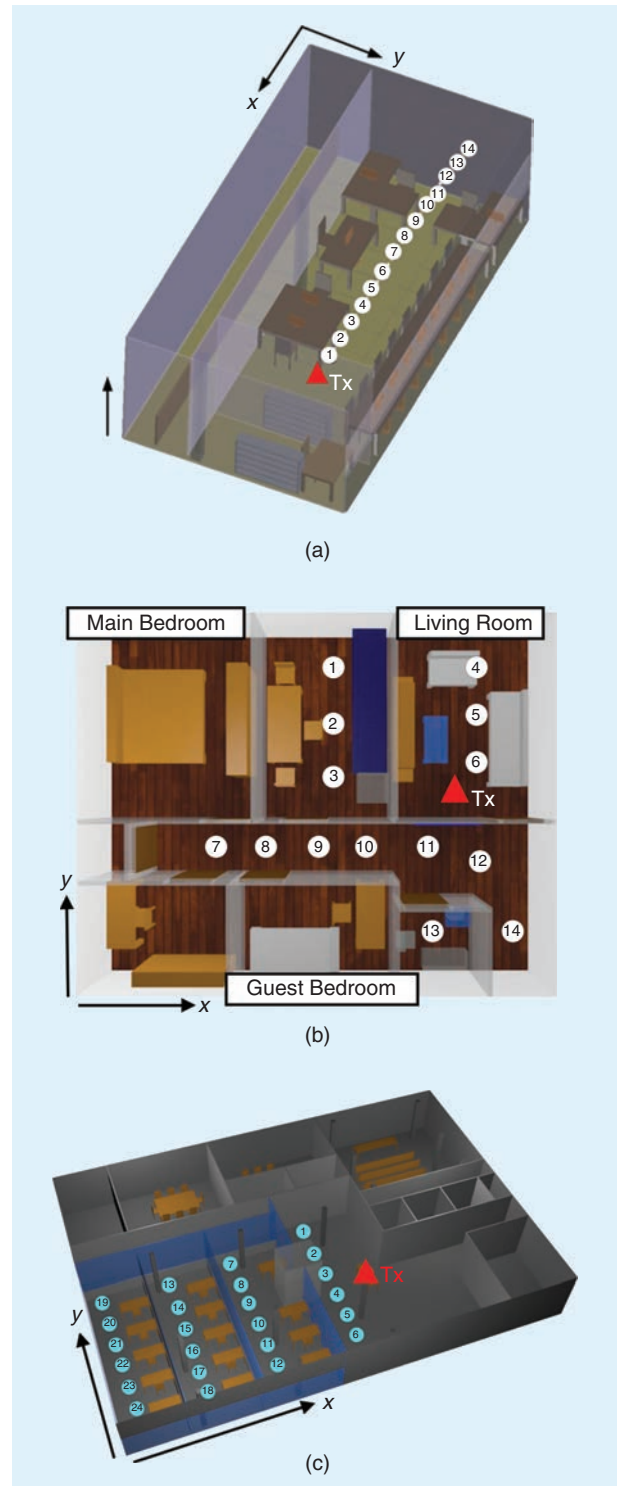
FIGURE 11. The measurement points for the scenarios considered: (a) office environment, (b) one-story house, and (c) floor with different rooms with the position of the Tx.

MEASUREMENT RESULTS AND DISCUSSION

Real measurements were made for each of the three scenarios to validate the results. For that purpose, a Tx antenna was connected to a signal generator at 2.4 GHz. The Tx antenna was been placed at the coordinates depicted with a red triangle in
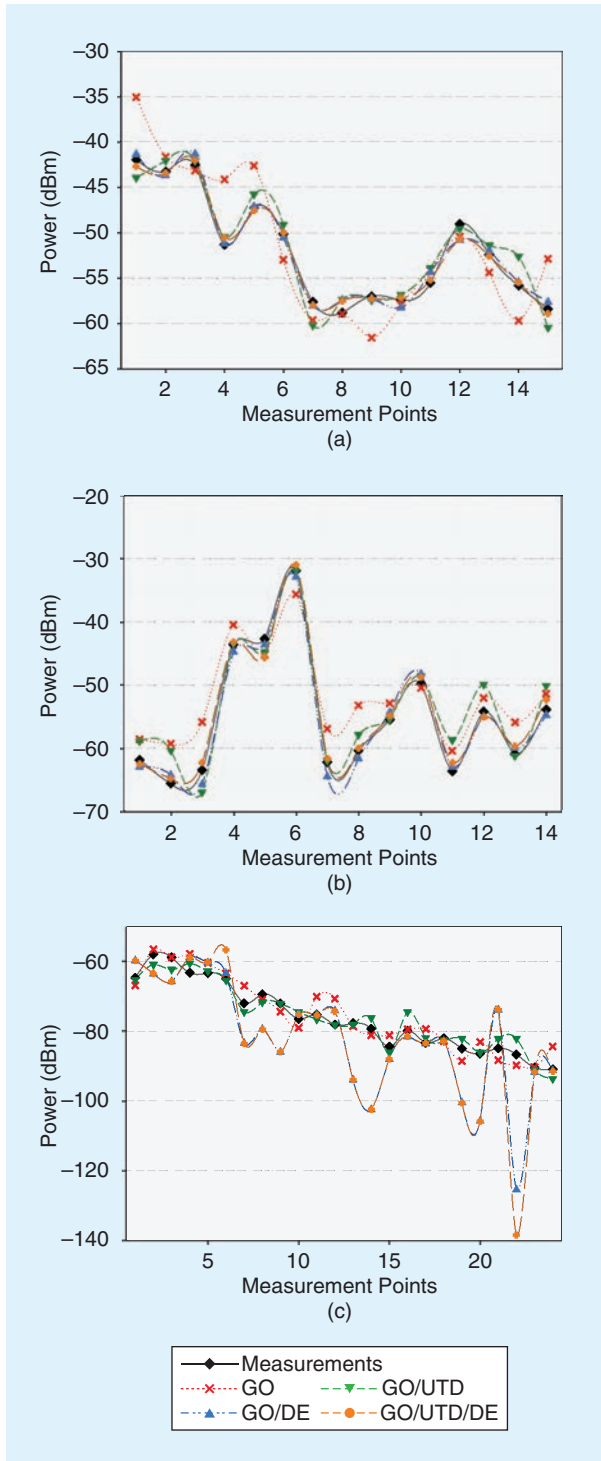
FIGURE 12. The comparison between the 3D RL simulation results and real measurements for 2.4 GHz frequency for the different simulation approaches: (a) office environment, (b) one-story house, and (c) floor with several rooms.

Figure 11 in the three scenarios considered. A portable Agilent N1996A was used as a signal generator and an Agilent N9912 Field Fox was the spectrum analyzer. Both transmitting and receiving antennas were omnidirectional antennas (Picea 2.4-GHz swivel antennas from Antenanova). Measurements were performed in the measurement points represented in Figure 11 for the three scenarios at a height of 0.80 m in all three cases.

Simulation and measurement results for the different simulation techniques are represented in Figure 12 for the first two scenarios, which have planes with obstacle densities higher than 10%, and for the third scenario, which has an obstacle density lower than 10%. For the three scenarios considered, the bandwidth considered for the measurements was 100 MHz and the measurement time was 60 s at each spatial point, considering the peak power detected values. The comparison has been made for the same spatial samples with the received power estimated by simulation and by the real measurements. From Figure 12, it can be seen that all of the proposed methods follow the received power measurement trend. Nevertheless, in the third scenario, the approaches considering the DE are not precise because the obstacle density is less than 10%.

Table 4 shows the mean error and standard deviation between the different approaches and real measurements for the three considered scenarios: the first two with planes with an obstacle density larger than 10% and the third one with obstacle density less than 10%. It can be seen that the full GO/UTD/DE technique is the most accurate for the first two cases with a mean error of 0.62 dB and a standard deviation of 0.73 dB for the office environment and a mean error of 1.01 dB and a standard deviation of 0.65 dB for the house. However, it is observed that in these two scenarios, for the GO/DE approach, the mean error only increased by 0.27 dB in the case of the office environment and by 0.22 dB in the case of the house, while the computational time is reduced 40 and 90% respectively, with respect to the full GO/UTD/DE approach.

Figure 13 shows the computational time required for the four techniques in each of the three scenarios. It can be seen from Figure 13 that the inclusion of the analysis of the diffracted rays takes a lot of time. However, the novel GO/DE technique, which does not account for the impact of edges because it considers the averaged received power field due to the different obstacles in the whole 3D environment, produced reasonable results. Table 4 also shows the mean error and standard deviation for the third scenario, which does not have any plane with an obstacle density larger than 10%. It can be seen that the mean error and standard deviation for the full GO/UTD/DE approach and the novel GO/DE technique increase significantly in this third scenario. Thus, the DE approach does not work in this scenario, with planes with obstacle densities less than 10%, as is shown in [43]. It can be concluded that it is highly important to achieve a good tradeoff between precision of the results and simulation computational time when these hybrid approaches are employed. The novel GO/DE technique is precise enough for complex indoor environments while saving a considerable amount of

TABLE 4. THE MEAN ERROR AND STANDARD DEVIATION FOR THE DIFFERENT APPROACHES.

Scenario	Obstacle Density	CASE 1: GO		CASE 2: GO+UTD		CASE 3: GO+DE		CASE 4: GO+UTD+DE	
		Mean Error (dB)	Standard Deviation (dB)	Mean Error (dB)	Standard Deviation (dB)	Mean Error (dB)	Standard Deviation (dB)	Mean Error (dB)	Standard Deviation (dB)
Office	>10%	3.01	2.30	1.37	0.81	0.89	0.96	0.62	0.73
One-story house	>10%	2.30	2.04	1.30	1.91	1.23	0.49	1.01	0.65
Floor with several rooms	<10%	2.86	1.98	1.89	1.44	8.29	9.27	9.09	11.19
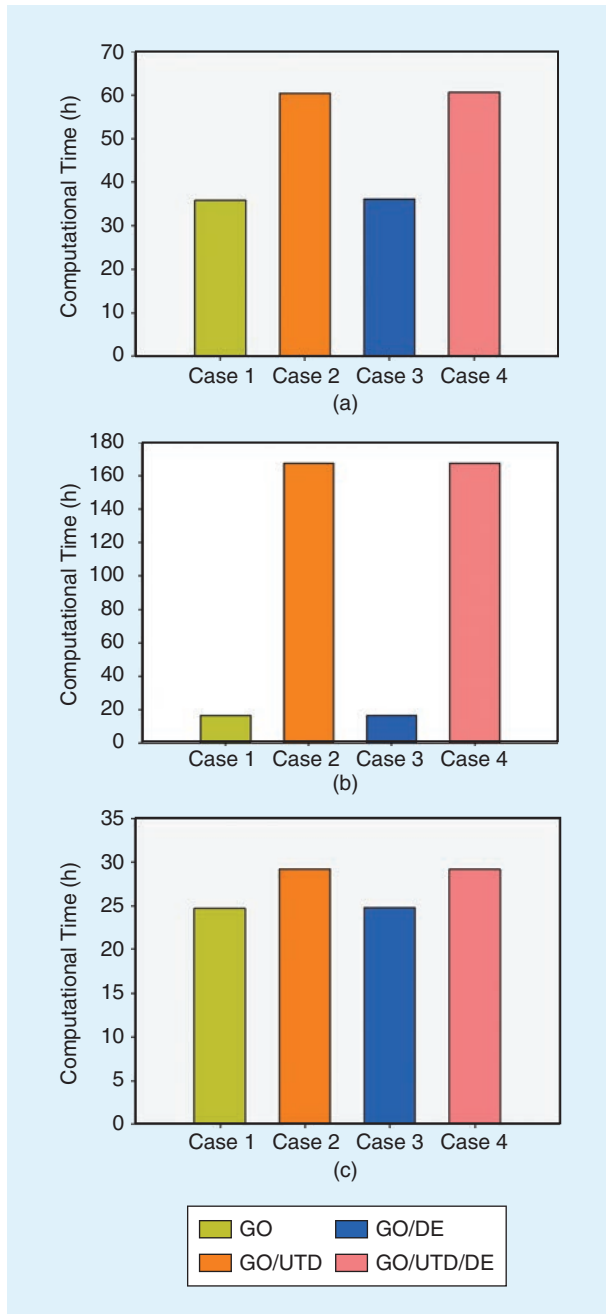
FIGURE 13. The computational time required for the complete simulation of the considered scenarios for the different simulation approaches: (a) office environment, (b) one-story house, and (c) floor with several rooms.

computational time when compared with the full GO/UTD/DE approach.

CONCLUSIONS

In this article, a new technique that combines a 3D RL with a DE (GO/DE) method based on the transport equation has been presented and validated in different realistic complex indoor environments. The new approach has been compared with the reference solution, GO with edge contributions and DE (GO/UTD/DE), in different simulations of real scenarios. The results show that, when applying the combined approaches, there is a small increase in mean error values, in the order of 1 dB. The new approach decreases simulation time by up to 90% while delivering accuracy levels comparable to the other approaches. Through reduced computational costs, the proposed hybrid methodology is practical for wireless channel characterization and hence coverage/capacity estimations in large, complex scenarios, such as large node density distributions of transceivers for context-aware environments including, for example, applications related to the Internet of Things and smart cities/smart regions.

Currently, a full 3D approach of scattering and absorption losses handled by the DE is being considered, with the aim of not needing to take the orthogonal 2D planes into account. This will be presented in future work.

ACKNOWLEDGMENT

AUTHOR INFORMATION

Leyre Azpilicueta (leyre.azpilicueta@tec.mx) is an associate professor and researcher at Tecnologico de Monterrey, Campus Monterrey, Mexico. Her research interests include radio propagation, mobile radio systems, ray tracing, and channel modeling. She is a Member of the IEEE.

Francisco Falcone (francisco.falcone@unavarra.es) is an associate professor at the Public University of Navarre (UPNA) and a researcher at the Institute for Smart Cities-UPNA, Spain. His research interests include artificial electromagnetic media, complex electromagnetic scenarios, and wireless system analysis. He is a Senior Member of the IEEE.

Ramakrishna Janaswamy (janaswamy@ecs.umass.edu) is a professor in the Department of Electrical & Computer

Engineering, University of Massachusetts, Amherst. His research interests include deterministic and stochastic radiowave propagation modeling, analytical and computational electromagnetics, antenna theory and design, and wireless communications. He is a Fellow of the IEEE.

REFERENCES

[1] T. Rappaport, *Wireless Communications: Principles and Practice* (Communications Engineering and Emerging Technologies Series), 2nd ed. Upper Saddle River, NJ: Prentice Hall, 2002.

[2] J. Kivinen, X. Zhao, and P. Vainikainen, "Empirical characterization of wideband indoor radio channel at 5.3 GHz," *IEEE Trans. Antennas Propag.*, vol. 49, no. 8, pp. 1192–1203, Aug. 2001.

[3] G. Durgin, T. S. Rappaport, and X. Hao, "Measurements and models for radio path loss and penetration loss in and around homes and trees at 5.85 GHz," *IEEE Trans. Commun.*, vol. 46, no. 11, pp. 1484–1496, Nov. 1998.

[4] M. I. S. Chowdhury, W. Zhang, and M. Kavehrad, "Combined deterministic and modified Monte Carlo method for calculating impulse responses of indoor optical wireless channels," *J. Lightw. Technol.*, vol. 32, no. 18, pp. 3132–3148, Sept. 15, 2014.

[5] V. Degli-Esposti et al., "A semi-deterministic model for outdoor-to-indoor prediction in urban areas," *IEEE Antennas Wireless Propag. Lett.*, vol. 16, pp. 2412–2415, June 2017.

[6] Y. Wu, Z. Chen, W. Fan, J. Wang, and J. Li, "A wave-equation-based spatial finite-difference method for electromagnetic time-domain modeling," *IEEE Antennas Wireless Propag. Lett.*, vol. 17, no. 5, pp. 794–798, May 2018.

[7] I. P. Shkarofsky and S. B. Nickerson, "Computer modeling of multipath propagation: Review of ray-tracing techniques," *Radio Sci.*, vol. 17, no. 5, pp. 1133–1158, Sept.–Oct. 1982.

[8] A. G. Kanatas and P. Constantinou, "A propagation prediction tool for urban mobile radio systems," *IEEE Trans. Veh. Technol.*, vol. 49, no. 4, pp. 1348–1355, July 2000.

[9] K. W. Kim and S. J. Oh, "Geometric optics-based propagation prediction model in urban street canyon environments," *IEEE Antennas Wireless Propag. Lett.*, vol. 15, pp. 1128–1131, Oct. 2016.

[10] D. Ullmo and H. U. Baranger, "Wireless propagation in buildings: A statistical scattering approach," *IEEE Trans. Veh. Technol.*, vol. 48, no. 3, pp. 947–955, 1999.

[11] R. Janaswamy, "An indoor pathloss model at 60 GHz based on transport theory," *IEEE Antennas Wireless Propag. Lett.*, vol. 5, pp. 58–60, Mar. 2006.

[12] Y. Corre and Y. Lostanlen, "Three-dimensional urban EM wave propagation model for radio network planning and optimization over large areas," *IEEE Trans. Veh. Technol.*, vol. 58, no. 7, pp. 3112–3123, Sept. 2009.

[13] E. M. Vitucci, F. Mani, V. Degli-Esposti, and C. Oestges, "Polarimetric properties of diffuse scattering from building walls: Experimental parameterization of a ray-tracing model," *IEEE Trans. Antennas Propag.*, vol. 60, no. 6, pp. 2961–2969, June 2012.

[14] F. Fuschini, H. El-Sallabi, V. Degli-Esposti, L. Vuokko, D. Guiducci, and P. Vainikainen, "Analysis of multipath propagation in urban environment through multidimensional measurements and advanced ray tracing simulation," *IEEE Trans. Antennas Propag.*, vol. 56, no. 3, pp. 848–857, Mar. 2008.

[15] J. H. Tarng, R.-S. Chang, J.-M. Huang, and Y.-M. Tu, "A new and efficient hybrid model for estimating space diversity in indoor environment," *IEEE Trans. Veh. Technol.*, vol. 49, no. 2, pp. 457–466, Mar. 2000.

[16] L. Azpilicueta, M. Rawat, K. Rawat, F. Ghannouchi, and F. Falcone, "A ray launching-neural network approach for radio wave propagation analysis in complex indoor environments," *IEEE Trans. Antennas Propag.*, vol. 62, no. 5, pp. 2777–2786, May 2014.

[17] F. Saez de Adana, O. Gutierrez Blanco, I. Gonzalez Diego, J. Perez Arriaga, and M. F. Catedra, "Propagation model based on ray tracing for the design of personal communication systems in indoor environments," *IEEE Trans. Veh. Technol.*, vol. 49, no. 6, pp. 2105–2112, Nov. 2000.

[18] J. P. Rossi, J. P. Barbot, and A. J. Levy, "Theory and measurement of the angle of arrival and time delay of UHF radiowaves using a ring array," *IEEE Trans. Antennas Propag.*, vol. 45, no. 5, pp. 876–884, May 1997.

[19] Y. Corre and Y. Lostanlen, "Three-dimensional urban EM wave propagation model for radio network planning and optimization over large areas," *IEEE Trans. Veh. Technol.*, vol. 58, no. 7, pp. 3112–3123, Sept. 2009.

[20] H. M. El-Sallabi, G. Liang, H. L. Bertoni, I. T. Rekanos, and P. Vainikainen, "Influence of diffraction coefficient and corner shape on ray prediction of power and delay spread in urban microcells," *IEEE Trans. Antennas Propag.*, vol. 50, no. 5, pp. 703–712, May 2002.

[21] C. H. Durney, D. A. Christensen, and R. W. Grow, "A mathematical technique for an exact small-signal field analysis of multiple-stream interaction in a finite longitudinal magnetic field," *IEEE Trans. Electron Devices*, vol. 16, no. 7, pp. 609–615, July 1969.

[22] Z. Zhijun and Y. Wei, "Damage of interconnects by electromigration induced surface evolution," *Tsinghua Sci. Technol.*, vol. 2, no. 2, pp. 574–577, June 1997.

[23] G. Wolfle, R. Wahl, P. Wertz, P. Wildbolz, and F. Landstorfer, "Deterministic propagation model for the planning of hybrid urban and indoor scenarios," in *Proc. 2005 IEEE 16th Int. Symp. Personal, Indoor and Mobile Radio Communications*, Berlin, pp. 659–663.

[24] F. Fuschini, E. M. Vitucci, M. Barbiroli, G. Falciasecca, and V. Degli-Esposti, "Ray tracing propagation modeling for future small-cell and indoor applications: A review of current techniques," *Radio Sci.*, vol. 50, no. 6, pp. 469–485, June 2015.

[25] L. Azpilicueta, F. Falcone, and R. Janaswamy, "A hybrid ray launching-diffusion equation approach for propagation prediction in complex environments," *IEEE Antennas Wireless Propag. Lett.*, vol. 16, pp. 214–217, May 2017.

[26] A. Cardama, *Antenas*, Barcelona, Spain: Edicions UPC, 1993.

[27] H. D. Hristov, R. Feick, W. Grote, and P. Fernandez, "Indoor signal focusing by means of Fresnel zone plate lens attached to building wall," *IEEE Trans. Antennas Propag.*, vol. 52, no. 4, pp. 933–940, Apr. 2004.

[28] J. Keller, "Diffraction of a convex cylinder," *IRE Trans. Antennas Propag.*, vol. 4, no. 3, pp. 312–321, July 1956.

[29] I. Kupiec, L. B. Felsen, S. Rosenbaum, J. B. Keller, and P. Chow, "Reflection and transmission by a random medium," *Radio Sci.*, vol. 4, no. 11, pp. 1067–1077, Nov. 1969.

[30] M. C. Liang, C. W. Chuang, and P. H. Pathak, "A generalized uniform geometrical theory of diffraction ray solution for the diffraction by a wedge with convex faces," *Radio Sci.*, vol. 31, no. 4, pp. 679–691, July–Aug. 1996.

[31] H. G. Booker and P. C. Clemmow, "A relation between the Sommerfeld theory of radio propagation over a flat earth and the theory of diffraction at a straight edge," *J. Inst. Electr. Eng.*, vol. 1950, no. 3, pp. 78–79, Mar. 1950.

[32] G. Deschamps, J. Boersma, and S.-W. Lee, "Three-dimensional half-plane diffraction: Exact solution and testing of uniform theories," *IEEE Trans. Antennas Propag.*, vol. 32, no. 3, pp. 264–271, Mar. 1984.

[33] K. Allsebrook and J. D. Parsons, "Mobile radio propagation in British cities at frequencies in the VHF and UHF bands," *IEEE Trans. Veh. Technol.*, vol. 26, no. 4, pp. 313–323, Nov. 1977.

[34] F. Ikegami, T. Takeuchi, and S. Yoshida, "Theoretical prediction of mean field strength for urban mobile radio," *IEEE Trans. Antennas Propag.*, vol. 39, no. 3, pp. 299–302, Mar. 1991.

[35] C. Tornevik, J. E. Berg, F. Lotse, and M. Madfors, "Propagation models, cell planning and channel allocation for indoor applications of cellular systems," in *Proc. IEEE 43rd Vehicular Technology Conf.*, Secaucus, NJ, 1993, pp. 867–870.

[36] S. Y. Seidel, T. S. Rappaport, and R. Singh, "Path loss and multipath delay statistics in four European cities for 900 MHz cellular and microcellular communications," *Electron. Lett.*, vol. 26, no. 20, pp. 1713–1715, Sept. 27, 1990.

[37] R. J. Luebbers, "Comparison of lossy wedge diffraction coefficients with application to mixed path propagation loss prediction," *IEEE Trans. Antennas Propag.*, vol. 36, no. 7, pp. 1031–1034, July 1988.

[38] L. Azpilicueta et al., "Optimization and design of wireless systems for the implementation of context aware scenarios in railway passenger vehicles," *IEEE Trans. Intell. Transp. Syst.*, vol. 18, no. 10, pp. 2838–2850, Oct. 2017.

[39] L. Azpilicueta et al., "Evaluation of deployment challenges of wireless sensor networks at signalized intersections," *Sensors*, vol. 16, no. 7, p. 1140, 2016.

[40] A. Córdoba et al., "SesToCross: Semantic expert system to manage single-lane road crossing," *IEEE Trans. Intell. Transp. Syst.*, vol. 18, no. 5, pp. 1221–1233, May 2017.

[41] F. Casino, L. Azpilicueta, P. Lopez-Iturri, E. Aguirre, F. Falcone, and A. Solanas, "Optimized wireless channel characterization in large complex environments by hybrid ray launching-collaborative filtering approach," *IEEE Antennas Wireless Propag. Lett.*, vol. 16, pp. 780–783, Aug. 2017.

[42] A. Ishimaru, *Wave Propagation and Scattering in Random Media*, vol. 1. New York: Academic, 1978.

[43] J. Xu and R. Janaswamy, "On the diffusion of electromagnetic waves and applicability of diffusion equation to multipath random media," *IEEE Trans. Antennas Propag.*, vol. 56, no. 4, pp. 1110–1121, Apr. 2008.

[44] C. A. Balanis, *Advanced Engineering Electromagnetics*, vol. 205. New York: Wiley, 1989.

[45] L. Azpilicueta, P. Lopez-Iturri, E. Aguirre, C. Vargas-Rosales, A. León, and F. Falcone, "Influence of meshing adaption in convergence performance of deterministic ray launching estimation in indoor scenarios," *J. Electromagn. Waves Applicat.*, vol. 31, no. 5, pp. 544–559, 2017.

Andrej Osterman and Patrik Ritoša

Radio Propagation Calculation

*A technique using 3D Fresnel zones
for decimeter radio waves on lidar data.*

This article discusses the Fresnel radio tool (FRT) model for radio-coverage prediction based on the Fresnel-zone calculation. The 3D Fresnel zones are calculated from the transmitter (Tx) source to each cell on a raster digital map. For numerical calculation purposes, Fresnel zones are cross sectioned to a finite number of fragments. The attenuation and phase shift of each segment can be adjusted according to the obstacle type. At the target receiver (Rx) point, contributions from each fragment, represented by complex numbers, are summed and converted to a signal strength.

The input data required for the FRT calculation are digital raster maps, a digital elevation model (DEM), a digital surface model (DSM), and land cover (LC). Raster maps with a resolution of 1 m are used, obtained from lidar cloud points. The FRT model comparison and validation are performed using a real LTE mobile network on the 800-MHz band. Several supplementary results are obtained, with the most astonishing result being the relative permittivity of vegetation. The FRT is compared to other models, including the Okomura–Hata, Ericsson 9999, and Cost231.

BACKGROUND

The FRT is a new approach to the propagation model that is based on a Friis formula and Fresnel zones. It is weakly related to the group of models described in International Telecommunication Union Recommendation P.526-13 [1] (that is, diffraction models), but at the same time, the FRT belongs more to the group of deterministic models [2]–[6] than empirical ones [7], [8]. However, this approach is not like the popular method of moments, finite element method, and finite difference time domain method [9], where a very accurate space description is required (less than half the wavelength). The accuracy of the input maps that are used here are coarser than the radio wavelength; strictly speaking, the size scale of the wavelength is in decimeters, and that of the

maps is in meters. The Friis formula serves as the basis of the FRT model. A new factor is appended to it, which represents the 3D Fresnel zones bounded between the Tx and Rx. Rays in the shape of a Fresnel ellipsoid suffuse the objects. On the Rx side, all of the rays are summed as complex numbers.

A majority of the propagation models treats objects as opaque for radio waves. In contrast, the FRT considers objects as transparent with two properties: attenuation and phase shift, both of which must be set for each type of object. For the sake of simplicity, only three object categories are included in this article: vegetation, buildings, and the ground. The phase shift is closely related to the permittivity of the objects. Comparing the propagation model with real measurements by seeking the minimum error enables the attenuation per meter and object permittivity to be obtained.

Although it appears that the FRT is similar to ray-tracing models [10]–[12], that is not quite true. Ray-tracing models consider the phenomenon of reflection; that is, rays are reflected from objects. However, each FRT ray is outstretched between the Tx and Rx, and reflection

> **The FRT is a new approach to the propagation model that is based on a Friis formula and Fresnel zones.**

is neglected. Furthermore, the FRT is more suitable for rural-area predictions because it considers diffraction and neglects reflection. To validate and calibrate the model, real-field LTE 800-MHz signals from commercial mobile-network base stations were measured and compared with the FRT. The same measurements were compared with the previously mentioned models, which are available from the open source radio-planning prediction-tool project [13].

RADIO-COVERAGE PREDICTIONS IN A REAL ENVIRONMENT

The basic approach to computing radio-coverage prediction uses a Friis formula for the free space: $P_{rx} = P_{tx} G_{tx} G_{rx} (\lambda/4\pi d)^2$, where P_{rx} and P_{tx} are the Tx and Rx power in watts, G_{tx} and G_{rx} are unitless gains for the Tx and Rx antenna, d is the distance between the Tx and Rx in meters, and λ is the wavelength in meters. The Friis formula can be written in logarithmic form as $P_{Rx}[\text{dBm}] = P_{Tx} + G_{Tx} + G_{Rx} + 20\log_{10}(\lambda/4\pi d)$, where P_{Tx} and P_{Rx} are the Tx and Rx power in decibels with reference to 1 mW (dBm), and G_{Tx} and G_{Rx} are gains for the Tx and Rx antenna in decibels isotropic (dBi). In a real propagation environment, the Friis formula can be extended with added variables that could represent additional phenomena in radio-wave propagation, such as diffraction, reflection, refraction, and scattering. This article addresses diffraction. The Friis formula takes the following form: $P_{Rx}[\text{dBm}] = P_{Tx} + G_{Tx} + G_{Rx} + 20\log_{10}(\lambda/4\pi d) + F_{frt}$.

The F_{frt} element represents the additional path-loss contribution that result from obstacles in the propagation path. F_{frt} can be determined by using Fresnel zones, and it depends on how much the zones are obstructed by obstacles in the propagation path. The value of F_{frt} is mainly negative, ($F_{frt} < 0$ dB), and contributes to additional signal losses. In a real environment, at least some areas of the Fresnel zones are blocked. However, a situation may arise where the Fresnel zones are obstructed in such a way that amplification of the received power occurs. A nice example is a Fresnel-zone focusing diffractor; if only the first Fresnel zone is opened, the signal is strengthened by $F_{frt} = 6$ dB. If the first seven odd Fresnel zones are opened, the signal is strengthened by $F_{frt} = 16.9$ dB [14].

FRESNEL ZONES

The FRT is based on a calculation of the Fresnel-zone obstruction between the radio Tx and Rx. The basic equation for the Fresnel zones is

$$F_n = \sqrt{n\lambda \frac{d_1 d_2}{d_1 + d_2}}, \tag{1}$$

where F_n represents the distance from a centerline in meters, and n is the real unitless number representing the stratum of the Fresnel zone. For the first Fresnel zone, $n < 1$, and for
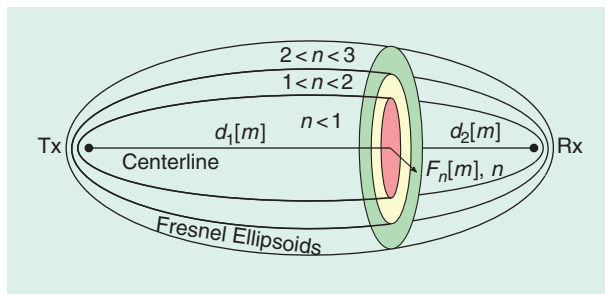

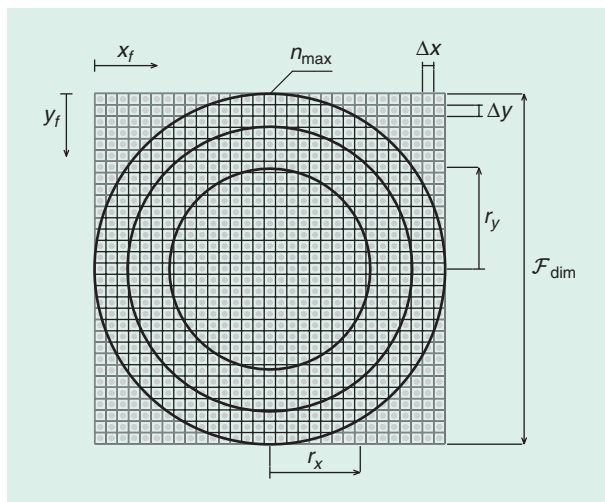**FIGURE 1.** The geometric representation of Fresnel zones.

FIGURE 2. The cross section of the Fresnel structure.

the second, $1 < n < 2$, and so on The wavelength is λ; the distances from the Tx and Rx are d_1 and d_2, respectively; and the distance between the Tx and Rx is $d = d_1 + d_2$. The geometric representation of Fresnel zones defined by (1) is presented in Figure 1.

For the purpose of numerical calculation, a cross section of the Fresnel-zone area is divided into arbitrarily small elements with dimensions $(\Delta x, \Delta y)$, as displayed in Figure 2, where $n_{\max}$ is the maximum number of Fresnel zones (for the case represented in Figure 2, $n_{\max} = 3$), $\mathcal{F}_{\dim} \cdot \mathcal{F}_{\dim}$ is the number of elements in the cross section, r_x and r_y are offsets from the centerline, and x_f and y_f are the element coordinates.

A horizontal plane of the Fresnel structure is depicted in Figure 3, where only the centerline and the circumference of the outer Fresnel zone are shown. In the figure, the parameters relevant to the numerical calculation are: d_x and d_y, the distances between the Rx and the Tx along the x and y axes, respectively; k_s, the slope for the centerline; and k_p, the slope perpendicular to k_s. The slope, k_s, and horizontal distance, r_x, from the centerline are relevant to the computation of the position of the calculation point (x_r, y_r) on the Fresnel ellipsoid.

A vertical plane of the Fresnel structure is displayed in Figure 4. The height of the centerline in the calculation point is evaluated by

$$h = (h_{\text{poi1}} + h_1) + \frac{d_1}{d_1 + d_2}((h_{\text{poi2}} + h_2) - (h_{\text{poi1}} + h_1)). \quad (2)$$

The height of each calculation point is obtained by summing h and r_y.

By defining

$$\Lambda = \lambda \frac{d_1 d_2}{d_1 + d_2}, \quad (3)$$

(1) is written as $F_n^2 = n\Lambda$. For the point on the edge of the cross section, $F_n = \mathcal{F}_{\dim}/2$, and $n = n_{\max}$. If $r_e = \sqrt{r_x^2 + r_y^2}$ is the distance from the center of the cross section, and n is a stratum of the Fresnel zone at distance r_e, we can write

$$n = \frac{r_e^2}{\Lambda}. \quad (4)$$

The distance from the center is

$$r_e = \sqrt{\left(x_f - \frac{\mathcal{F}_{\dim}}{2}\right)^2 + \left(\frac{\mathcal{F}_{\dim}}{2} - y_f\right)^2}. \quad (5)$$

Equation (5) is inserted into (4):

$$n = \frac{\left(x_f - \frac{\mathcal{F}_{\dim}}{2}\right)^2 + \left(\frac{\mathcal{F}_{\dim}}{2} - y_f\right)^2}{\Lambda}. \quad (6)$$

Equation (6) is written in a more useful form for later use:

$$n = \left(\left(\frac{x_f - \mathcal{F}_{\dim}/2}{\mathcal{F}_{\dim}/2}\right)^2 + \left(\frac{\mathcal{F}_{\dim}/2 - y_f}{\mathcal{F}_{\dim}/2}\right)^2\right) \cdot n_{\max}. \quad (7)$$

The offsets from the centerline, r_x and r_y, for each element $(\Delta x, \Delta y)$ are calculated by (8) and (9):

$$r_x = \frac{(x_f - \mathcal{F}_{\dim}/2)}{\mathcal{F}_{\dim}/2} \cdot \sqrt{\lambda n_{\max}} \cdot \sqrt{\frac{d_1 d_2}{d_1 + d_2}} \, [m], \quad (8)$$

$$r_y = \frac{(\mathcal{F}_{\dim}/2 - y_f)}{\mathcal{F}_{\dim}/2} \cdot \sqrt{\lambda n_{\max}} \cdot \sqrt{\frac{d_1 d_2}{d_1 + d_2}} \, [m]. \quad (9)$$

ELECTRIC-FIELD INTENSITY CALCULATION

The electric-field intensity on the Rx side is calculated according to the Kirchhoff law:
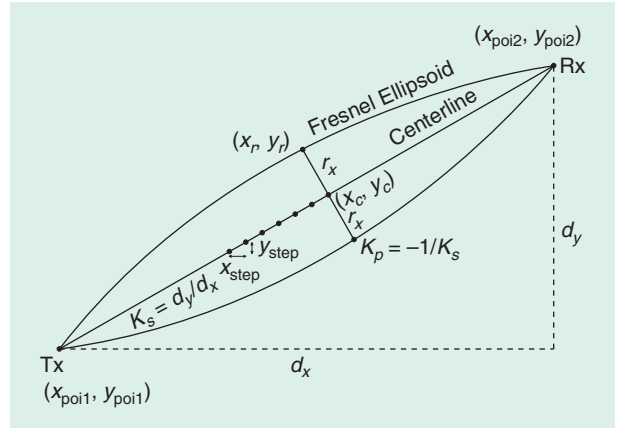

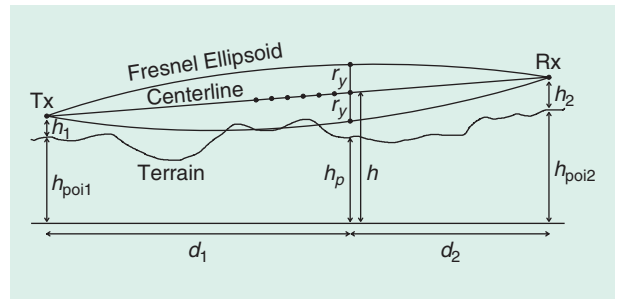FIGURE 3. The horizontal plane of the Fresnel structure. The black dots represent calculation points.

FIGURE 4. The vertical plane of the Fresnel structure. The black dots represent calculation points.
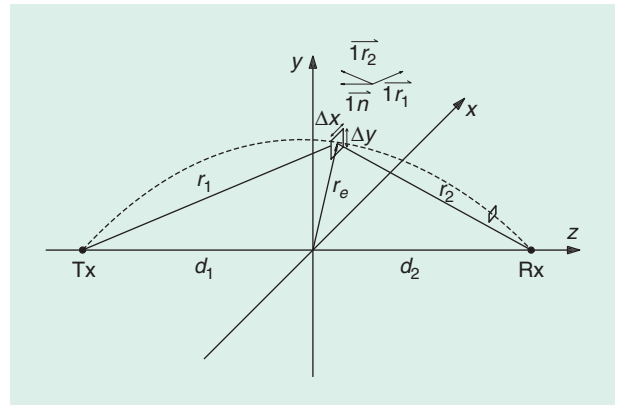

FIGURE 5. The scaling element along the Fresnel ellipsoid.

$$\vec{E}(\mathrm{Rx}) = \frac{1}{4\pi} \int_{A_1} \left(G \frac{\partial \vec{E}}{\partial n} - \vec{E} \frac{\partial G}{\partial n} \right) dA_1. \tag{10}$$

Observing Figure 5, the fields are written in waveform:

$$\vec{E} = \vec{1_E} C \frac{e^{-j\beta r_1}}{r_1}, \tag{11}$$

$$G = \frac{e^{-j\beta r_2}}{r_2}, \tag{12}$$

where β is the phase-shift constant, $\beta = 2\pi/\lambda = \omega/c_0$. The conditions on the small surface elements $(\Delta x, \Delta y)$ are

$$\frac{\partial G}{\partial n} = \vec{1_n} \vec{1_{r_2}} \frac{\partial G}{\partial r_2} \approx \vec{1_n} \vec{1_{r_1}} (-j\beta \vec{E}), \tag{13}$$

$$\frac{\partial \vec{E}}{\partial n} = \vec{1_n} \vec{1_{r_1}} \frac{\partial \vec{E}}{\partial r_1} \approx \vec{1_n} \vec{1_{r_2}} (-j\beta G), \tag{14}$$
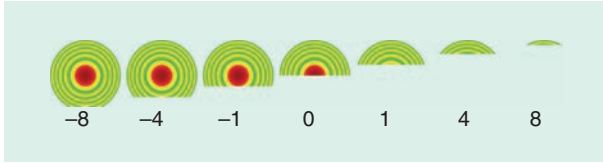

FIGURE 6. The demonstration of a knife-edge obstacle for 11 Fresnel zones for a circular aperture. The numbers under the figures are n.
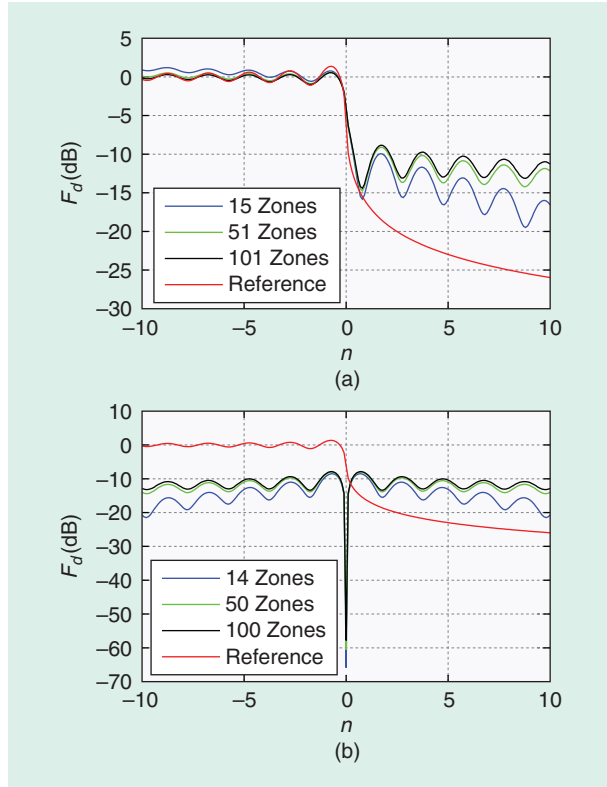

FIGURE 7. The numerical calculation of a knife-edge obstacle for a limited number of Fresnel zones and a circular aperture, computed with (30). (a) The odd number of Fresnel zones. (b) The even number of Fresnel zones.

and upon insertion into (10),

$$\vec{E}(\mathrm{Rx}) = -\frac{j\beta}{4\pi} \int_{A_1} (G\vec{E}\vec{1_n}\vec{1_{r_1}} - G\vec{E}\vec{1_n}\vec{1_{r_2}}) dA_1. \tag{15}$$

Since the area of interest is the far field, it is simplified as

$$r_x, r_y \ll d_1, d_2 \quad \Rightarrow \quad \vec{1_n}\vec{1_{r_1}} \approx -1, \quad \vec{1_n}\vec{1_{r_2}} \approx 1, \tag{16}$$

$$r_1 = \sqrt{r_x^2 + r_y^2 + d_1^2} \approx d_1 + \frac{r_x^2 + r_y^2}{2d_1}, \tag{17}$$

$$r_2 = \sqrt{r_x^2 + r_y^2 + d_2^2} \approx d_2 + \frac{r_x^2 + r_y^2}{2d_2}, \tag{18}$$

and then

$$\vec{E}(\mathrm{Rx}) = \frac{j\beta}{4\pi} \int_{A_1} \vec{1_n}(\vec{1_{r_2}} - \vec{1_{r_1}}) G\vec{E} dA_1. \tag{19}$$

Equation (17) is inserted into (11):

$$\vec{E} = \vec{1_E} C \frac{e^{-j\beta r_1}}{r_1} \approx \vec{1_E} C \frac{1}{d_1} e^{-j\beta d_1} e^{-\frac{j\beta}{2d_1}(r_x^2 + r_y^2)}, \tag{20}$$

and (18) is inserted into (12):

$$G = \frac{e^{-j\beta r_2}}{r_2} \approx \frac{1}{d_2} e^{-j\beta d_2} e^{-\frac{j\beta}{2d_2}(r_x^2 + r_y^2)}. \tag{21}$$

Equations (20) and (21) are inserted into (19):

$$\vec{E}(\mathrm{Rx}) \doteq \vec{1_E} C \frac{j\beta}{2\pi} \frac{e^{-j\beta d}}{d_1 d_2} \int_{A_1} e^{-j\beta \frac{d}{2d_1 d_2}(r_x^2 + r_y^2)} dr_x dr_y. \tag{22}$$

The scaling of element $(\Delta x, \Delta y)$ along the radio link is

$$\Delta x = \frac{2}{\mathcal{F}_{\dim}} \sqrt{\lambda n_{\max}} \sqrt{\frac{d_1 d_2}{d}}, \tag{23}$$

$$\Delta y = \frac{2}{\mathcal{F}_{\dim}} \sqrt{\lambda n_{\max}} \sqrt{\frac{d_1 d_2}{d}}, \tag{24}$$

$$\Delta x \cdot \Delta y = \frac{4\lambda n_{\max}}{\mathcal{F}_{\dim}^2} \frac{d_1 d_2}{d}. \tag{25}$$

The scaling of r_e^2 along the radio link is obtained by (8) and (9):

$$
\begin{aligned}
r_e^2 &= r_x^2 + r_y^2 \\
&= \left(\left(\frac{x_f - \mathcal{F}_{\dim}/2}{\mathcal{F}_{\dim}/2} \right)^2 + \left(\frac{\mathcal{F}_{\dim}/2 - y_f}{\mathcal{F}_{\dim}/2} \right)^2 \right) \cdot \lambda n_{\max} \cdot \frac{d_1 d_2}{d}.
\end{aligned} \tag{26}
$$

Equations (7) and (26) are combined to obtain a simple form:

$$r_x^2 + r_y^2 = n \cdot \lambda \cdot \frac{d_1 d_2}{d}. \tag{27}$$

It is assumed that the phase shift inside a sufficiently small element $(\Delta x, \Delta y)$ has a constant value; therefore, the integral from (22) is replaced with a sum:

$$\vec{E}(\mathrm{Rx}) \doteq \vec{1_E} C \frac{j\beta}{2\pi} e^{-j\beta d} \sum_{\mathrm{elem}} \frac{1}{d_1 d_2} e^{-j\beta \frac{d}{2d_1 d_2}(r_x^2 + r_y^2)} \Delta x \Delta y. \tag{28}$$

Equations (25) and (27) are merged with (28) and simplified:

$$\vec{E}(\text{Rx}) \doteq \overrightarrow{1_E} C \frac{j\beta}{2\pi} e^{-j\beta d} \frac{1}{d} \frac{4\lambda n_{\max}}{\mathcal{F}_{\dim}^2} \sum_{\text{elem}} e^{-\frac{j}{2}\beta n\lambda}. \qquad (29)$$

Instead of β we use $2\pi/\lambda$ and obtain the final equation:

$$\vec{E}(\text{Rx}) \doteq \overrightarrow{1_E} C j e^{-j\beta d} \frac{4 n_{\max}}{d \mathcal{F}_{\dim}^2} \sum_i e^{-j\pi n}. \qquad (30)$$

The power at the Rx point is $P(\text{Rx}) = |\vec{E}(\text{Rx})|^2/Z$, where $Z = (120\pi)\,\Omega \doteq 377\,\Omega$ in free space. The development of (30) is described in more detail in [15].

DIFFRACTION FROM A CIRCULAR APERTURE

To verify our approach for the received signal strength calculation with (30), a simulation of the knife-edge diffraction is performed. Figure 6 illustrates knife-edge obstruction on a limited number of Fresnel zones for the circular aperture. The results of the numerical calculation using (30) are given in Figure 7. The reference is represented with a red line and calculated from the following equation, where $C(x) = \int_0^x \cos(t^2)\,dt$ and $S(x) = \int_0^x \sin(t^2)\,dt$ are Fresnel integrals:

$$F_d = 20 \log \left\{ \frac{1}{\sqrt{2}} \sqrt{[0.5 - C(\nu)]^2 + [0.5 - S(\nu)]^2} \right\}. \qquad (31)$$

As shown in Figure 7, a special case of a Fresnel-interference diffractor is obtained with a limited number of Fresnel zones. If an odd number of Fresnel zones is taken into account [Figure 7(a)], the main distortion is obtained at the scene, where the first Fresnel zone is obstructed $(n > 1)$. If an even number of Fresnel zones is considered [Figure 7(b)], a substantially more unusable result is obtained. The reason for that result is that a limited number of Fresnel zones (a restricted circular area) is taken into account, and each zone contributes the same amount of electrical-field intensity to the outcome. To overcome that effect, (30) is modified so that the electric-field intensity decreases from the maximum value to zero from the center to the edge of the Fresnel intersection according to the equation $\eta_r = 1 - n/n_{\max}$. Hence, (30) is modified as follows:

$$\vec{E}(\text{Rx}) \doteq \overrightarrow{1_E} C j e^{-j\beta d} \frac{4 n_{\max}}{d \mathcal{F}_{\dim}^2} \sum_i \eta_r e^{-j\pi n}. \qquad (32)$$

Since the overall electric-field intensity, $\vec{E}(\text{Rx})$, is degraded, the shortfall should be compensated with the variable C. The knife-edge simulation with (32) is shown in Figure 8. With an increasing number of Fresnel zones, the numerical calculation approaches the red reference line [defined by (31)], as shown in Figure 9. However, the error increases when all of the Fresnel zones are completely obstructed; therefore, the path loss moves toward infinity.

FIGURE 8. The numerical calculation of the knife-edge obstacle for a limited number of Fresnel zones with a circular aperture and a linear reduction in the electric-field intensity toward the edge of the cross section, determined by (32). (a) The odd number of Fresnel zones. (b) The even number of Fresnel zones.
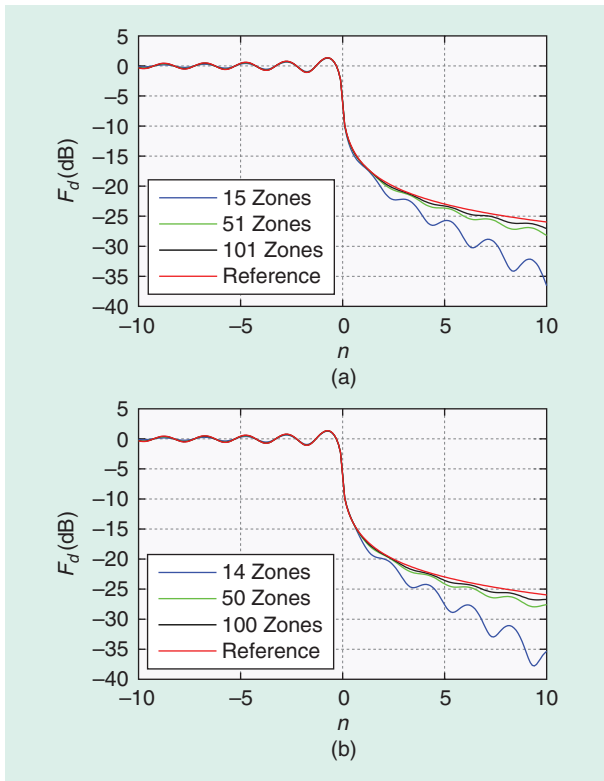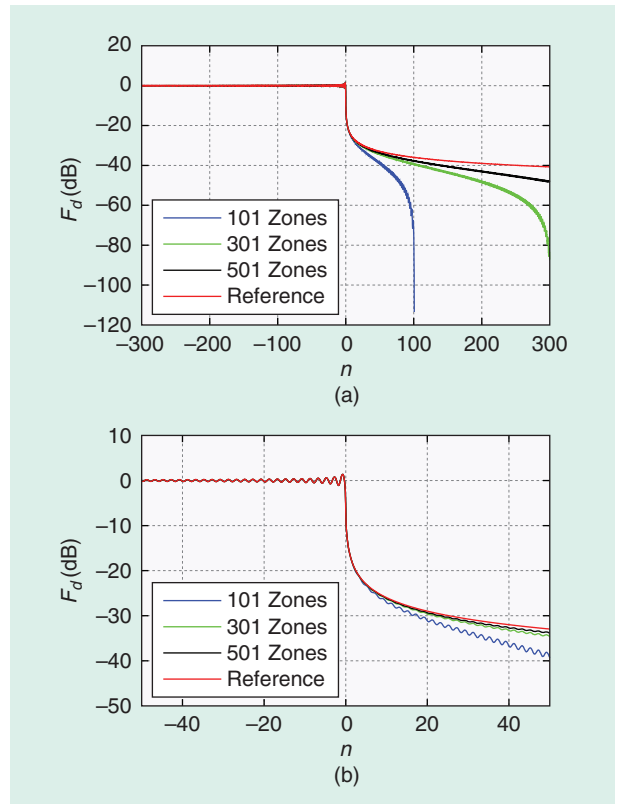

FIGURE 9. (a) The numerical calculation of the knife-edge obstacle for a finite number of Fresnel zones with a circular aperture and a linear reduction in the electric-field intensity toward the edge of the cross section, computed by (32). (b) A zoomed-in version of the information in (a).

DIFFRACTION FROM A SQUARE APERTURE

A better approach than using a circular aperture would be to use a square one (Figure 10). The dimmed factor takes the value $\eta_r = 1 - n_{xy}/n_{\max}$, where $n_{xy} = \max(n_x, n_y)$, n_x is the Fresnel cross section's offset from center along the x-axis, and n_y is the Fresnel cross section's offset from center along the y-axis. In Figure 11 the red curve represents the reference, the black curve denotes the dimmed Fresnel cross section, and the gray curve indicates the evenly radiated square Fresnel cross section. The evenly radiated square diffraction case (the gray curve) is used for the final calculation because it floats near the reference curve. A calculation error is still present, but it is slightly smaller than in the case of the dimmed circular aperture; therefore, this method is more appropriate. The advantage of the evenly radiated square aperture compared to the dimmed circular one is presented in "The FRT" section. The impact of the number of Fresnel zones used on the standard deviation is described in the "Voronoi Diagrams to Reduce Computational Complexity" section.

THE FRT

Images of obstacles between the Tx and Rx can be obtained using digital raster maps; that is, the DEM and DSM. Obstacles are considered to be the opaque or translucent for Fresnel elements, as shown in the example in Figure 12. From here, a numerical calculation of the electric-field intensity and the power of the remaining free-path elements in the Fresnel cross section is suggested.

A cross section of the FRT model is represented in Figure 13. The Tx and Rx are bounded by virtual rays in the shape of Fresnel ellipsoids in the 3D structure. For the sake of clarity, only two dimensions are shown. In the example, the ray calculation points are spaced at a distance of 1 m. Each ray, which represents the element $(\Delta x, \Delta y)$, starts at the Tx with a predefined complex number, $\eta_r e^{-j\pi n}$, of the dimmed Fresnel zone cross section or with $e^{-j\pi n}$ in the case of an evenly radiated Fresnel zone cross section. Each calculation point changes the ray's complex number according to the signal attenuation-phase–shift value pair $(a_{i,j}, b_{i,j})$, where i is the ray index, and j is the calculation-point index. The value of $a_{i,j}$ ranges between zero and one; the obstructed elements get zero, and the free path

> **A majority of the propagation models treats objects as opaque for radio waves.**

elements get one. Values between zero and one represent a partial signal attenuation of the obstacle for a particular element. The phase shift, $b_{i,j}$, is in radians per meter. Values $a_{i,j}$ and $b_{i,j}$ depend on land usage in the particular locations of the calculation point. If the calculation point is located in the air, the following numbers are used: $a_{i,j} = 1$, and $b_{i,j} = 0$. If the calculation point is located in vegetation, the value $a_{i,j}$ is less than one (it can be, for example, 0.99), and the value $b_{i,j}$ is not equal to zero (it can be, for instance, 0.02). In this way, each ray on its path from the Tx to the Rx accumulates signal attenuation $a_i = \Pi_j a_{i,j}$ and a phase shift, $b_i = \Sigma_j b_{i,j}$. At the Rx point, contributions from all of the rays are summed as described in (33), resulting in a corresponding Rx field strength:

$$\vec{E}(\mathrm{Rx}) \doteq \vec{1_E} C j e^{-j\beta d} \frac{4n_{\max}}{d\mathcal{F}_{\dim}^2} \sum_i \eta_r a_i e^{-j(\pi n + b_i)}. \tag{33}$$
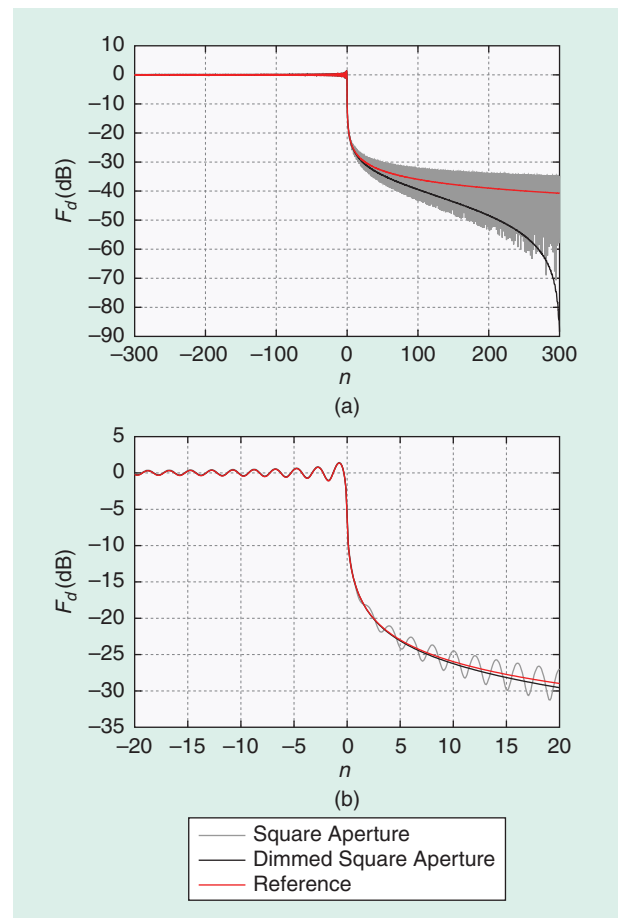
FIGURE 11. (a) The numerical simulation of a knife-edge obstacle for 301 Fresnel zones with a square aperture. The black curve represents a linear reduction in the electric-field intensity toward the edge of the cross section, while the gray curve signifies evenly radiated Fresnel zones. (b) A zoomed-in version of the information in (a).
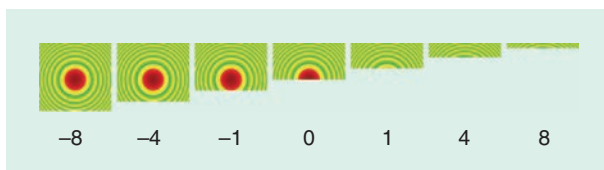

FIGURE 10. The demonstration of a knife-edge obstacle for 11-plus Fresnel zones for a square aperture. The numbers under the figures are n.

The variable F_{frt} in the Friis equation is calculated by squaring the electric-field intensity: $F_{frt} = 10\log(|\vec{E}(\text{Rx})|^2/Z)$.

VORONOI DIAGRAMS TO REDUCE COMPUTATIONAL COMPLEXITY

Thus far, for each element $(\Delta x, \Delta y)$ in the Fresnel cross section, an individual ray was used. If, for example, the Fresnel cross section is divided into $4{,}000 \times 4{,}000$ elements, more than 12.5 million rays (or 16 million, in the case of a square Fresnel cross section) are generated, and the complexity of the computation becomes enormous. To reduce the number of rays and computational difficulty, several elements can be combined (added) at the Tx side. A Voronoi diagram is used to determine which elements are added. In Figure 14(a), the Fresnel cross section, which contains a huge number of rays, is displayed. The rays are not visible in the figure and can be imagined by observing Figure 2. In Figure 14(b), a Voronoi diagram with a reduced number of combined rays, called *seed rays*, is presented. The seed rays are displayed as dots. In Figure 14(c), both figures are bonded together. The seed rays are specified beforehand in the Fresnel cross section, and for each one there is a corresponding area called the *Voronoi cell*. It is composed of the Fresnel cross section elements that are closer to the seed ray than to any other. That is, predefined complex numbers, $\eta_r e^{-j\pi n}$, from several elements $(\Delta x, \Delta y)$ in the associated Voronoi cell are summed at the Tx side to generate each seed ray. In practical calculations, a few hundred (approximately 300) seed rays are specified; therefore, instead of using 12.5 (or 16) million rays, 300 seed rays are utilized. This simplification is affordable because the digital map resolution determines the overall accuracy, and very dense ray usage does not contribute to more accurate results. In practical running tests, the accuracy of the propagation results noticeably worsens if fewer than 200 seed rays are included.

> The FRT is less accurate in urban areas or near water bodies where reflection effects come to the forefront.

IMPLEMENTATION OF RADIO-COVERAGE PREDICTION

The research focus on the FRT radio-coverage prediction model was for decimeter radio waves for suburban and rural areas, where the diffraction effects of radio-wave propagation are dominant. The FRT is less accurate in urban areas or near water bodies where reflection effects come to the forefront. For the test polygon, an LTE mobile network at 800 MHz [16] was used. Coverage predictions and measurements were made for rural, suburban, and urban LTE base stations. The calculated coverage predictions were calibrated with signal-strength measurements that were made with a Rohde and Schwarz TSMW [17] instrument installed in a dedicated measurement car.

For practical implementation of the FRT radio-coverage prediction algorithm, several requirements must be fulfilled. The first step is to obtain terrain data. For that purpose, free lidar data covering the terrain of Slovenia were procured [18]. Afterward, the raw lidar data were converted to the raster format, which was suitable for use in the coverage-prediction model. Suburban three-cell LTE base stations with several different types of objects in the surrounding area were chosen for the test polygon. Those objects included a forest, houses, fields, a highway, rural roads (gravel and paved), hills, and so on.

FIGURE 13. The Fresnel ellipsoids and calculation points. Only two dimensions are displayed; however, the rays are stretched in the 3D structure.

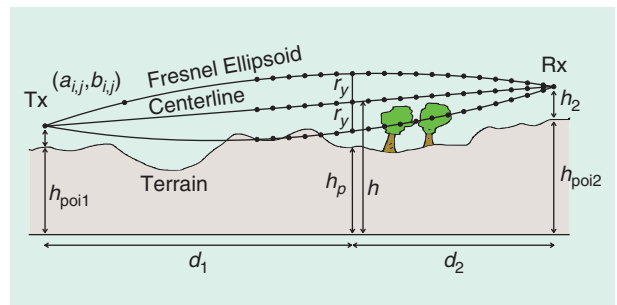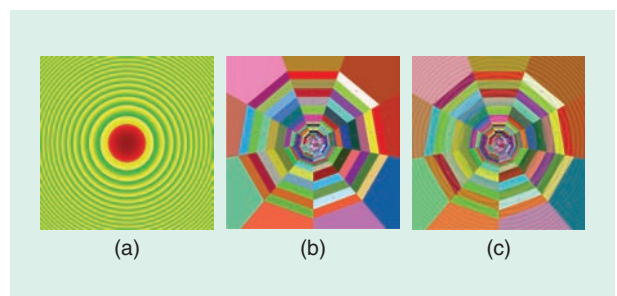**FIGURE 12.** The obstacles between the Tx and Rx in the Fresnel cross section.

FIGURE 14. (a) The Fresnel cross section. (b) The Voronoi diagram. (c) The Fresnel cross section and Voronoi diagram combined.

DIGITAL RASTER MAPS FROM RAW LIDAR DATA

Three types of raster digital maps are needed as input data in the radio-coverage prediction module: DEM, DSM, and LC, all with a 1-m resolution. The necessary lidar maps were obtained on the free web service eVoide [18], where the data are arranged in square-kilometer increments. Three types of data are available per square kilometer: DEM, relief point cloud (RPC), and georeferenced and classified point cloud (GCPC). The DEM is used directly as input data for the radio-coverage prediction module, whereas the DSM and LC are made from the GCPC and DEM. The RPC is not used in this case. The section of the lidar GCPC data is shown in Figure 15.

Figure 16 reveals samples of the square-kilometer DEM, DSM, and LC maps. The DSM is obtained from lidar data in such a way that for each square meter the GCPC map point with the maximum value of component z is found. Up to 30 cloud points per square meter are usually contained in the lidar data. However, due to the type of terrain, some of the square meters remain without a radar reflection (for example, water), resulting in spots with undefined data values. To overcome that problem, the missing cells were interpolated with the surrounding cells' values.

> **If various ground types could be distinguished, independent attenuations and phase shifts could be associated with each kind.**

The LC is obtained from the GCPC [19] by reading each point classification value and determining which one prevails. In that way, the following classifications are obtained: ground, low vegetation, medium vegetation, and high vegetation. Further work is planned to obtain a more precise classification of the LC; that is, different types of vegetation (leafy and needle-shaped trees), different kinds of buildings (small and massive), water, and so on. Exact classification is crucial for the accurate operation of the FRT algorithm, since different attenuations and phase shifts of a radio wave are considered for each classification type.

PROPAGATION CALCULATION

From the Tx to each square meter of the land, the 3D model of the Fresnel zones is calculated, as shown in Figure 17. Each line from the Tx to the endpoint on the map represents one FRT calculation. The height of the potential Rx is set to 1.8 m (the usual height of a handheld mobile phone).

The number of times that the DEM, DSM, and LC values are read in each calculation point is determined by the number of seed rays. Stated another way, each seed ray at the calculation point must read the DEM, DSM, and LC, and based on that data, determine its location in space. The location of the seed rays can be in free space, near objects (buildings and vegetation), and on the ground. If the location at a particular calculation point is not free space, the complex value of the seed ray changes according to the type of object (building, vegetation, ground, and so on), as described in the section "The FRT."

PROPAGATION-PARAMETERS TUNING USING THE FRT

The field measurements of the signal strength for one suburban LTE base station were performed in June 2017. At that time
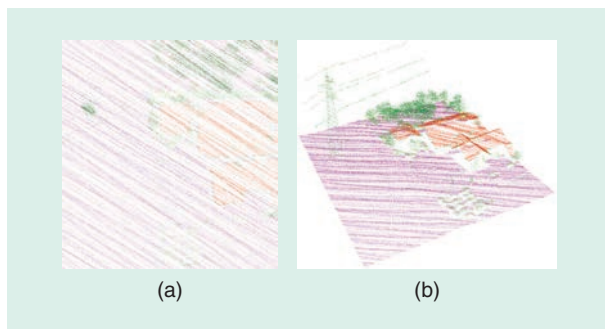

FIGURE 15. The (a) 2D and (b) 3D views of the lidar georeferenced and classified point cloud.
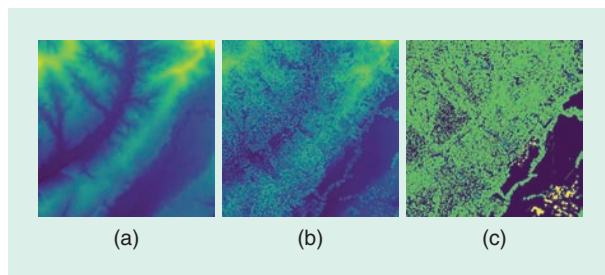

FIGURE 16. (a) The DEM. (b) The DSM. (c) The LC. All of the raster maps are in dimensions of 1 km² and have a resolution of 1 m. (Data from [18].)
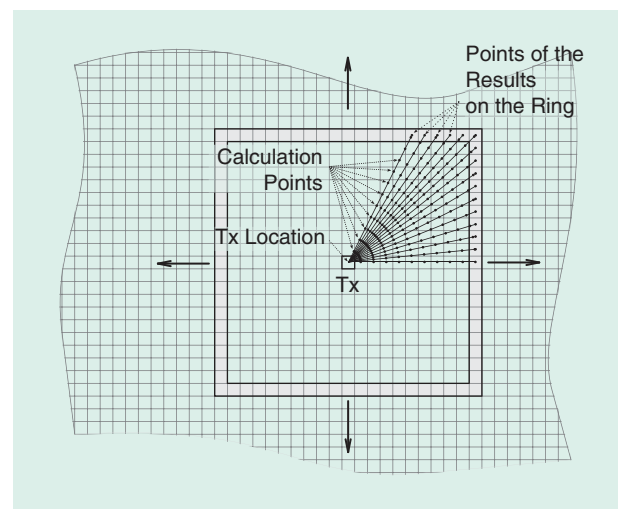

FIGURE 17. The horizontal plane of the FRT calculation.

of year, vegetation in Slovenia is lush, and a strong radio-wave attenuation through the forest is expected. During several hours of measurement around the base station, 105,176 signal-strength samples were recorded with their GPS position.

The criteria for the model calibration is the standard deviation, $\sigma = \sqrt{\sum (x_i - \bar{x})^2 / (n-1)}$, and the average error, $\mu = \Sigma (x_i - \bar{x})/n$, where $x_i = P_{Rxi} - P_{MEASi}$ is the difference between the calculated power, P_{Rxi}, and measured power, P_{MEASi}. Initially, to increase the radio-prediction accuracy, the standard deviation, σ, is observed while the signal attenuation and phase shift through different types of objects are adjusted. For that task, a measurement test set from all three cells (A, B, and C) of the mobile-network base station is used.

ATTENUATION AND PHASE-SHIFT PARAMETERS FOR VEGETATION

Coarse attenuation and phase-shift parameter optimization for vegetation can be seen in Figure 18. A singular and very deep minimum at 0.995 is obtained for vegetation attenuation, as shown in Figure 18(a). The phase-shift variation can be observed in Figure 18(b), where it reaches a minimum value near zero. The phase-shift values are repeated every 2π radians. A more accurate attenuation and phase-shift analysis near the expected minimum is given in Figure 19. The minimum

standard deviation is obtained at values $ph = 0.02$ rd/m for the phase shift and $a = 0.99 = 0.01005$ Np/m $= 0.086$ dB/m for the attenuation.

Based on the obtained value for the phase shift in vegetation, $ph = \varphi = 0.02$ rd/m, the corresponding relative permittivity is calculated, assuming that the relative permittivity for air is $\epsilon_{ra} = 1.0006$ [20]. The phase-shift constant in air is $\beta_a \simeq \omega \sqrt{\mu_0 \mu_{ra} \varepsilon_0 \varepsilon_{ra}}$, and for vegetation it is $\beta_v \simeq \omega \sqrt{\mu_0 \mu_{rv} \varepsilon_0 \varepsilon_{rv}}$. It is presumed that $\mu_{ra} = \mu_{rv}$ and $\beta_v = \beta_a + \varphi$. The quotient of both phase-shift constants is written in (34), and after a short derivation, (35) is obtained for the vegetation's relative permittivity. Filling in (35) with real values gives the result for the relative permittivity for vegetation: $\epsilon_{rv} = 1.002988$.

$$\frac{\beta_a + \varphi}{\beta_a} = \frac{\omega \sqrt{\mu_0 \mu_{rv} \varepsilon_0 \varepsilon_{rv}}}{\omega \sqrt{\mu_0 \mu_{ra} \varepsilon_0 \varepsilon_{ra}}}, \tag{34}$$

$$\varepsilon_{rv} = \varepsilon_{ra} \left(\frac{\beta_a + \varphi}{\beta_a} \right)^2. \tag{35}$$

ATTENUATION AND PHASE-SHIFT PARAMETERS FOR BUILDINGS

Using a procedure similar to the one for vegetation, the attenuation and phase-shift adjustment for buildings can be performed. The coarse-attenuation and phase-shift adjustment
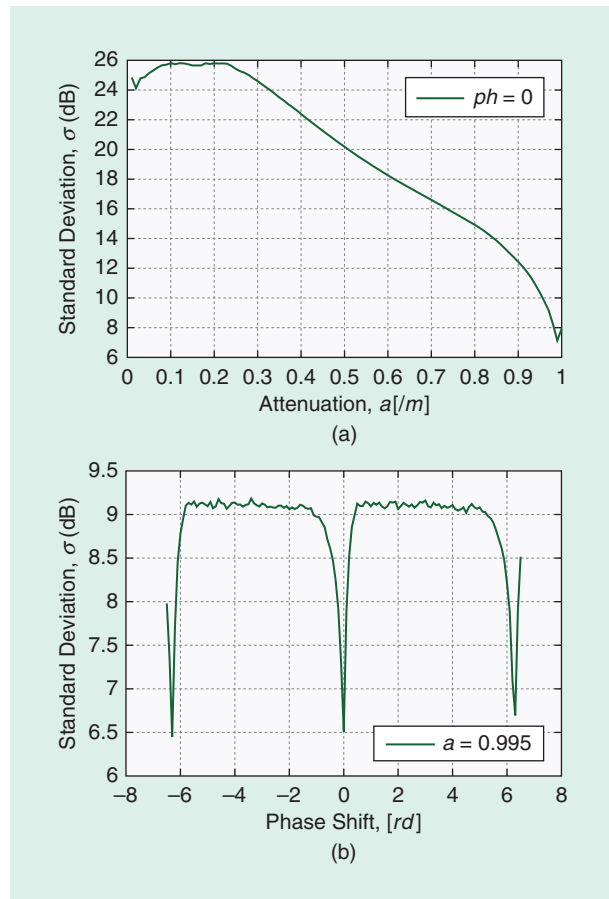

FIGURE 18. The (a) coarse-attenuation and (b) phase-shift adjustment for vegetation.
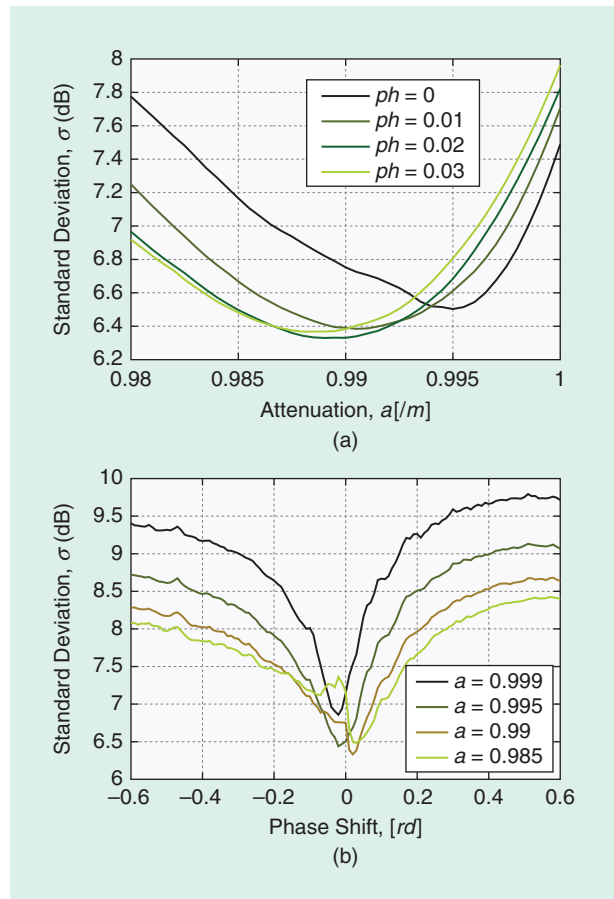
FIGURE 19. The (a) fine-attenuation and (b) phase-shift adjustment for vegetation.

for buildings is displayed in Figure 20. The singular and deep minimum is obtained at 0.9706 [Figure 20(a)], and the phase shift has a slightly positive value [Figure 20(b)]. An observation of the attenuation and phase shift in more detail is shown in Figure 21. In Figure 21(a), several curves for the different phase shifts are displayed, while in Figure 21(b), several curves for different attenuations are shown. From both figures, the attenuation and phase shift at the smallest standard deviation can be seen: $ph = 0.12$ rd/m, and $a = 0.945 = 0.05657$ Np/m $= 0.4865$ dB/m.

ATTENUATION AND PHASE-SHIFT ADJUSTMENT FOR THE GROUND

The ground attenuation and phase-shift adjustment provide manifold results with several minima. The phase-shift delay, 0 rd/m, shown in Figure 22(b) as a dark-red curve, has a minimum at $a = 0.04$ ($\alpha = 3.22$ Np/m 27.7 dB/m). However, note that the phase-shift delay has a main minimum near 1.2 rd/m, and if the black curve is observed, there are several local minima. In Figure 22(a), the black curve represents the attenuation with a phase-shift delay of 1.2 rd/m and repeatedly manifests several minima.

At that moment, only one type of ground is investigated, and the achieved result presents new possibilities for ground-characteristics analysis. Namely, if various ground types could be distinguished, independent attenuations and phase shifts could be associated with each kind. Therefore, this article proposes a new type of map layer, named the ground type (GT), with the following classification: field, forest ground, paved road, gravel road, water, marsh, the ground under buildings, and so on. However, the GT is left for future study.

HEIGHT OF THE Rx ANTENNA AND EARTH'S RADIUS

Figure 23(a) illustrates the ability of the module to calculate the exact Rx antenna height. The curve on the graph has a strong minimum at approximately 1.8 m, which is, in fact, the roof height of the measuring car to which the antenna was attached. Figure 23(b) shows the standard deviation as a function of Earth's radius. The graph is quite fuzzy; however, two minima are important there. One minimum is near Earth's radius of 6,400 km. The second interesting minimum is near 8,000 km, which could be the consequence of radio-wave refraction through the atmosphere.

FIGURE 20. The (a) coarse-attenuation and (b) phase-shift adjustment for buildings.
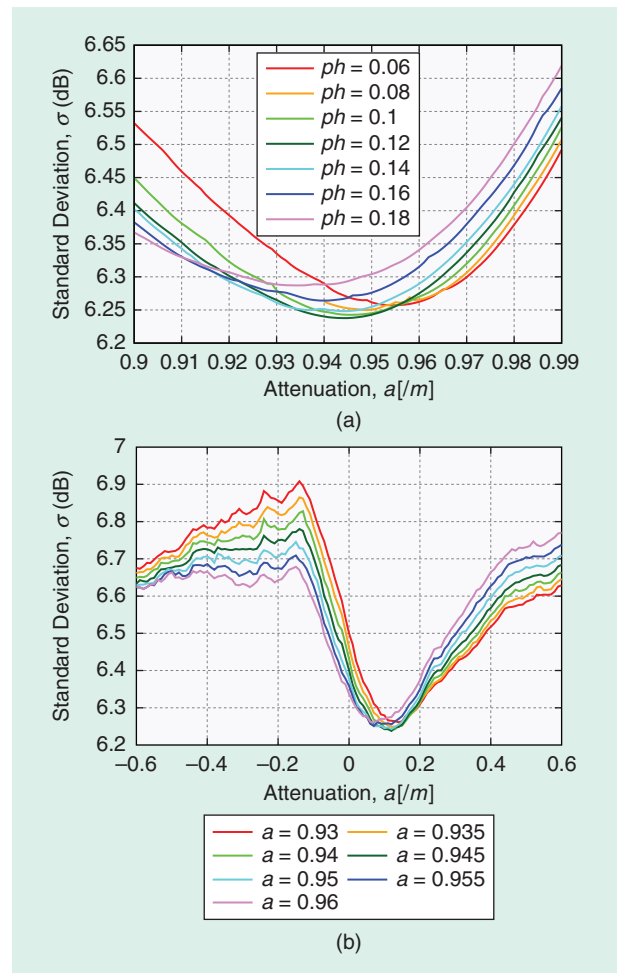
FIGURE 21. The (a) fine-attenuation and (b) phase-shift adjustment for buildings.

COMPARISON OF DIMMED CIRCULAR AND EVENLY SQUARE APERTURES

After calibrating the FRT module, the following values were obtained: for vegetation, $a\,[/m] = 0.99$ and $ph\,[rd] = 0.02$; for buildings, $a\,[/m] = 0.945$ and $ph\,[rd] = 0.12$; for the ground, $a\,[/m] = 0.035$ and $ph\,[rd] = 1.2$. Using those parameters, a test was performed with a dimmed circular aperture, and it produced the standard deviation $\sigma = 6.16551$ dB. When an evenly radiating square aperture was used, the result was $\sigma = 6.14029$ dB. Apparently, the method with an evenly radiating square aperture gives slightly better results than the one with a dimmed circular aperture.

FRESNEL ZONES AND THE CALCULATION ERROR

Figure 24 displays the impact that the number of Fresnel zones had on the calculation error for the evenly radiating square aperture. More than 60 Fresnel zones should be considered to achieve a reasonably low error.

PREDICTION CALCULATION AND MODEL COMPARISON

A large amount of data from a live network was used to test and compare the FRT algorithm with other propagation models. Measurement data from a live 800-MHz LTE network were used. The test area consisted of 160 base stations with a total of 454 cells. Field measurements, using the measurement car, were conducted from 2015 to 2017. For obtaining real-world general network conditions, different types of cells were included: rural (55.4%), suburban (32.9%), and urban (11.7%), with an average of 34,000 measurement points per cell. The maximum calculation distance was 7 km from the base-station antenna. The measurement points were 1–3 m apart (depending on the

FIGURE 23. The (a) height of the Rx antenna and (b) Earth's radius.

FIGURE 22. The (a) attenuation and (b) phase-shift adjustment of the ground.
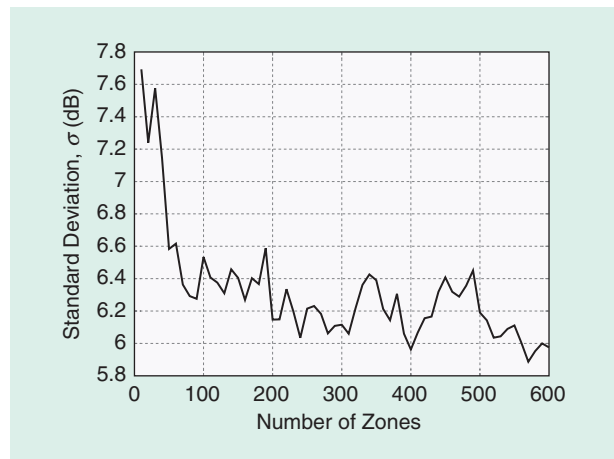
FIGURE 24. The impact of the number of Fresnel zones on the standard deviation.

vehicle speed). The first set consisted of 165 cells, the second had 142, and the third included 147.

Table 1 lists the results for all of the different models that were considered, where the first set was used to tune the model-specific parameters. Based on the obtained data, the remaining cell propagation (the second and third sets) was calculated and compared with the respective measurements. The presented error results consist of the standard deviation and average error. Even though the FRT does not consider reflections, while other models statistically do, it has less error than the other three.

The data sample for one cell is shown in Figure 25 as an example of the described procedure. The azimuth was 150°, the transmission power was 20 W, and the bandwidth was 10 MHz. Directional antenna Kathrein K742265 [21] was used, and it had the following characteristics: a gain of 18.8 dBi,

> There are several benefits that distinguish the FRT algorithm, including the estimation of object properties (the attenuation and phase shift), a smaller error, and a very clear physics structure.
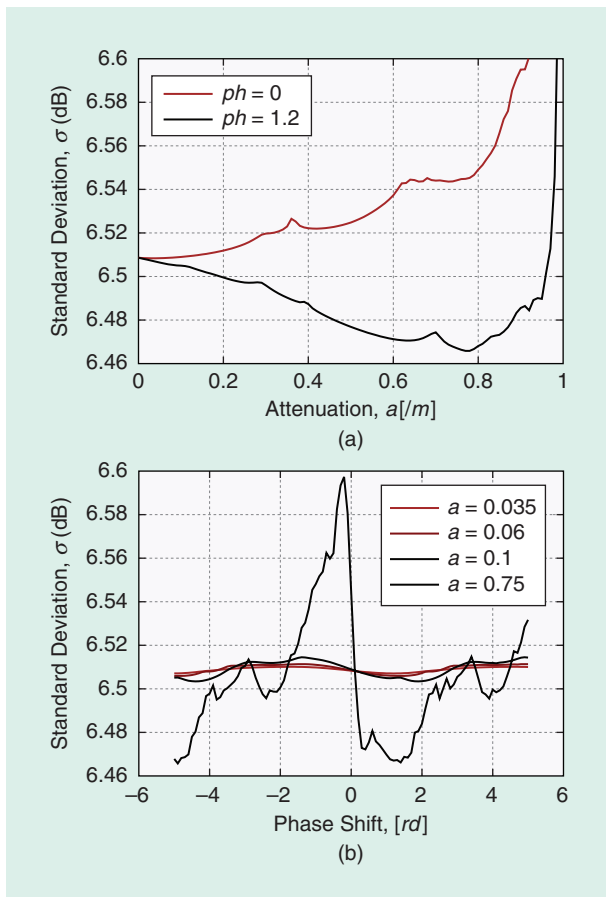
a horizontal beamwidth of 66°, and a vertical beamwidth of 5.2°. The down-tilt was 3°. The height of the antennas was 35 m. The receiving antenna was a Rohde & Schwarz TSMW ZE6 at 3 dBi with a magnetic base mounted on the car roof. The Rx was a Rohde & Schwarz TSMW [17] universal radio-network analyzer (with measurement uncertainties of less than 1 dB). Several details can be observed in the figure, including houses, forests, tree avenues, hills, roads, and so on. Since the FRT is a 3D model, diffraction behind obstacles can be recognized.

COMPUTATIONAL TIME AND RESTRICTIONS

In Figure 26, the calculation time of one radio cell coverage prediction for the FRT, Okomura–Hata, Ericsson 9999, and Cost231 is shown. For that test, raster maps with a resolution of 1 m were used, and the number of Fresnel seed rays for the

TABLE 1. THE COMPARISON BETWEEN THE FOUR TYPES OF PROPAGATION MODELS.

		FRT	Ericsson 9999	Okomura–Hata	Cost231
Set 1	σ (dB)	7.29	9.3	8.82	10.62
Set 2	σ (dB)	7.49	9.38	8.8	10.02
	μ (dB)	0.15	−0.32	1.01	2.58
Set 3	σ (dB)	7.39	9.1	8.49	10.53
	μ (dB)	−0.41	−0.45	−2.39	−4.41
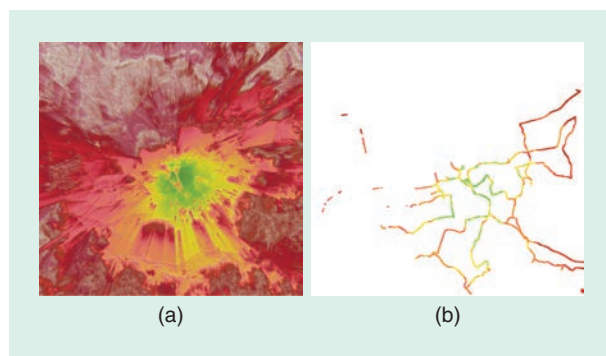
FIGURE 25. The (a) FRT LTE 800-MHz propagation for one LTE cell and (b) measurement locations. The dimension of the map is 6 × 6 km, and the resolution is 1 m. The azimuth is 150°. The colors represent the signal strength: green is better than −80 dBm, yellow is between −80 dBm and −95 dBm, orange is between −95 dBm and −115 dBm, and red is worse than −115 dBm.

FIGURE 26. (a) The calculation time versus the distance for four propagation algorithms for maps with a 1-m resolution. (b) A zoomed-in version of the information in (a).

FRT algorithm was 300. Because the FRT algorithm complexity is $O(r^3)$, the computation was carried out on a GPU [22]. The other three models were computed on a CPU.

The FRT algorithm is limited by the GPU's global memory, which prevents the processing of raster maps that are greater than a certain size. The maximum map area A for the FRT algorithm with the resolution R that can be calculated on the GPU is $A[m^2] < (R[m])^2 \cdot M[B]/16$ or $A[km^2] < (R[m])^2 \cdot M[GB] \cdot 67.11$, where M is the global-memory size.

CONCLUSIONS

In this article, a novel FRT algorithm for radio-coverage prediction at decimeter wavelengths based on 3D Fresnel zones was presented. The model was based on the Friis formula and Fresnel zones. A numerical equation for the radio-signal strength was developed on the basis of a cross section of Fresnel zones. Input raster maps (DEM, DSM, and LC) with a resolution of 1 m were obtained from lidar cloud data, which were freely available for the territory of Slovenia [18]. To perform real radio-coverage prediction calculations, several strategies and optimizations were discussed; that is, dimmed Fresnel cross sections to avoid diffraction problems, the reduction of Fresnel rays with Voronoi diagrams, and so on.

A live LTE 800-MHz network was measured and compared with the coverage prediction, which was made with the FRT, Ericsson 9999, Okomura–Hata, and Cost231 models. For the FRT algorithm, the attenuation and the phase shift were adjusted for each type of object, including vegetation and buildings, and the standard deviation and average error were employed as model-calibration criteria. For each kind of object, the attenuation and the phase shift were obtained. Additionally, the relative permittivity for different types of objects was calculated.

A similar procedure of adjusting the attenuation and phase shift was made for the ground. Several wave propagation phenomena were incorporated into the results graphs (Figure 22), and several minima were obtained. To distinguish the minima, the GT map layer with a detailed classification of the ground was proposed to give separate graphs for each ground categorization.

There are several benefits that distinguish the FRT algorithm, including the estimation of object properties (the attenuation and phase shift), a smaller error, and a very clear physics structure,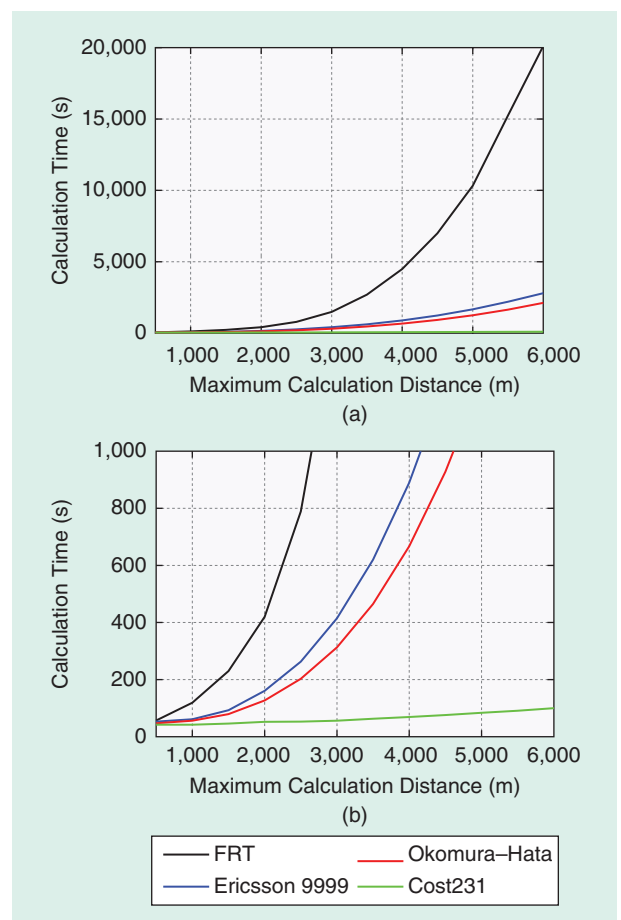 which enables easier future development. Mobile providers produce daily measurements of their networks. With the described technique, it would be possible to study vegetation properties. For example, the attenuation and phase shift for a cornfield can be determined on different frequency bands, and from the obtained data, the health of the vegetation can be concluded. Of course, this is solely speculation, and detailed research could determine whether the approach would work. Future projects will include the introduction of a new ground-type map layer, extension of the LC map layer classification, and experiments with other frequencies and geometries for different wave propagation phenomena, such reflections from the ground.

AUTHOR INFORMATION

Andrej Osterman (andrej.osterman@guest.arnes.si) works in the development of radio propagation prediction models and the preparation of statistics and scripts for mobile radio networks.

Patrik Ritoša (patrik.ritosa@gmail.com) is currently working on data analytics in the banking industry. His past work includes mobile network radio planning and 5G research projects.

REFERENCES

[1] ITU-R P.526-13, *Propagation by diffraction*, Series of ITU-R Recommendations, 2013.
[2] M. Lebherz, W. Wiesbeck, and W. Krank, "A versatile wave propagation model for the VHF/UHF range considering three-dimensional terrain," *IEEE Trans. Antennas Propag.*, vol. 40, no. 10, pp. 1121–1131, 1992.
[3] M. C. Lawton and J. McGeehan, "The application of a deterministic ray launching algorithm for the prediction of radio channel characteristics in small-cell environments," *IEEE Trans. Veh. Technol.*, vol. 43, no. 4, pp. 955–969, 1994.
[4] H. L. Bertoni, W. Honcharenko, L. Macel, and H. H. Xia, "UHF propagation prediction for wireless personal communications," *Proc. IEEE*, vol. 82, no. 9, pp. 1333–1359, 1994.
[5] J.-P. Rossi and Y. Gabillet, "A mixed ray launching/tracing method for full 3-d UHF propagation modeling and comparison with wide-band measurements," *IEEE Trans. Antennas Propag.*, vol. 50, no. 4, pp. 517–523, 2002.
[6] K. Guan, Z. Zhong, B. Ai, and T. Kürner, "Semi-deterministic path-loss modeling for viaduct and cutting scenarios of high-speed railway," *IEEE Antennas Wireless Propag. Lett.*, vol. 12, pp. 789–792, Dec. 2013.
[7] Y. Okumura, "Field strength and its variability in VHF and UHF land-mobile radio service," *Rev. Electr. Commun. Lab*, vol. 16, pp. 825–873, Sept.–Oct. 1968.
[8] M. Hata, "Empirical formula for propagation loss in land mobile radio services," *IEEE Trans. Veh. Technol.*, vol. 29, no. 3, pp. 317–325, 1980.
[9] J.-M. Jin, *The Finite Element Method in Electromagnetics*. Hoboken, NJ: Wiley, 2015.
[10] W. M. O'Brien, E. M. Kenny, and P. J. Cullen, "An efficient implementation of a three-dimensional microcell propagation tool for indoor and outdoor urban environments," *IEEE Trans. Veh. Technol.*, vol. 49, no. 2, pp. 622–630, 2000.
[11] M. F. Iskander and Z. Yun, "Propagation prediction models for wireless communication systems," *IEEE Trans. Microw. Theory Techn.*, vol. 50, no. 3, pp. 662–673, 2002.
[12] Y. Corre and Y. Lostanlen, "Three-dimensional urban EM wave propagation model for radio network planning and optimization over large areas," *IEEE Trans. Veh. Technol.*, vol. 58, no. 7, pp. 3112–3123, 2009.
[13] A. Hrovat, A. Vilhar, I. Ozimek, T. Javornik, and E. Kocan, "Grass-raplat-radio planning tool for grass GIS system," in *Proc. 2013 21st Int. Conf. IEEE Applied Electromagnetics and Communications (ICECom)*, pp. 1–5.
[14] H. D. Hristov, *Fresnal Zones in Wireless Links, Zone Plate Lenses and Antennas*. Norwood, MA: Artech House, 2000.
[15] A. Osterman, "Parallel visibility and Fresnel zones calculation using graphics processing units, (Vzporedno računanje vidnosti in Fresnelovih con na grafičnih procesnih enotah)," Ph.D thesis, 2015.
[16] T. Slovenije, "TS mobile coverage." Accessed on: Mar. 29, 2018. [Online]. Available: http://www.telekom.si/pomoc-in-podpora/teme-pomoci/pokritost-in-dostopnost/pokritost-mobilnega-omrezja
[17] Rohde and Schwarz, "Rohde and Schwarz TSMW." Accessed on: Dec. 15, 2018. [Online]. Available: http://www.livingston-products.com/products/pdf/156522_1_en.pdf
[18] Agencija RS ZA Okolje, "LIDAR eVode." Accessed on: Dec. 14, 2017. [Online]. Available: http://gis.arso.gov.si/evode/profile.aspx?id=atlas_voda_Lidar@Arso
[19] D. Mongus, N. Lukač, and B. Žalik, "Ground and building extraction from LiDAR data based on differential morphological profiles and locally fitted surfaces," *ISPRS J. Photogrammetry Remote Sens.*, vol. 93, pp. 145–156, Jan. 2014.
[20] C. A. Balanis, *Advanced Engineering Electromagnetics*. New York: Wiley, 1999.
[21] Kathrein Scala Division, "Kathrein antenna pattern 742265." Accessed on: Dec. 15, 2018. [Online]. Available: http://a2dcorp.us/pdf/kathrein/742265.pdf
[22] A. Osterman, L. Benedičič, and P. Ritoša, "An IO-efficient parallel implementation of an R2 viewshed algorithm for large terrain maps on a CUDA GPU," *Int. J. Geographical Inform. Sci.*, vol. 28, no. 11, pp. 2304–2327, 2014.

2020 IEEE International Symposium on Antennas and Propagation and North American Radio Science Meeting
5-10 July 2020 • Montréal, QC, Canada

www.2020apsursi.org

The 2020 IEEE AP-S Symposium on Antennas and Propagation and CNC/USNC-URSI joint meeting will be held from July 5-10, 2020, at the Fairmont The Queen Elizabeth Hotel in Montréal, Quebec, Canada. Founded in 1642, Montréal is the second-largest French-speaking city in the world and is often called the "Paris" of North America. The city hosted both EXPO 67 and the 1976 Summer Olympics, and is currently home to several outstanding universities, the Canadian Space Agency, and Transport Canada's Motor Vehicle Test Centre. Wireless technology is a very important part of the local industry scene. *A key component of this meeting will be industry participation and tours of local industry sites.*

The symposium and meeting are co-sponsored by the IEEE Antennas and Propagation Society (AP-S), and both the Canadian and U.S. National Committees (CNC/USNC) of the International Union of Radio Science (URSI). The technical sessions, workshops, and short courses will be coordinated among the groups to provide a comprehensive and well-balanced program that will promote the exchange of information on state-of-the-art research in antennas, propagation, electromagnetic engineering, and radio science. *The paper submission deadline is Friday, January 17, 2020 (23h 59m at International Date Line, UTC -12 hours; this is equivalent to 6:59 am Saturday, January 18, Eastern US Time).*

Steering Committee

General Chair:
Ahmed Kishk — ahmed.kishk@concordia.ca

General Co-Chairs:
Lot Shafai — lot.shafai@umanitoba.ca
David G. Michelson — davem@ece.ubc.ca
Yahia M. M. Antar — antar-y@rmc.ca

Finance Chair:
David G. Michelson — davem@ece.ubc.ca

Technical Program Chairs:
George V. Eleftheriades — gelefth@ece.utoronto.ca
Ke Wu — ke.wu@polymtl.ca
Ashwin K. Iyer — iyer@ece.ualberta.ca
Marco Antoniades — mantoniades@ryerson.ca

URSI TPC Co-Chair:
Y. M. M. Antar — antar-y@rmc.ca

URSI/AP Liaison:
Ross Stone — r.stone@ieee.org

Special Sessions Chairs:
Derek McNamara — dmcnamar@uottawa.ca
Shulabh Gupta — shulabhgupta@cunet.carleton.ca

Student Paper Competition Chair:
Robert Paknys — robert.paknys@concordia.ca
Michael Newkirk — mhnewkirk@ieee.org

Student Design Contest Chair:
Sean Hum — sean.hum@utoronto.ca

Short Courses and Workshops:
Tayeb Denidni — denidni@emt.inrs.ca

Young Professionals:
Tarek Djerafi — tarik.djerafi@emt.inrs.ca
Mohamed Bakr — mbakr@mail.ece.mcmaster.ca

Local Arrangements and Technical Tours:
Jean-Jacques Laurin — jean-jacques.laurin@polymtl.ca
David G. Michelson — davem@ece.ubc.ca

Publicity Chairs:
Abdelrazek Sebak — abdo@ece.concordia.ca
Mohammad S. Sharawi — mohammad.sharawi@polymtl.ca

Sponsors and Exhibits:
Pedram Mousavi — pmousavi@ualberta.ca
Daniel Janse Van Rensburg — drensburg@nsi-mi.com

Hospitality:
Susan Stone — SueLStone@hotmail.com
Joanne Wilton — jjwilton@mindspring.com
Judy Long — judimlong@swbell.net

Women in Engineering:
Natalia K. Nikolova — talia@mcmaster.ca
Mojgan Daneshmand — mojgan@ece.ualberta.ca

International Advisory Committee:
Zhizhang (David) Chen — z.chen@dal.ca (Chair)
Yang Hao — y.hao@qmul.ac.uk
H. Nakano — hymat@hosei.ac.jp
Ludger Klinkenbusch — klinkenbusch@tf.uni-kiel.de
Maria Pour — maria.pour@uah.edu
Satish Sharma — ssharma@sdsu.edu
Luk Kwai Man — eekmluk@cityu.edu.hk
Stefano Maci — macis@dii.unisi.it
Atif Shamim — atif.shamim@kaust.edu.sa
Raed Shubair — rshubair@mit.edu
Karu Esselle — karu.esselle@mq.edu.au
Richard Ziolkowski — richard.ziolkowski@uts.edu.au
Yejun He — heyejun@126.com

Paper Submission: Authors are invited to submit contributions for review and possible presentation at the Symposium or Meeting (the "Conference") on topics of interest to AP-S and CNC/USNC-URSI, including advancements and innovations in the fields of electromagnetics, antennas, and wave propagation. Suggested topics and general information are listed on the Website. In addition to regularly scheduled sessions for oral and poster presentations, there will be a student paper competition, as well as special sessions, workshops, and short courses that will address timely topics and state-of-the-art advancements in these fields.

- AP-S submissions must be in standard IEEE two-column format and must be two pages in length.

- CNC/USNC-URSI submissions may be in either a one-page, one-column format with a minimum length of 250 words or in the IEEE two-page, two-column format with a length of two pages.

- In all cases, only accepted and presented submissions that are in the IEEE two-page two-column format and substantially fill the two pages will be submitted for possible inclusion in IEEE Xplore if the author chooses submission to Xplore.

- All accepted and presented submissions will appear in the proceedings distributed at the Conference.

- Presenting authors will be required to register for the Conference by Friday, May 22, 2020, in order for their paper(s) to be included in the Conference.

- A complete list of AP-S and URSI topics, as well as detailed instructions including formats and templates, will be available on the conference Website - www.2020apsursi.org – by October 2019.

AP-S Student Paper Competition: Eligible entries in the Student Paper Competition must have only one student author, and that student must be the first author. Each additional coauthor must submit a signed letter indicating that his/her contribution is primarily advisory. Letters must be in PDF format and must be uploaded to the Conference's student paper Website in the indicated area at the time the paper is submitted. All Student Paper Competition entries will be evaluated using a double-blind review process. Detailed instructions are available on the Conference Website. For additional information, contact Robert Paknys (robert.paknys@concordia.ca) or Michael Newkirk (mhnewkirk@ieee.org).

CNC-/USNC-URSI Student Paper Competition: The CNC- and USNC-URSI are jointly admninistrering the 2020 Student Paper Competition, which is open to all students participating in the conference who are enrolled at colleges or universities in Canada or the U.S. Prizes will be awarded to five student papers. Awards (payable in USD) will be made for First Prize in the amount of $1000, Second Prize in the amount of $750, Third Prize in the amount of $500, Fourth Prize in the amount of $250, and Fifth Prize in the amount of $150. The deadline for submission of full papers on the conference website is Monday, March 11, 2020. Full details will be posted to the Conference website by October 2019.

CNC-/USNC-URSI Student Travel Grants: The CNC- and USNC-URSI are pleased to announce that there will be student travel grants to qualifying students attending Canadian and U.S. universities to help defray the costs of attending the 2020 URSI North American Radio Science Meeting. Travel awards will consist of an $800 stipend to partially offset the costs of travel and attending the conference. The awards will be dispersed contingent on the availability of funding in the awards program. To be eligible for the travel grants, students are required to apply via the Conference website. Full details will be posted by October 2019.

Special Sessions: Requests to organize special sessions should be submitted to Derek McNamara (dmcnamar@uottawa.ca) or Shulabh Gupta (shulabhgupta@cunet.carleton.ca) no later than Tuesday, October 8, 2019. Each proposal should include the title of the special session, a brief description of the topic, an indication of whether the proposed session is for AP-S, CNC/USNC-URSI, or is joint, and justification for its designation as a special session. All proposals should be submitted in PDF format. Special sessions will be selected and finalized by the end of November 2019. At that time, additional instructions will be provided to the organizers of the special sessions chosen for inclusion in the Conference. The associated papers or abstracts will be due Friday, January 17, 2020. A list of special sessions will be posted at the Conference website in December 2019.

Exhibits: Industrial, academic, and book exhibits will be open from Tuesday, July 7, 2020 to Thursday, July 9, 2020 (inclusive). Exhibitor registration and additional information can be found on the Conference website.

Short Courses/Workshops/Tutorials: Several short courses and tutorials on topics of special and current interest will be solicited by the technical program committee and organized for the Conference. Individuals who wish to organize a short course or workshop should contact Tayeb Denidni (denidni@emt.inrs.ca) by Friday, November 15, 2019.

List of AP-S/URSI Topics and Updates: The most current Call for Papers, including the detailed list of AP-S and URSI topics, is available on the Conference website, http://www.2020apsursi.org.

Raymond P. Wasky

2019 ASIA-PACIFIC MICROWAVE CONFERENCE (APMC 2019)

10–13 December 2019, Singapore, email: lee@acedaytons -direct.com. http://www.apmc2019.org/.

SECOND INDIAN CONFERENCE ON ANTENNAS AND PROPAGATON (InCAP)

18–22 December 2019, Ahmedabad, India. (Papers: closed.) Contacts: Dr. Sudhakar Rao, organizing cochair, InCAP2019, +1 215 500 9655, email: skraoks@yahoo.com; or conference email: https://www.incap2019.org/contact-us.php; or Integrated Conference and Event Management, B-128, Sector-5, Noida 201301, National Capital Region, Delhi, India. +91 96500 17933, email: aman@iceindia.in. http://www.incap2019.org.

IEEE RADIO AND WIRELESS SYMPOSIUM (RWS2020)

26–29 January 2020, San Antonio, Texas, United States. Contact: Elsie Vega, 445 Hoes Lane, Piscataway, NJ 08854, United States. +1 732 981 3428, email: elsie.vega@ieee .org. http://radiowirelessweek.org.

INTERNATIONAL WORKSHOP ON ANTENNA TECHNOLOGY (IWAT 2020)

25–28 February 2020, Bucharest, Romania. (Papers: closed.) Contacts: Razvan D. Tamas, general chair, Constanta Maritime University, email: tamas@ieee.org; or Dr. Liliana Achitei, Constanta Maritime University, email: contact@iwat2020.org. http://www.iwat2020.org/.

2020 EUROPEAN CONFERENCE ON ANTENNAS AND PROPAGATION (EuCAP 2020)

15–20 March 2020, Copenhagen, Denmark. (Papers: closed.) Contact: Olav Breinbjerg, conference chair, email: ob@elektro .dtu.dk. http://www.eucap2020.org/.

2020 INTERNATIONAL APPLIED COMPUTATIONAL ELECTROMAGNETICS SOCIETY (ACES) SYMPOSIUM

22–26 March 2020, Monterey, California, United States. (Papers: closed.) http://www.aces-society.org/conference/Monterey_2020/.

2020 IEEE INTERNATIONAL CONFERENCE ON COMPUTATIONAL ELECTROMAGNETICS (ICCEM 2020)

25–27 March 2020, Singapore. (Papers: closed.) Contacts: Ziliang Liu, conference secretary, email: tslliuz@ nus.edu.sg; or Chao-Fu Wang, general chair, National University of Singapore, 5A Engineering Drive 1, #09-02, 117411, Singapore. +65 6516 7813, fax: +65 6872 6840, email: cfwang@nus.edu.sg. http://www.iccem2020.org.

IEEE INTERNATIONAL CONFERENCE ON COMMUNICATIONS (ICC 2020)

7–11 June 2020, Dublin, Ireland. (Papers: closed.) https:// icc2020.ieee-icc.org.

2020 IEEE/MTT-S INTERNATIONAL MICROWAVE SYMPOSIUM (IMS 2020)

21–26 June 2020, Los Angeles, California, United States. (Papers: 4 December 2019, Hawaii Standard Time.) Submit 3–4 page papers in PDF format, not to exceed 2 MB in size, to http://www.ims-ieee.org. Hardcopy and email submissions are not accepted. Contact: Elsie Vega, 445 Hoes Lane, Piscataway, NJ 08854, United States. +1 732 981 3428, email: elsie.vega@ieee.org. http://www .ims2019.org.

2020 IEEE INTERNATIONAL SYMPOSIUM ON ANTENNAS AND PROPAGATION AND URSI NORTH AMERICAN RADIO SCIENCE MEETING

19–24 July 2020, Montréal, Canada. Contact: Ahmed Kishk, Concordia University, email: kishk@encs.concordia.ca. https://2020apsursi.org.

IEEE INTERNATIONAL GEOSCIENCE AND REMOTE SENSING SYMPOSIUM (IGARSS 2020)

19–24 July 2020, Waikoloa, Hawaii, United States. (Symposium and student papers: 15 January 2020.) +1 979 846 6800, email: info@igarss2020.org. http://www.igarss2020 .org.

INTERNATIONAL CONFERENCE ON ELECTROMAGNETICS IN ADVANCED APPLICATIONS (ICEAA 2020) AND IEEE-APS TOPICAL CONFERENCE ON ANTENNAS AND PROPAGATION IN WIRELESS COMMUNICATIONS (IEEE APWC 2020)

10–14 August 2020, Honolulu, Hawaii, United States. (Abstracts: 6 March 2020.) Contacts: Prof. Roberto D. Graglia, chair of organizing committee, Dipartimento di Elettronica e TLC, Politecnico di Torino, Corso Duca degli Abruzzi, 24, 10129 Torino, Italy, email: roberto.graglia@polito.it; or Prof. Piergiorgio L.E. Uslenghi, chair of scientific committee, Department of ECE (MC 154), University of Illinois at Chicago, 851 South Morgan Street, Chicago, IL 60607-7053, United States, email: uslenghi@uic.edu. http://www.iceaa.net.

43rd SCIENTIFIC ASSEMBLY OF THE COMMITTEE ON SPACE RESEARCH (COSPAR)

15–23 August 2020, Sydney, Australia. (Papers: 14 February 2020.) Contacts: Emma Bowyer, managing director, ICMS Australia, GPO Box 3270, Sydney NSW 2001, Australia. +61 (0) 2 9254 5000, fax: +61 (0) 2 9251 3552, email: emmab@icmsaust.com.au; or Selina Moscatt, email: enquiries@cospar2020.org. http://www.cospar2020.org/.

33rd GENERAL ASSEMBLY AND SCIENTIFIC SYMPOSIUM (GASS) OF THE INTERNATIONAL UNION OF RADIO SCIENCE (URSI GASS 2020)

29 August–5 September 2020, Rome, Italy. (Papers: 31 January 2020.) Session, short course, and workshop proposals should be addressed to: spc@ursi2020.org. For other questions related to scientific aspects, contact the URSI secretary at: gass@ursi.org. For all questions related to registration and attendance at GASS, refer to the symposium website: http://www.ursi2020.org. For inquiries about the GASS Student Paper Competition, please visit: https://www.ursi2020.org/grants-award/. Contact: URSI Secretariat, c/o INTEC, Tech Lane Ghent Science Park—Campus A, Technologiepark-Zwijnaarde 126, B-9052 Gent, Belgium, email: gass@ursi.org. http://www.ursi2020.org.

INTERNATIONAL SYMPOSIUM ON ELECTROMAGNETIC COMPATIBILITY (EMC EUROPE 2020)

7–11 September 2020, Rome, Italy. (Papers: 15 February 2020.) +39.0221006.203 287 202; or +39.0221006.231 287 202, emails: General information: info@emceurope2020.org; Chairs: chairs@emceurope2020.org; or Technical Program: tpc@emceurope2020.org. http://www.emceurope2020.org/.

2020 IEEE RADAR CONFERENCE

21–25 September 2020, Florence, Italy. (Papers: 30 March 2020.) Papers will open at the end of February 2020. For additional information, refer to the conference website: http://www.radaraconf20.org. Contact: Fulvio Gini, general cochair, the University of Pisa, Italy. +39 050 2217550, email: f.gini@ing.unipi.it; or Maria Sabrina Greco, general cochair, the University of Pisa, Italy. +39 050 2217620, email: m.greco@ing.unipi.it. http://www.radaraconf20.org.

EIGHTH ANNUAL IEEE INTERNATIONAL CONFERENCE ON WIRELESS FOR SPACE AND EXTREME ENVIRONMENTS (WiSEE2020)

12–14 October 2020, Vicenza, Italy. (Papers: 1 July 2020.) Contact: wisee20-chairs@edas.info. https://attend.ieee.org/wisee-2020/.

AOC 57th INTERNATIONAL SYMPOSIUM AND CONVENTION

8–10 December 2020, Washington, D.C., United States. Amy Belicev, Association of Old Crows, 1555 King Street, Suite 500, Alexandria, VA 22314, United States. +1 703 549 1600, email: belicev@crows.org. http://www.crows.org.

THIRD URSI ATLANTIC RADIO SCIENCE CONFERENCE (URSI AT-RASC)

23–28 May 2021, Gran Canaria, Canary Islands. (Papers: 4 January 2021.) Contact: URSI Secretariat, c/o INTEC, Ghent University, Technologiepark-Zwijnaarde 126, B-9052 Gent, Belgium. +32 (0) 9 264 33 20, fax: +32 (0) 9 264 42 88, email: at-rasc@ursi.org. http://www.at-rasc.com/.

FUTURE AP-S SYMPOSIA

2020 IEEE INTERNATIONAL SYMPOSIUM ON ANTENNAS AND PROPAGATION AND URSI NORTH AMERICAN RADIO SCIENCE MEETING

19–24 July 2020, Montréal, Canada. Ahmed Kishk, Concordia University, email: kishk@encs.concordia.ca. https://2020apsursi.org.

Raymond P. Wasky

SHORT COURSES

ANTENNA AND ARRAY FUNDAMENTALS
10–12 December 2019, Columbia, Maryland, United States. Applied Technology Institute, 349 Berkshire Drive, Riva, MD 21140-1433, United States, +1 888 501 2100 (toll-free U.S.) or +1 410 956 8805, fax: +1 410 956 5785, email: ati@ATIcourses .com. http://www.ATIcourses.com.

FUNDAMENTALS OF RADAR SIGNAL PROCESSING
27–30 January 2020, Atlanta, Georgia, United States.

BASIC RADAR CONCEPTS
28–30 January 2020, Denver, Colorado, United States. Georgia Institute of Technology, Professional Education, P.O. Box 93686, Atlanta, GA 30377-0686, United States, +1 404 385 3500, fax: +1 404 894 8925. http://www.pe.gatech.edu.

MODELING AND SIMULATION OF PHASED ARRAY ANTENNAS
11–13 February 2020, Atlanta, Georgia, United States.

ADVANCED RF ELECTRONIC WARFARE PRINCIPLES
24–28 February 2020, Atlanta, Georgia, United States.

PRINCIPLES OF MODERN RADAR
24–28 February 2020, Denver, Colorado, United States.

MODERN ELECTRONIC AND DIGITAL SCANNED ARRAY ANTENNAS
24–28 February 2020, San Diego, California, United States.

PRINCIPLES OF PULSE DOPPLER RADAR
25–27 February 2020, Atlanta, Georgia, United States.

PRINCIPLES OF MILLIMETER-WAVE RADAR ELECTRONIC WARFARE
26–27 February 2020, Atlanta, Georgia, United States. Georgia Institute of Technology, Professional Educa-tion, P.O. Box 93686, Atlanta, GA 30377-0686, United States, +1 404 385 3500, fax: +1 404 894 8925. http://www .pe.gatech.edu.

SONAR PRINCIPLES AND ASW ANALYSIS
24–26 February 2020, Columbia, Maryland, United States. Applied Technology Institute, 349 Berkshire Drive, Riva, MD 21140-1433, United States, +1 888 501 2100 (toll-free U.S.) or +1 410 956 8805, fax: +1 410 956 5785, email: ati@ATIcourses .com. http://www.ATIcourses.com.

EARTH STATION AND TERMINAL DESIGN
3–6 March 2020, Columbia, Maryland, United States.

UNDERWATER ACOUSTIC MODELING AND SIMULATION
9–12 March 2020, Columbia, Maryland, United States.

SATELLITE COMMUNICATIONS DESIGN AND ENGINEERING
17–19 March 2020, Columbia, Maryland, United States.

SYNTHETIC APERTURE RADAR IMAGE FORMATION PROCESSING
17–20 March 2020, Atlanta, Georgia, United States.

ELECTRONIC WARFARE: PROTECTION AND ELECTRONIC ATTACK
17–20 March 2020, Columbia, Maryland, United States.

ACOUSTICS FUNDAMENTALS, MEASUREMENTS, AND APPLICATIONS
24–26 March 2020, Columbia, Maryland, United States. Applied Technology Institute, 349 Berkshire Drive, Riva, MD 21140-1433, United States, +1 888 501 2100 (toll-free U.S.) or +1 410 956 8805, fax: +1 410 956 5785, email: ati@ATIcourses .com. http://www.ATIcourses.com.

RADAR WARNING RECEIVERS FUNDAMENTALS
1–2 April 2020, Atlanta, Georgia, United States.

The EurAAP Leopold B. Felsen Award for Excellence in Electrodynamics

The Felsen Awards were conceived by Michael and Judy Felsen, heirs of the late Prof. Leopold B. Felsen (1924-2005), with the main purpose to keep alive Prof. Felsen's memory and scientific legacy, as well as to foster academic excellence in the electromagnetics community. The basic idea was to give recognition to outstanding scientific contributions from early stage researchers in electrodynamics, with emphasis on wave interactions with complex environments, subjects that were at the core of Prof. Felsen's research. Originally, several Felsen Awards were established, targeting national communities connected with former collaborators and students of Prof. Felsen.

Among these, the Felsen Awards established jointly by the University of Siena (Prof. Stefano Maci) and the University of Sannio (Prof. Vincenzo Galdi) in Italy were subsequently transformed and extended to a broader, international dimension. In agreement with the Felsen Family and in close cooperation with Prof. Juan R. Mosig, at that time chairing the European Association of Antennas and Propagation (EurAAP) Board, a global EurAAP Felsen Award for Excellence in Electrodynamics was established, and endowed with a generous year prize of US$5,000. To provide a world-class frame and broad visibility within the electromagnetics, antenna and propagation communities, the Award was connected with the annual European Conferences on Antennas and Propagation (EuCAP). An Award jury was created, formed by Profs. Vincenzo Galdi, Ehud Heyman, Raj Mittra, Juan Mosig, and Werner Wiesbeck. Starting from EuCAP'2015, the EurAAP Felsen Award has been delivered annually, and the complete list of Awardees is:

2015:   Francesco Andriulli (Telecom Bretagne / Institut Mines-Telecom, France)

2016:   Yakir Hadad (University of Texas, USA)

2017:   Juan Sebastian Gomez Diaz (University of California, Davis, USA)

2018:   ex aequo, Giorgio Carluccio (Delft University of Technology, The Netherlands) and Özgür Ergül (Middle East Technical University, Turkey)

2019:   Francesco Monticone (Cornell University, USA)

The 2019 Award, delivered during the EuCAP'2019 Conference in Krakow, Poland, was particularly eventful. For the first time, Michael Felsen was able to attend the ceremony with his wife and deliver personally the Award. In his speech, Prof. Felsen's son expressed his proudness in seeing the Felsen Award fully consolidated as one of the most prestigious prizes in our community. Then, with moving words, he went on recalling the connections of his family with Poland, the story of his father escaping the Nazi Holocaust and establishing in the USA as the distinguished professor that we remember, and finally his last wishes on his deathbed from which the Award was originated.

The next 2020 EurAAP Felsen Award will be delivered in Copenhagen, Denmark, during the EuCAP'2020 Conference (March 15—20, 2020). Information and application forms for the 2020 edition of the Award are available at: http://www.euraap.org/publications-and-news/EurAAP-Awards/EurAAP-Awards-Description

Potential candidates, nominators and endorsers are strongly encouraged to apply before the deadline of January 31, 2020.

—Juan R. Mosig (juan.mosig@epfl.ch),
Vincenzo Galdi (vgaldi@unisannio.it)

DEADLINE: JANUARY 31, 2020

The EurAAP Felsen Award 2019 ceremony: C. Mangenot, EurAAP Chair; Francesco Monticone, award winner and Michael Felsen

Rajeev Bansal

Roman Invisibility Cloak?

Let me start by retelling an old joke [1]:

Drilling 100 ft deep, German archaeologists found bits of copper in core samples collected from several parts of their country. After laboratory testing, they announced that 10,000 years ago, ancient German tribes had a nationwide telephone network. When the news reached England, British scientists undertook their own archaeological excavations and came across some pieces of glass at a depth of 200 ft. Their conclusion: 20,000 years ago, the ancient British had a fiber-optic network. Across the Channel, the French were outraged. Their scientist dug even deeper but couldn't find anything except dirt and rocks. However, the French papers had the last word: 30,000 years ago, the ancient French had a satellite-based wireless phone system.

Well, the French scientists have been digging holes again, and this time they seem to have found a version of Harry Potter's invisibility cloak [2]–[5]. First, a bit of background. As members of our technical community would recall, metamaterials can be synthesized by arranging [4]:

certain regular patterns of objects [that] can interact with waves in a way that steers them and modifies

> **The researchers drilled a periodic array of boreholes into topsoil and discovered that sound waves reflected most of their energy back toward the source when they encountered the first two rows of holes.**

their behavior. A curious feature of this phenomenon is that the objects themselves are much smaller than the waves themselves. But the combined effect of many objects arranged in a regular pattern has an important influence on the waves.

In 2006, a suitably designed grid of metal resonators was used to divert microwaves gently around a region of space. "To an outside observer *looking with microwave eyes* [italics mine], this region of space, and anything in it, disappears. In effect, the team had built the world's first invisibility cloak" [4]. The concept can be extended (at least in principle) to both light waves and sound (seismic) waves [2].

French civil engineer Stephane Brûlé, a coauthor of [5], "demonstrated the possibility of this kind of large-scale acoustic and seismic cloaking a few years ago with colleagues from the Fresnel Institute in Marseille. The researchers drilled a periodic array

of boreholes into topsoil and discovered that sound waves reflected most of their energy back toward the source when they encountered the first two rows of holes" [3]. While Brûlé was on vacation in the town of Autun in France, "he saw an aerial photograph showing the foundations of a Gallo-Roman theatre buried under a field just up the road. Although barely discernable, the markings in the field showed the outline of the first century AD building and he reckoned the semicircular structure bore an uncanny resemblance to one half of an invisibility cloak" [2]. Brûlé discovered similar features in the foundational structures of the Colosseum in Rome [3].

So did the Roman engineers know about metamaterials and their role in cloaking structures against the violent seismic waves of an earthquake? As physicist Greg Gbur noted [3]:

I doubt that the builders of structures in that era intentionally designed their buildings to be earthquake resistant, or even that they were able to unconsciously evolve their designs over time to make them more secure—the time scales seem too short. I could imagine, however, that there might be a sort of 'natural selection' that occurred, where megastructures built with inadvertent

earthquake cloaking might have survived longer than their counterparts, allowing us to see their remains now.

Does this archaeological find have an application to the design of smart cities in the future? Brûlé and his colleagues have developed computer models to show "how skyscrapers arranged in a circle could act as an invisibility cloak that creates a safe zone at its center" [4]. Urban planners, please take note.

REFERENCES

[1] R. Bansal, "What goes up…," *IEEE Antennas Propag. Mag.*, vol. 42, no. 3, pp. 102–103, June 2000.
[2] E. Cartlidge, "Did the Romans build seismic invisibility cloaks?" *Physics World*. Accessed on: Sept. 9, 2019. [Online]. Available: https://physicsworld.com/a/did-the-romans-build-seismic-invisibility-cloaks/
[3] J. Ouellette, "Study says ancient Romans may have built 'invisibility cloaks' into structures," *Ars Technica*. Accessed on: Sept. 9, 2019. [Online]. Available: https://arstechnica.com/science/2019/05/study-says-ancient-romans-may-have-built-invisibility-cloaks-into-structures/
[4] Emerging Technology, "Roman amphitheaters act like seismic invisibility cloaks," *MIT Technology Review*. Accessed on: Sept. 9, 2019. [Online]. Available: https://www.technologyreview.com/s/613550/roman-amphitheaters-act-like-seismic-invisibility-cloaks/
[5] S. Brûlé, S. Enoch, and S. Guenneau, Role of nanophotonics in the birth of seismic megastructures. Sept. 9, 2019. [Online]. Available: https://arxiv.org/abs/1904.05323

COURSES

RADAR WARNING RECEIVER SYSTEM DESIGN AND ANALYSIS
14–16 April 2020, Shalimar, Florida, United States.

ANTENNA ENGINEERING
20–24 April 2020, Atlanta, Georgia, United States.

PHASED ARRAY RADAR SYSTEMS
21–24 April 2020, Atlanta, Georgia, United States. Georgia Institute of Technology, Professional Education, P.O. Box 93686, Atlanta, GA 30377-0686, United States, +1 404 385 3500, fax: +1 404 894 8925. http://www.pe.gatech.edu.

AESA RADAR AND ITS APPLICATIONS
28–30 April 2020, Columbia, Maryland, United States. Applied Technology Institute, 349 Berkshire Drive, Riva, MD 21140-1433, United States, +1 888 501 2100 (toll-free U.S.) or +1 410 956 8805, fax: +1 410 956 5785, email: ati@ATIcourses.com. http://www.ATIcourses.com.

NEAR-FIELD ANTENNA MEASUREMENT TECHNIQUES
4–8 May 2020, Boulder, Colorado, United States.

MODELING AND SIMULATION OF ANTENNAS
5–8 May 2020, Atlanta, Georgia, United States. Georgia Institute of Technology, Professional Education, P.O. Box 93686, Atlanta, GA 30377-0686, United States, +1 404 385 3500, fax: +1 404 894 8925. http://www.pe.gatech.edu.

RADAR SYSTEMS ENGINEEERING
2–4 June 2020, Atlanta, Georgia, United States.

RADAR CROSS SECTION REDUCTION
8–10 June 2020, Atlanta, Georgia, United States.

MODELING AND SIMULATION OF RADAR SYSTEMS
8–11 June 2020, Las Vegas, Nevada, United States.

FUNDAMENTALS OF RADAR SIGNAL PROCESSING
8–11 June 2020, Las Vegas, Nevada, United States.

BASIC ANTENNA CONCEPTS
9–11 June 2020, Las Vegas, Nevada, United States.

RADAR SOFTWARE DEVELOPMENT
16–18 June 2020, Atlanta, Georgia, United States.

BASIC RADAR CONCEPTS
23–25 June 2020, Las Vegas, Nevada, United States. Georgia Institute of Technology, Professional Education, P.O. Box 93686, Atlanta, GA 30377-0686, United States, +1 404 385 3500, fax: +1 404 894 8925. http://www.pe.gatech.edu.

AIRBORNE AESA RADAR
14–16 July 2020, Las Vegas, Nevada, United States.

PRINICIPLES OF PULSE DOPPLER RADAR
14–16 July 2020, Las Vegas, Nevada, United States.

PRINCIPLES OF MODERN RADAR
27–31 July 2020, Las Vegas, Nevada, United States. Georgia Institute of Technology, Professional Education, P.O. Box 93686, Atlanta, GA 30377-0686, United States, +1 404 385 3500, fax: +1 404 894 8925. http://www.pe.gatech.edu.

A Father Has Two Sons or a Parent Has Two Children?

Dan Jiao

EDITOR'S NOTE

In this "Women in Engineering" column, Prof. Dan Jiao from the School of Electrical and Computer Engineering at Purdue University and chair of the IEEE Antennas and Propagation Society (AP-S) Women in Engineering Committee, analyzes the state of women in engineering and career prospects and opportunities within the AP-S. She also recalls recent AP-S panel events on the subject organized at IEEE International Conferences.

Francesca Vipiana

Prof. Jiao is a recipient of many awards recognizing her scientific career, including the 2013 S.A. Schelkunoff Prize Paper Award of the IEEE AP-S and the 2008 National Science Foundation Career Award. Moreover, she was among 21 female faculty selected across the United States as a 2014–2015 fellow of the Executive Leadership in Academic Technology and Engineering at Drexel, a national leadership program for women in the academic science, technology, engineering, and mathematics fields.

In my research, I often deal with a binary tree. My male students like to say, "a father node has two sons," even though I correct them repeatedly, saying, "remember, a parent has two children." The next time, during our research meeting, it comes back again! I am positive that my students will eventually get it right, but they did not invent these words—they are written in the books.

Once in my Electrical and Computer Engineering (ECE) 618 (computational electromagnetics) class, I gave the following riddle to my students:

A father and his son are in a car accident. The father is killed, and the son is seriously injured. The son is taken to the hospital where the surgeon says, "I cannot operate, because this boy is my son."

A son has two fathers? Most of my students did not figure it out. After taking a few minutes, some of them finally realized that the boy's mother could be a surgeon.

As you can see, even when we have the best of intentions, we may have certain unconscious gender bias rooted in our minds. Research shows that our culture's strong gender stereotypes extend beyond image to performance, leading to the misbelief that men are more competent than women. Managers—both male and female—continue to favor men over equally qualified women in hiring, compensation, performance evaluation, and promotion decisions [1]. This limits opportunities for women and deprives organizations of valuable talent [1]. The problem is a difficult one to solve. However, let's start by getting to know the problem, become aware of the bias, and work on inclusion and diversity daily in our society.

As of May 2018, we had 8,080 members in the IEEE Antennas and Propagation Society (AP-S), out of whom 616—7.6%—were women (Figure 1). Of these 616 women members, 14 are IEEE Fellows and 98 are Senior Members. Given such a low percentage of women members, we need to encourage women at all levels to join the AP-S. To do so, in the past two years we have held several special Women in AP panel and networking events at AP-S conferences as well as conferences sponsored by the Society. The goal of these panel events is to stimulate discussions of the problem and increase awareness of the challenges women face during their careers and professional development. In addition, we brainstorm together with the audience on how to overcome these challenges and how to create a more diverse and inclusive environment to better support a woman's career in the AP-S.

One event was organized in the 2019 IEEE Microwave Theory and Techniques Society's (MTT-S's) International Conference on Numerical

Electromagnetic and Multiphysics Modeling and Optimization (NEMO), held in Cambridge, Massachusetts 29–31 May 2019. NEMO is an annual focal event on electromagnetic- and multiphysics-based computer-aided design, which rotates between Europe, North America, and Asia. The women's panel and networking event (see https://nemo-ieee.org/2019/index.html) at NEMO was financially cosponsored by the IEEE AP-S and MTT-S, and it was very well attended.

Prof. Wenquan Che, who is the chair of the Women in Microwave Subcommittee for the IEEE MTT-S Administrative Committee (AdCom), as well as the representative for MTT-S at the IEEE Women in Engineering Society, chaired the event. The panelists included a diverse group of female and male leaders from both academia and industry (Figure 2):

- Maurizio Bozzi, a professor at the University of Pavia, Italy, an elected member of the AdCom of the

FIGURE 1. The membership of women in the IEEE AP-S as of May 2018 (note that not all members provided their gender information).

IEEE MTT-S for term 2017–2019, and the chair of the Meetings and Symposia Committee of MTT-S AdCom
- Malgorzata Celuch, a cofounder and the chief executive officer (CEO) of Quick Wave Software for Electromagnetic Design, a Polish high-tech company, and previously

a faculty member with Warsaw University, Poland
- Dan Jiao (myself), a professor at Purdue University, West Lafayette, Indiana, and chair of the Women in Engineering (WIE) committee in IEEE AP-S
- Dominique Schreurs, a professor with University of Leuven, Belgium,
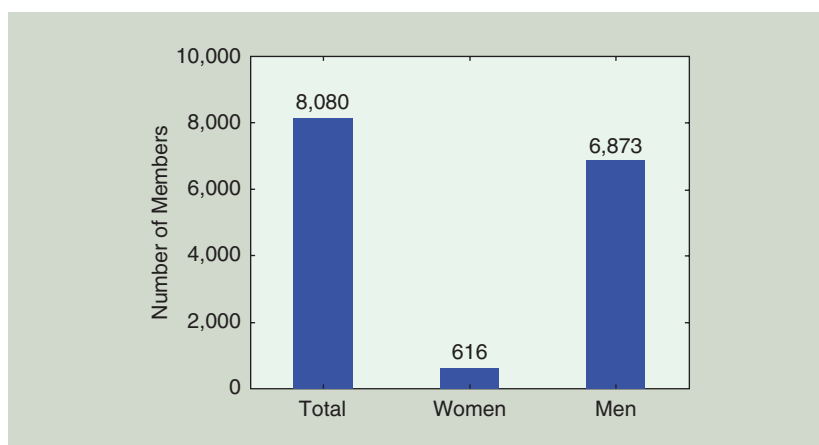

Call for Special Issues/Sections

IEEE Antennas and Propagation Magazine is inviting proposals for special issues (6 papers) or special sections (2–4 papers).

IEEE Antennas and Propagation Magazine publishes feature articles and columns that describe engineering activities within its scope, taking place in industry, government, and universities. Emphasis is placed on providing the reader with a general understanding of either a particular subject or of the technical challenges being addressed by various organizations, as well as their capabilities to cope with these challenges. Review, tutorial, and historical articles are welcome.

The focus of special issues/sections could be on either established or emerging research topics relevant for the IEEE Antennas and Propagation Society. Cross-disciplinary topics are equally welcome.

Guidelines for Submission:

A special issue/cluster proposal should be sent to Editor-in-Chief Prof. Francesco P. Andriulli (apm-eic@ieee.org) and it should contain:

1) The proposed title of the special issue/section.
2) A short abstract describing the topic and its relevancy for the AP-S community.
3) The list of prospective guest editors with affiliations.
4) A tentative list of potential contributors.

The proposals will be evaluated based on

- Relevancy and impact
- Potential to attract quality contributions
- Scientific standing of guest editors.

and the first female MTT-S president (April 2018–2019)

- Harry Skinner, Intel fellow, and director of RF Platform Technologies at Intel Labs, Santa Clara, California, leading Intel's research into radio-frequency interference and radio-frequency resiliency, front-end solutions, and antenna systems
- Qijun Zhang, a chancellor's professor with Carleton University, Ottawa, Ontario, Canada, and a fellow of the Canadian Academy of Engineering; chair of the Department of Electronics, Carleton University 2009–2011, and the Interim Associate Dean of Faculty of Engineering and Design 2016–2017.

The event was started by an interesting talk given by Prof. Maurizio Bozzi, "Is Engineering a Profession for Women?" Prof. Bozzi shared with the audience data from AlmaLaurea and the Ministry of University and Research (MIUR). AlmaLaurea is an Italian inter-university consortium established in 1994 and currently counts 75 universities as members. The consortium is supported and funded by the universities and by MIUR. The data shows that the number of female students in engineering master courses was 21.9%, 25.1%, and 23.2% for the years 2007, 2012, and 2017, respectively. It also shows that all performance parameters were practically identical between male and female students; the difference lies in the perception of the role of the engineer, be it soldering transistors or saving human lives. In addition, Prof. Bozzi reported that, in Italian universities (Figure 3), female assistant professors in electromagnetic fields accounted for 21.4% in 2017, which is close to the number of the female students in the discipline. However, this number dropped to 15.6% at the associate professor level; and further dropped to 2.2% at the full professor level. Prof. Bozzi concluded his talk by making a crucial observation: male and female faculty members have a similar starting point, but female members seem to experience a more difficult career path.

Following Prof. Bozzi's opening speech, panelists had a lively discussion. One panelist commented that the reason for women's underrepresentation in the field is because, traditionally, they are expected to have more responsibilities at home. The time when they should be promoted to associate or full professors is often when they have children or aging parents to take care of. If these responsibilities are not equally shared by men, it is unavoidable that many women would have to pause their careers. For example, one female faculty member found that she had to compete with her students for a promotion when she returned to school after taking care of family responsibilities. Another panelist asked whether this problem can be better addressed by establishing different evaluation systems to allow for diverse career paths. Some also pointed out that women may measure their successes in a different way. Some women may not be energized by goals like becoming president, CEO, or a highly accomplished professor. That is understandable because people make diverse choices.

However, for women who want to pursue these career goals, the AP-S, institutions, organizations, and so forth should provide equal-opportunity, support work-life balance, and eliminate unacceptable biases so that women's potentials can be fully realized. For example, research

FIGURE 2. The organizers and panelists at the NEMO 2019 women's panel and networking event (from left): Wenquan Che, Maurizio Bozzi, Dan Jiao, Qijun Zhang, Malgorzata Celuch, Harry Skinner, and Dominique Schreurs.
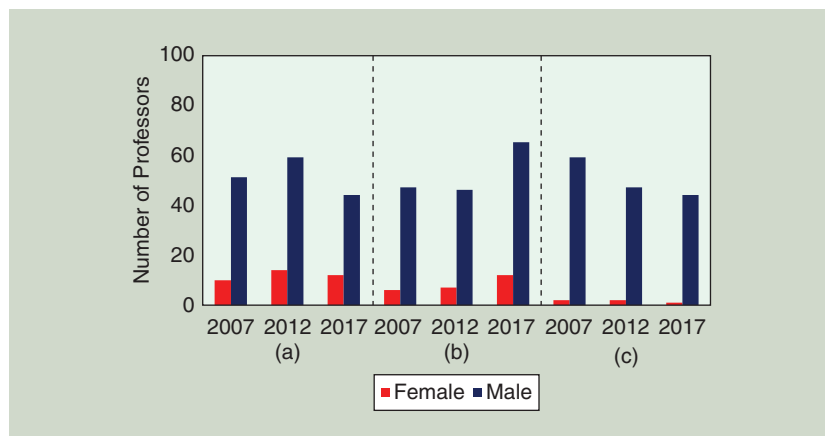

FIGURE 3. The number of female professors in electromagnetic fields in Italian universities: (a) assistant professors, (b) associate professors, and (c) full professors. (Source: MIUR; used with permission.)

showed that "success and likeability are positively correlated for men and negatively correlated for women" [4]. When a man is successful, he is liked by both men and women; when a woman is successful, people of both genders like her less [4]. Thus, it hurts a woman to become successful in her professional life. It is thus important to let people be aware of such biases and understand that these are not acceptable.

In addition, a breakfast panel event generously sponsored by Raytheon was organized during the AP-S's 2018 flagship conference, the IEEE International Symposium on Antennas and Propagation and USNC-URSI Radio Science 2018 Symposium, held in Boston, Massachusetts 8–13 July; see https://www.2018apsursi.org/WIE.asp. Many thanks to the following 2018 panelists for contributing their precious time and efforts to support this event (Figure 4):

- Weng Chew, distinguished professor, School of Electrical Engineering, Purdue University, West Lafayette, Indiana, and 2018 president of the AP-S
- Ellen Ferraro, director of research and technology, Integrated Defense Systems Advanced Technology, Raytheon Company, Waltham, Massachusetts
- Susan Hagness, Philip Dunham Reed Professor, Department of Electrical and Computer Engi-

neering, University of Wisconsin, Madison
- Leo Kempel, dean, College of Engineering, Michigan State University, East Lansing
- Francesca Vipiana, associate professor of electronics and telecommunications, Politecnico di Torino, Italy
- Mona Zaghloul, professor, director, George Washington University Institute of Microelectromechanical Systems and VLSI Technologies, Washington, DC.

Prof. Alkim Akyurtlu of the University of Massachusetts, Lowell, and I moderated this event. I found the panel discussions very eye-opening. For example, several years ago, the souvenir given to newly elevated IEEE Fellows was not something that would be used or appreciated by women. As another example, one of the panelists had always been the only female student in her class and research group during both her undergraduate and graduate study. She had to work with gender differences to navigate through the male-dominated system.

> **Male and female faculty members have a similar starting point, but female members seem to experience a more difficult career path.**

Today, the situation has been improved significantly for women, but we still face deep problems in gender equality.

One study that particularly strikes me was conducted by my university's ADVANCE–Purdue Center on female faculty experiences in the classroom [2], [3]. The objective of this study was to understand the classroom experiences of female STEM faculty regarding student interactions and perceptions. The results indicated that the overall evaluation score for female instructors was minus 0.467 that of male instructors with 5 representing a full score. Student course evaluations also revealed that women professors face the added burden of emotional labor. *Emotional labor* is defined as the performance of certain emotions as part of one's job. For example, occupations traditionally held by women (e.g., nurses), often require stereotypical "feminine emotional displays" (e.g., nurturing, soothing), and emotional labor is as essential to these jobs as mental or physical labor (Figure 5). Unlike men, women were expected to be 1) friendly and likeable; 2) encouraging and enabling toward students; 3) understanding, caring, and kind; and 4) pretty (only from male student responses). Women professors received criticism if they failed to demonstrate enough emotional labor or were not pretty enough. In addition, 27% of

FIGURE 4. The panelists and organizers of Women in Antennas and Propagation Panel at the IEEE AP-S/URSI 2018 Symposium (from left): Payal Majumdar, Dan Jiao, Ellen Ferraro, Francesca Vipiana, Alkim Akyurtlu, Leo Kempel, Mona Zaghloul, Weng Chew, and Michael Shields.

Emotional Labor
- Performance of Certain Emotions as Part of One's Job
- Occupations Traditionally Held by Women Often Require Stereotypic "Feminine Emotional Displays"
- Emotional Labor Is as Essential to the Job as Mental or Physical Labor

FIGURE 5. The added burden of emotional labor faced by women professors.

women faculty indicated they had been disrespected by students, versus 2% of the STEM male respondents, and 22% indicated that they experienced some form of gender inequity. For example, they observed or were aware of receiving different treatment by students than their male counterparts.

A father has two sons, or a parent has two children? There is still a long way to go for the latter to be realized. But let's just do *something*. This something could be as simple as realizing that a surgeon can be a woman; sharing your family responsibilities; not viewing an ambitious and driven woman negatively; thinking about whether you have the same standards for caring and attractiveness in your male professors; attending WIE events; or simply joining the AP-S so that we have more women in our profession!

CONCLUSIONS

While I was preparing the final version of this article, I received our Society's 2019 membership data. We currently have 806 female IEEE AP-S members, which constitute 9% out of the overall 8,937 Society members. This is a very significant improvement compared to 2018. In addition, out of these 806 female members, 15 are IEEE Fellows and 123 are Senior Members, thanks to the efforts made by our women members and membership committee, as well as both female and male colleagues in our Society as a whole. Let's keep it up and work toward a more fruitful year in 2020! If you have any suggestions or comments regarding the issues discussed in this article, please feel free to contact me at djiao@purdue. edu. I look forward to hearing from you.

AUTHOR INFORMATION

Dan Jiao (djiao@purdue.edu) is a professor in the School of Electrical and Computer Engineering at Purdue University, West Lafayette, Indiana. Her research interests include computational electromagnetics, high-speed very large-scale integration circuit design and analysis, applied electromagnetics, and fast and high-capacity algorithms. She currently serves as the chair of the Women in Engineering Committee in the IEEE Antennas and Propagation Society.

REFERENCES

[1] A. Grant and S. Sandberg, "When talking about bias backfires," *NY Times*, Dec. 2014. [Online]. Available: https://www.nytimes.com/2014/12/07/opinion/sunday/adam-grant-and-sheryl-sandberg-on-discrimination-at-work.html
[2] E. A. Hoffmann, "Evaluation of women and men professors: How gender scripts affect students' assessments," presented at the ADVANCE-Purdue Gender and STEM Research Symp. 3, 2013. [Online]. Available: https://docs.lib.purdue.edu/advancegsr/2013/presentations/3
[3] S. R. Geier and C. L. Sahley "Women faculty in STEM colleges at Purdue University: Perceptions of the classroom environment related to student interactions," presented at the ADVANCE-Purdue Gender and STEM Research Symp. 9, 2013. [Online]. Available: https://docs.lib.purdue.edu/advancegsr/2013/presentations/9
[4] S. Sandberg, *Lean In*. New York: Knopf, 2013.

2020 IEEE CONFERENCE ON ANTENNA MEASUREMENT AND APPLICATIONS (CAMA)

23–25 NOVEMBER 2020, ANTIBES JUAN-LES-PINS, FRANCE

The 2020 IEEE CAMA wishes to promote women in electrical engineering.

We are about to celebrate the centenary of the first French woman to graduate college with an engineering degree, however, women currently represent 25% of engineers in France but only 4% as far as electrical engineering are concerned.

The 2020 IEEE CAMA conference, which will be held from 23 to 25 November 2020 in Antibes Juan-les-Pins, France, will promote women in this field by organizing a special session titled "Women in EM-Modeling and Measurements for Microwave Imaging Systems," organized by Prof. Claire Migliaccio.

Microwave imaging is becoming more important in our daily lives through a large panel of applications such as in the medical field, transportation, the nondestructive control of food, or homeland security. The objective of this session is to present the latest advances in measurement and numerical modeling mainly oriented toward microwave imaging.

Organizer

Prof. Claire Migliaccio, University of Nice Sophia Antipolis

Supervisor and Supervisee Expectations

Qammer H. Abbasi

There are different styles of supervision discussed in the literature [1]–[3]. They are based on either structure and support, purpose and process, a supervisor's knowledge and skills, or the nature and level of supervision required. These styles include [1]:

1) laissez-faire: where a supervisor has less interaction with the student and provides few specific directions for research
2) pastoral: where a supervisor provides considerable personal care and support, almost on a daily basis
3) contractual: where a supervisor administers direction and exercises good management skills and interpersonal relationships.

Due to different styles of supervision and the varying expectations between students and supervisors, the level of satisfaction between supervisor and student is decreasing day by day, and the reasons for this are rightly pointed out in [4]. They are not limited to:

1) an unrealistic expectation from a student without considering inclusivity with other students
2) an undefined student–supervisor relationship level (whether it should be more friendly and approachable or more serious and to the point)
3) an undefined level of the commitment that should be given to the stu-

---

EDITOR'S NOTE

The Young Professionals Committee (YPC) of the IEEE Antennas and Propagation Society (AP-S) is committed to encouraging and supporting young professionals to be more engaged and actively participate in the Society. We are happy to announce that two additional members, Dr. Qammer H. Abbasi (University of Glasgow) and Dr. Anton Menshov (CEMWorks, Inc.), have just officially joined the YPC. Dr. Abbasi has contributed to this interesting article on the important topic of supervisor–supervisee expectations.

Hao Xin

We would like to thank all of the Society members who attended the wonderful AP-S YPC event at the World of Coca Cola on 19 July 2019 in Atlanta, Georgia. We extend our invitation for more members, especially those who work in industry, to join the YPC as volunteers.

---

dent by his or her supervisor. The possible solution to satisfy these issues is the training of supervisors (especially early career) and the proper mentoring of new supervisors by senior staff members who have worked with a large pool of students and have vast experience.

When we set expectations, it seems that the Goldilocks Rule should be considered: "too little or too much, and it is no good." According to [5], the student–supervisor relationship should not have any hindrance between the parties, and a possible solution to remove this barrier is to arrange a more friendly meeting with the student outside the office, over a cup of coffee for example, to boost the student's confidence. This can ultimately contribute to the neutral

and leveling atmosphere that aligns with a collaborative approach to supervision. Students at a different stage of degree (either junior or senior, sharp or weak) should be treated differently, and supervision should be flexible in terms of the student's phase. There should also be a balance in student–supervisor meetings. Less frequent meetings do not help develop a supervisory-student relationship and may create a less friendly relationship with the student. It is the responsibility of the supervisor to provide students following support:

1) guidance and support in terms of research direction and resources
2) reasonable opportunities for development and training by letting them attend short courses, conferences, and training

3) timely feedback on written manuscripts and examination training by performing mock exercises
4) correct expectations and a balanced relationship, as mentioned previously
5) instruction and guidance to the student on effective management, intellectual property rights, and retention of research data.

To better understand the expectations between students and their supervisors, discussions were held with many students and supervisors both in developed and developing countries. Both students and supervisors were asked the most important attributes they expected from each other. The conclusion from this discussion was that encouragement and friendly attitude are the two most desired supervisor attributes expected by students. Students tend to avoid supervisors who set hard deadlines for them. They also mostly prefer biweekly meetings and do not much appreciate the idea of on-demand meetings. As for supervisor expectations, they would like to supervise students who are responsive and become independent early in their research so that the supervisors can oversee their studies. Supervisors are not interested in the social activities of their student and are more concerned with assigned task delivery only.

ACKNOWLEDGMENTS

AUTHOR INFORMATION

Qammer H. Abbasi (qammer.abbasi@glasgow.ac.uk) is an assistant professor at the James Watt School of Engineering, University of Glasgow, and a visiting assistant with Queen Mary University of London. He is an IEEE Antennas and Propagation Society Young Professionals Committee member and also an Institution of Engineering and Technology Technical and Professional Networks Committee member on antenna and propagation. He has contributed to a research portfolio of around £4 million, seven books, and more than 250 leading international technical journal and peer-reviewed conference papers. His research has been featured on the BBC, Scotland TV, and many other media houses.

REFERENCES

[1] T. Gatfield, "An investigation into PhD Supervisory Management Styles: Development of a dynamic conceptual model and its managerial implications," *J. Higher Educ. Policy Manage.*, vol. 27, no. 3, pp. 311–325, 2005.
[2] N. Murphy, J. Bain, and L. Conrad, "Orientations to research higher degree supervision," *Higher Educ.*, vol. 53, no. 2, pp. 209–234, 2007.
[3] A. Lee, "How are doctoral students supervised? Concepts of doctoral research supervision," *Stud. Higher Educ.*, vol. 33, no. 3, pp. 267–281, 2008.
[4] G. Turner, "Learning to supervise: Four journeys," *Innovations Educ. Teaching Int.*, vol. 52, no. 1, pp. 86–98, 2015.
[5] S. R. Hemer, "Informality, power and relationships in postgraduate supervision: Supervising PhD candidates over coffee," *Higher Educ. Res. Develop.*, vol. 31, no. 6, pp. 827–839, 2012.

CORRECTION

In the article, "Paving the Way for Higher-Volume Cost-Effective Space Antennas" published in the October 2019 issue of *IEEE Antennas and Propagation Magazine* [1], the authors mistakenly omitted a coauthor: the name Nicholas Bouchard Kinch (MDA Montréal, Canada) should have been included in the byline as follows: Karim Glatre, Louis Hildebrand, Nicholas Bouchard Kinch, Erick Charbonneau, Jeremy Perrin, and Eric Amyotte.

AUTHOR INFORMATION

Nicholas Bouchard Kinch (Nicholas.BouchardKinch@mdacorporation.com) is a manufacturing engineer at MDA, Montréal, Canada, who leads manufacturing automation including robotic assembly and test and Industry 4.0 innovations that link automated systems to MES, ERP and QMS infrastructures; transforming MDA's focus to align to NewSpace constellation program requirements.

REFERENCE

[1] K. Glâtre, L. Hildebrand, E. Charbonneau, J. Perrin, and E. Amyotte, "Paving the way for higher-volume cost-effective space antennas: Designing for manufacturing, assembly, integration, and test," *IEEE Antennas Propag. Mag.*, vol. 61, no. 5, pp. 47–53, Oct. 2019. doi: 10.1109/MAP.2019.2932313.

CALL FOR PAPERS

ICEAA '20
IEEE APWC '20

ICEAA - IEEE APWC

August 10-14, 2020, Honolulu, Hawaii, USA

www.iceaa-offshore.org

August 10-14, 2020 - Honolulu, Hawaii, USA

ICEAA 2020
International Conference on
Electromagnetics in Advanced Applications

IEEE APWC 2020
IEEE-APS Topical Conference on
Antennas and Propagation in
Wireless Communications

The twenty-second edition of the International Conference on Electromagnetics in Advanced Applications (ICEAA 2020) is supported by the Politecnico di Torino, and by the Torino Wireless Foundation with the principal technical cosponsorship of the IEEE Antennas and Propagation Society and the technical cosponsorship of the International Union of Radio Science (URSI). It is coupled to the tenth edition of the IEEE-APS Topical Conference on Antennas and Propagation in Wireless Communications (APWC 2020). The two conferences consist of invited and contributed papers, and share a common organization, registration fee, submission site, workshops and short courses, banquet, and social events. The proceedings of the conferences will be submitted to the IEEE Xplore Digital Library.

Information for Authors

Authors must submit a full-page abstract electronically by March 6, 2020. Authors of accepted contributions must submit the full paper, executed copyright form and registration electronically by June 1, 2020. Instructions are found on the website. Each registered author may present no more than two papers. All papers must be presented by one of the authors. Please refer to the website for details.

Deadlines:

Abstract submission	March 6, 2020
Notification of acceptance	April 10, 2020
Full paper and presenter registration	May 25, 2020

ICEAA Topics

1. Adaptive and reconfigurable antennas
2. Complex media
3. Electromagnetic applications to biomedicine
4. Electromagnetic applications to nanotechnology
5. Electromagnetic education
6. Electromagnetic measurements
7. Electromagnetic modeling of devices and circuits
8. Electromagnetic packaging
9. Electromagnetic properties of materials
10. Electromagnetic theory
11. EMC/EMI/EMP
12. Finite methods
13. Frequency selective surfaces
14. High power electromagnetics
15. Integral equation and hybrid methods
16. Intentional EMI
17. Inverse scattering and remote sensing
18. Metamaterials and metasurfaces
19. Optoelectronics and photonics
20. Phased and adaptive arrays
21. Plasma and plasma-wave interactions
22. Printed and conformal antennas
23. Radar cross section and asymptotic techniques
24. Radar imaging
25. Radio astronomy (including SKA)
26. Random and nonlinear electromagnetics
27. Reflector antennas
28. Technologies for mm and sub-mm waves

IEEE APWC Topics

1. Active antennas
2. Antennas and arrays for security systems
3. Channel modeling
4. Channel sounding techniques for MIMO systems
5. Cognitive radio
6. Communication satellite antennas
7. DOA estimation
8. EMC in communication systems
9. Emergency communication technologies
10. Indoor and urban propagation
11. Low-profile wideband antennas
12. MIMO systems
13. Mobile networks
14. Multi-band and UWB antennas and systems
15. OFDM and multi-carrier systems
16. Propagation models
17. Radio astronomy (including SKA)
18. RFID technologies
19. Signal processing antennas and arrays
20. Small mobile device antennas
21. Smart antennas and arrays
22. Space-time coding
23. Vehicular antennas
24. Wireless communications
25. Wireless mesh networks
26. Wireless power transmission and harvesting
27. Wireless security
28. Wireless sensor networks

All inquiries should be directed to:

Prof. Roberto D. Graglia
Chair of Organizing Committee
Dipartimento di Elettronica e TLC
Politecnico di Torino
Corso Duca degli Abruzzi, 24
10129 Torino, ITALY
roberto.graglia@polito.it

Prof. Piergiorgio L. E. Uslenghi
Chair of Scientific Committee
Department of ECE (MC 154)
University of Illinois at Chicago
851 South Morgan Street
Chicago, Illinois 60607-7053, USA
uslenghi@uic.edu

POSTDOCTORAL POSITION

Pennsylvania State University

The Computational Electromagnetics and Antennas Research Lab at The Pennsylvania State University is seeking highly qualified individuals for postdoctoral positions. Applicants should visit http://cearl.ee.psu.edu/ or contact Prof. Douglas H. Werner (dhw@psu.edu) for more information.

FACULTY POSITION

Fuzhou University, Fujian, China

There are multiple faculty openings for postdoctoral fellows and assistant/associate/full professors in electronics and communications at Fuzhou University, Fujian, China. Mandarin or English speakers are welcome. Competitive financial packages will be provided. Email inquiries or applications to dean_pie@fzu.edu.cn.

IEEE ANTENNAS AND PROPAGATION SOCIETY

Consider Publishing with the IEEE Press

IEEE Press books are published by John Wiley and Sons, and are reviewed by IEEE Societies and their members. The IEEE Press Liaison Committee of the Antennas and Propagation Society solicits, reviews and in some cases sponsors texts for the IEEE Press. The IEEE Antennas and Propagation Society (AP-S) shares in the proceeds from sales of sponsored books.

The goal of the committee is to seek new and some reprinted texts in the area of antenna and propagation theory and system design. The committee also works with the editor of the IEEE series on Electromagnetic Wave Propagation and Applications to find reviewers and to provide sponsorship for selected mutually agreed titles.

At present, the committee is soliciting books on antennas and propagation in general, but specifically in the areas of 5G technology, MIMO and orbital angular momentum systems, metasurface propagation and radiation, and wearable antennas.

Authors interested in publication with the Press may contact any of the committee members or the Press directly. These individuals are listed below:

AP-S/IEEE Press Liaison Committee: Gary Brown, Bob Mailloux (Chair: mrmailloux@comcast.net), Ross Stone, Daniel Weile and Douglas Werner (Editor of EM Wave Propagation and Applications series).

IEEE Press: Mary Hatcher (mhatcher@wiley.com)

Submitting your draft or manuscript to the Liaison Committee will assure that it will be read or reviewed by knowledgeable colleagues in the AP-S community.

The Tale of Two Electromagnetics Friends, Yahya and Nader: From the University of Tehran to Receiving Ellis Island Medals of Honor

by Yahya Rahmat-Samii and Nader Engheta

The Medal

As written on the official website of Ellis Island Honors Society: *"The Ellis Island Medals of Honor embody the spirit of America in their salute to tolerance, brotherhood, diversity and patriotism."* They are presented each year *"to a select group of individuals whose accomplishments in their field and inspired service to the nation"* are worthy of commendations. The Ellis Island Honors Society, the medal's sponsoring organization, is proud that since its founding in 1986, the Medal (see above) has been officially recognized by the US House of Representatives and the U.S. Senate as "one of our nation's most prestigious awards" and its honorees are recorded annually in the Congressional Record.

The award description states: The Ellis Island Medals of Honor recognizes "individuals who have made it their mission to share, with those less fortunate, their wealth of knowledge, indomitable courage, boundless compassion, unique talents and selfless generosity." They do so while acknowledging their debt to their ethnic heritage and they uphold the ideals and spirit of America. Since the medal was founded, distinguished and diverse Americans including Presidents Ronald Reagan and William J. Clinton, as well as five other presidents of the United States have been honored.

Award Ceremony

On May 11, 2019, both Prof. Yahya Rahmat-Samii and Prof. Nader Engheta received the prestigious Ellis Island Medals of Honor at an elegant and spectacular award ceremony held on the historical Ellis Island, New York. After a beautiful sunset ride on a boat to Ellis Island from New York, the award ceremony was held in the grand hall of the historical building where over 11 million immigrants have passed through to come to the United States. The U.S. military flags were on display at the entrance and the invited attendees were paraded in with their formal attire. The place is now a museum displaying many historical photos of people who arrived here including Albert Einstein. It was a breathtaking formal dinner ceremony attended by the awardees and their families. Yahya and Nader and their families were at the same table in the ceremony hall.

Each awardees' name was individually called upon and the awardees walked to an ornate stage and received their medals. Their names, affiliations and contributions were read and their photos were shown on a big screen. At the end of the ceremony, the awardees and their families were taken back to the boat and cruised by the Statue of Liberty with amazing fireworks planned specifically for this event. The 2019 medal recipients were all highly accomplished individuals including, Representative Adam Schiff of California, former Google Chair and CEO Eric Schmidt, MasterCard CEO Ajay Banga, IBM CEO Ginni Rometty, former Apple CEO John Sculley, former PepsiCo CEO Indra Nooyi, Dr. Sanjay Gupta of CNN, Vice Admiral Mary Jackson, and others. In previous years, seven U.S. presidents, Nobel Laureate Elie Wiesel, Muhammad Ali, Rosa Parks, and Lee Iacocca also received the honor, to just name a few. A complete list of past Medalists can be found on www.EIHonors.org; video of the event can be viewed at www.EIHonorsVideo.org.

Tale of Two Friends

Now about the tale of the two electromagnetics friends, Yahya and Nader. They were both born in Tehran, Iran, and both graduated from University of Tehran with the highest distinctions from the engineering faculty in the electrical Engineering Department. They both came to the United States receiving their Ph.D. degrees focusing on the subject of electromagnetics. Yahya finished at the University of Illinois, Urbana-Champaign, and Nader graduated from Caltech. Upon graduation Yahya joined NASA/CalTech/JPL and became one of the youngest Senior Research Scientists at JPL. Subsequently he joined UCLA as a full professor and advanced to the rank of Distinguished Professor and the holder of the Northrop Grumman Chair in Electromagnetics. Similarly for Nader, after receiving his Ph.D. from Caltech and spending one year as a postdoctoral fellow at Caltech and four years as a Senior Research Scientist at Kaman Sciences Corporation's Dikewood Division in Santa Monica, California, Nader joined the faculty of the University of Pennsylvania where he is currently the H. Nedwill Ramsey Professor, with affiliations in the Departments of Electrical and Systems Engineering, Bioengineering, Materials Science and Engineering, and Physics and Astronomy. They both received the IEEE Electromagnetics Award, the IEEE Antennas and Propagation Distinguished Achievement Award and the URSI Medals. Besides the aforementioned similar awards, Yahya and Nader have received numerous other top awards for their research activities.

Yahya and Nader are electromagnetics friends with common languages in Farsi, English, and Maxwell's equations who both received the coveted Ellis Island Medals of Honor (Nader, left, and Yahya, right) in May 2019.

Yahya Rahmat-Samii (rahmat@ee.ucla.edu) is a Distinguished Professor, holds the Northrop-Grumman Chair in electromagnetics at UCLA, is a Fellow of the IEEE, URSI, ACES, AMTA and EMA, was elected to the U.S. National Academy of Engineering, and is a recipient of the 2011 IEEE Electromagnetics Award, 2011 UCLA Distinguished Teaching Award, 2007 IEEE Chen-To Tai Distinguished Educator Award, and 2005 Booker Gold Medal of URSI.

Nader Engheta (engheta@ee.upenn.edu) is the H. Nedwill Ramsey Professor at University of Pennsylvania, a Fellow of the IEEE, OSA, APS, SPIE, URSI, MRS, and AAAS, was elected to the U.S. National Academy of Inventors, and is a recipient of the 2012 IEEE Electromagnetics Award, 2014 Balthasar van der Pol Gold Medal of URSI, and 2015 Gold Medal of SPIE.

Fred E. Gardiol

C ross out, in the grid, all the words that appear in the list below—they may appear horizontally, vertically, or diagonally. Five letters should then remain, indicating features and functions characterizing a range, a product, a service, or a result.

L	A	B	M	Y	C	O	R	S	S	N	E	I	L	A
A	I	R	O	I	E	R	U	L	I	N	G	N	S	C
C	O	T	T	O	N	I	R	A	R	N	R	T	M	I
I	N	C	T	X	T	O	S	I	I	N	E	E	R	B
H	A	S	B	E	E	N	O	D	S	R	D	N	S	A
T	B	G	E	N	R	E	N	C	O	U	N	T	E	R
Y	R	D	N	E	P	E	I	I	S	A	I	S	H	A
M	U	I	N	I	L	O	D	A	G	I	M	B	A	L
D	E	O	U	O	R	M	U	Z	C	I	E	O	B	Y
E	G	S	T	R	E	A	M	P	S	T	R	A	I	M
Y	L	A	R	T	C	E	P	S	A	N	K	O	T	E
R	I	G	H	T	N	N	I	T	N	E	B	M	A	L
T	B	A	N	T	U	O	N	S	C	G	U	M	B	O
N	N	N	O	A	N	Z	G	E	H	R	O	A	L	D
E	V	R	E	S	B	O	E	J	O	U	R	N	E	Y

Aisha, Aliens, Arabica, Asteroid
Bake, Bangle, Bennu, Boot, Bilge, Breen
Center, Cotton, Cymbal
Dial, Dinosaur, Dude, Dumping
Encounter, Entry, Extra
Gadolinium, Gimbal, Gumbo

Habitable, Has been
Intent
Jest, Journey
Lambent, Lending, Littered
Medusa, Melody, Mentor, Methane, Missions, Mylar, Mythical
Observe, Origin, Orion, Ormuz, Osiris, Oxen, Ozone
Paring, Pendry

Reminder, Reno, Right, Roald, Ruling
Sagan, Sancho, Snout, Spectral, Stream, Suite
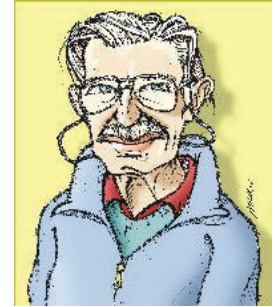Tactic
Urban, Urgent

LEOPOLD B FELSEN

EXCELLENCE in ELECTROMAGNETICS AWARD

Leopold B. Felsen Fund bestows an award for Excellence in Electromagnetics to promote contributions of the Turkish students/researchers to the field of Electromagnetics each year (since 2007).

This year, in 2019, there were 9 applications of very high quality. Following the request of late Prof. Felsen, Doctor Honoris Causa of Doğuş University, while selecting the candidates, being a member or a student of Doğuş University and publications resulting from research done in Turkey are considered a plus. After a meticulous examination process, the Selection Committee bestows this year's 2,500 US $ award to:

**Polat GÖKTAŞ
Bilkent University**

Picture: Polat (L), with his PhD advisor Prof. Dr. Ayhan Altıntaş (R) from Bilkent University in the Award Ceremony during EMC TURKIYE 2019 Conference.

Picture: (L-R) Levent Sevgi, Polat Göktaş, and Ayhan Altıntaş with the award check in the Award Ceremony during EMC TURKIYE 2019 Conference.

**Prof. Dr. Levent Sevgi
Chair / Award Committee**

ADVERTISING & SALES

The Advertisers Index contained in this issue is compiled as a service to our readers and advertisers: the publisher is not liable for errors or omissions although every effort is made to ensure its accuracy. Be sure to let our advertisers know you found them through *IEEE Antennas & Propagation Magazine.*

COMPANY	PAGE NUMBER	WEBSITE	PHONE
Antenna World	9	antennatesting.com	+1 305 850 7779
Comsol	3	comsol.blog/EM-simulations	
EMCoS Ltd.	5	www.emcos.com	
Remcom	CVR 4	www.remcom.com/5g-mimo	+1 888 7 REMCOM
WIPL-D	7	www.wipl-d.com	

SOCIETY OFFICERS & ADMINISTRATIVE COMMITTEE

OFFICERS
Koichi Ito—*President*
Center for Frontier Medical Engineering
Chiba University, Japan
Email: ito.koichi@faculty.chiba-u.jp

Mahta Moghaddam—*President-Elect*
University of Southern California
Electrical Engineering
3737 Watt Way, PHE 634
Los Angeles, CA 90089
Phone: +1 213 740 4712
Email: mahta@usc.edu

Donald M. McPherson—*Treasurer*
SRC
7502 Round Pond Rd.
North Syracuse, NY 13212
Phone: +1 315 452 8000
Email: dmcpherson@ieee.org

Felix Vega—*Secretary*
National University of Colombia, Bogota
Electrical and Electronic Engineering Department
Edificio 411 off 210
Ciudad Universitaria, Bogota, Colombia
Email: jfvegas@unal.edu.co

ADMINISTRATIVE COMMITTEE
2019
Agostino Monorchio
Don McPherson
Zhongxiang Shen
Felix Vega

2020
Francesco Andriulli
Ajay Poddar
Rod Waterhouse
Monai Krairiksh

2021
Andrea Alù
Takeshi Fukusako
Yang Hao
Guido Lombardi

HONORARY LIFE MEMBER
W. Ross Stone

PAST PRESIDENTS
Weng Cho Chew, 2018
Ahmed A. Kishk, 2017
Michael A. Jensen, 2016
Roberto D. Graglia, 2015

CALL FOR PROPOSALS TO HOST THE JOINT IEEE AP-S INTERNATIONAL SYMPOSIUM ON ANTENNAS AND PROPAGATION/USNC-URSI RADIO SCIENCE MEETING

The IEEE Antennas and Propagation Society (AP-S) and the US National Committee (USNC) of the International Union of Radio Science (URSI) invite letters of interest from appropriate groups wishing to host the joint IEEE AP-S International Symposium on Antennas and Propagation/USNC-URSI Radio Science Meeting to be held in June or July of 2022 and later years. Proposals from all IEEE Regions are welcome; however, it is expected that a joint symposium will be held in Regions 8-10 not more frequently than every third year (the joint symposium will be held in Region 10 in 2021).

A group approved to host the joint symposium will be expected to undertake the following major tasks:

1) Provide a volunteer local Organizing Committee to organize all aspects of the symposium, working with a professional conference organizer
2) Select one or more possible venues fulfilling all necessary requirements for the symposium
3) Establish a Technical Program Committee to ensure the quality of the symposium
4) Fulfill all of the other requirements identified in the Meetings Handbook.

Proposals to host the symposium may be submitted by an authorized representative of a university, research institute, or any appropriate nonprofit organization.
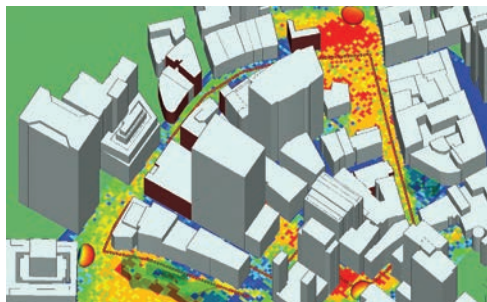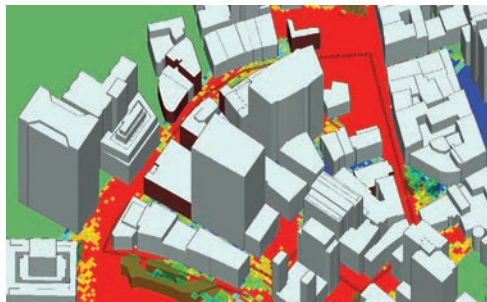
Letter of interest: Groups wishing to host the symposium should submit a detailed letter of interest to Dave Michelson, Chair of the Meetings Committee, at davem@ece.ubc.ca. At a minimum, the letter should contain the following:

1) A brief description of the proposed host group, its location, and composition
2) The proposed location and venue(s) of the symposium, with an explanation of their advantages
3) The proposed dates (may be approximate)
4) Basic budget data using the parameters in the Meetings Handbook
5) Possible social activities
6) Possible sponsors
7) Any concurrent meetings and information on co-organizers, if any
8) Any special advantages offered by the proposal.

The Meetings Handbook (available at www.ieeeaps.org, by request from Dave Michelson, or from the AP-S Secretary) should be consulted before preparing a letter of interest. All letters of interest should be received by **February 1** or **May 15** for consideration at one of the two Meetings Committee meetings held each year. Questions regarding the availability of a year or the preparation of a letter of interest should be sent to Dave Michelson at davem@ece.ubc.ca.

Wireless InSite™

Beamforming with massive MIMO (top) shows significant improvement to throughput over links between single antennas (bottom)

Software for Simulating 5G mmWave and MIMO Systems

Remcom's unique ray tracing capability simulates the detailed multipath of large MIMO arrays while overcoming the limitations of traditional ray tracing methods.

- 3D ray tracing valid up to 100 GHz
- Simulate massive MIMO arrays
- MIMO beamforming, spatial multiplexing, and diversity techniques
- Throughput and capacity for MIMO systems
- Diffuse scattering
- High-performance computing

Learn more at | **www.remcom.com/5g-mimo** ▶▶▶

+1.888.7.REMCOM (US/CAN) | +1.814.861.1299 | **www.remcom.com**

REMCOM®